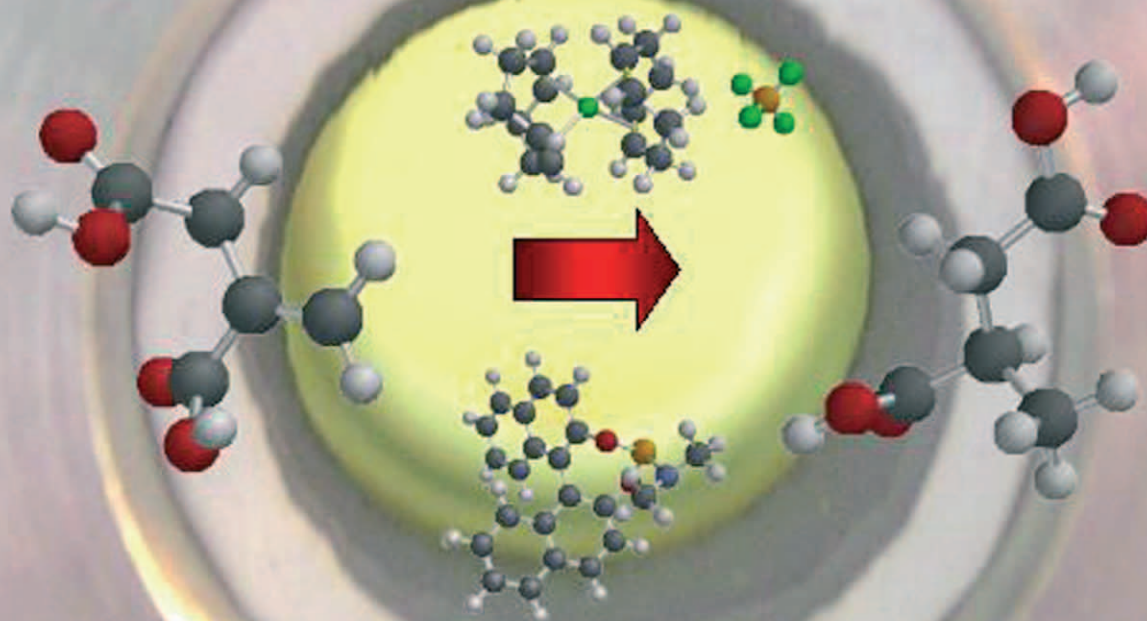


Green Chemistry

Cutting-edge research for a greener sustainable future

www.rsc.org/greenchem

Volume 7 | Number 10 | October 2005 | Pages 689–752



Downloaded on 06 November 2010
Published on 23 September 2005 on <http://pubs.rsc.org> | doi:10.1039/B512992N

ISSN 1463-9262

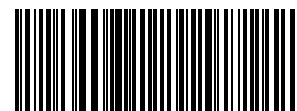
RSC Publishing

Godinez-Salomon *et al.*
Scavengers for cyanides

Abbott *et al.*
Hydrogenation in a supercritical HFC

Morita *et al.*
Conversion of primary alcohols in water

Wu *et al.*
Synthesis of ionic liquids in sCO₂



1463-9262 (2005) 7:10;1-4

Elegant Solutions

Ten Beautiful Experiments in Chemistry

Where does the true beauty reside in experimental chemistry?

In the clarity of the experiment's conception? the design of the instruments? the nature of the knowledge gained or of the product made?

'Philip Ball is one of the most prolific and imaginative of contemporary science writers.'
Chemistry in Britain

Winner of the Aventis Prize for Science Books 2005,

Philip Ball,
offers ten suggestions in his latest book

Hardcover | 0 85404 674 7 | 208 pages | 2005 | £19.95 | RSC member price £12.75

RSC Publishing

www.rsc.org/elegantsolutions

IN THIS ISSUE

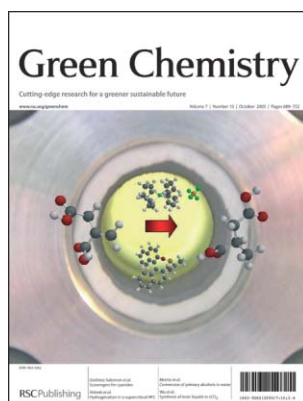
ISSN 1463-9262 CODEN GRCHFJ 7(10) 689–752 (2005)

In this issue...

Himeshima and Amao describe the production of hydrogen from a cellulose derivative, using the light-harvesting function of Mg chlorophyll-a



Chemical biology articles published in this journal also appear in the *Chemical Biology Virtual Journal*: www.rsc.org/chembiol



Cover

The cover image represents the use of supercritical HFC 134a for the asymmetric hydrogenation of prochiral olefins which allows high solute concentrations and standard catalysts to be used.

Image reproduced by permission of A. P. Abbott from *Green Chem.*, 2005, 7(10), 721.

CHEMICAL TECHNOLOGY

T37

Chemical Technology highlights the latest applications and technological aspects of research across the chemical sciences.

Chemical Technology

October 2005/Volume 2/Issue 10

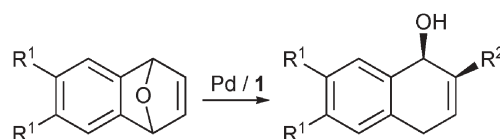
www.rsc.org/chemicaltechnology

HIGHLIGHT

699

Highlights

Markus Hölscher reviews some of the recent literature in green chemistry



EDITORIAL STAFF

Editor

Harpal Minhas

Assistant editors

Nina Athey-Pollard, Merlin Fox, Katie Gibb

News writer

Markus Hölscher

Publishing assistant

Jackie Cockrill

Team leader, serials production

Stephen Wilkes

Technical editors

Katherine Davies, Christopher Ingle, Kathryn Lees

Administration coordinator

Sonya Spring

Editorial secretaries

Lynne Braybrook, Rebecca Gotobed, Julie Thompson

Publisher

Adrian Kybett

Green Chemistry (print: ISSN 1463-9262; electronic: ISSN 1463-9270) is published 12 times a year by the Royal Society of Chemistry, Thomas Graham House, Science Park, Milton Road, Cambridge, UK CB4 0WF.

All orders, with cheques made payable to the Royal Society of Chemistry, should be sent to RSC Distribution Services, c/o Portland Customer Services, Commerce Way, Colchester, Essex, UK CO2 8HP. Tel +44 (0) 1206 226050; E-mail sales@rscdistribution.org

2005 Annual (print + electronic) subscription price: £795; US\$1310. 2005 Annual (electronic) subscription price: £715; US\$1180. Customers in Canada will be subject to a surcharge to cover GST. Customers in the EU subscribing to the electronic version only will be charged VAT.

If you take an institutional subscription to any RSC journal you are entitled to free, site-wide web access to that journal. You can arrange access via Internet Protocol (IP) address at www.rsc.org/ip. Customers should make payments by cheque in sterling payable on a UK clearing bank or in US dollars payable on a US clearing bank. Periodicals postage paid at Rahway, NJ, USA and at additional mailing offices. Airfreight and mailing in the USA by Mercury Airfreight International Ltd., 365 Blair Road, Avenel, NJ 07001, USA.

US Postmaster: send address changes to Green Chemistry, c/o Mercury Airfreight International Ltd., 365 Blair Road, Avenel, NJ 07001. All despatches outside the UK by Consolidated Airfreight.

PRINTED IN THE UK

Advertisement sales: Tel +44 (0) 1223 432243; Fax +44 (0) 1223 426017; E-mail advertising@rsc.org

Green Chemistry

Cutting-edge research for a greener sustainable future

www.rsc.org/greenchem

Green Chemistry focuses on cutting-edge research that attempts to reduce the environmental impact of the chemical enterprise by developing a technology base that is inherently non-toxic to living things and the environment.

EDITORIAL BOARD

Chair

Professor Colin Raston,
Department of Chemistry
University of Western Australia
Perth, Australia
E-mail clraston@chem.uwa.edu.au

Scientific editor

Professor Walter Leitner,
RWTH-Aachen, Germany
E-mail leitner@itmc.rwth-aachen.de

Professor Joan Brennecke,
University of Notre Dame, USA

Professor Steve Howdle, University of Nottingham, UK

Dr Janet Scott, Centre for Green Chemistry, Monash University, Australia

Dr A Michael Warhurst,
WWF, Brussels, Belgium

Professor Tom Welton,
Imperial College, UK
E-mail t.welton@ic.ac.uk

Professor Roshan Jachuck,
Clarkson University, USA
E-mail rjachuck@clarkson.edu

Dr Paul Anastas, Green Chemistry Institute, USA
Email p_anastas@acs.org

Professor Buxing Han, Chinese Academy of Sciences
Email hanbx@iccas.ac.cn

Associate editor for the Americas

Professor C. J. Li, McGill University, Canada
E-mail cj.li@mcgill.ca

INTERNATIONAL ADVISORY EDITORIAL BOARD

James Clark, York, UK

Avelino Corma, Universidad Politécnica de Valencia, Spain

Mark Harmer, DuPont Central R&D, USA

Herbert Hugl, Lanxess Fine Chemicals, Germany

Makato Misono, Kogakuin University, Japan

Robin D. Rogers, Centre for Green Manufacturing, USA

Kenneth Seddon, Queen's University, Belfast, UK

Roger Sheldon, Delft University of Technology, The Netherlands

Gary Sheldrake, Queen's University, Belfast, UK

Pietro Tundo, Università ca Foscari di Venezia, Italy

Tracy Williamson, Environmental Protection Agency, USA

INFORMATION FOR AUTHORS

Full details of how to submit material for publication in Green Chemistry are given in the Instructions for Authors (available from <http://www.rsc.org/authors>). Submissions should be sent via ReSource: <http://www.rsc.org/resource>.

Authors may reproduce/republish portions of their published contribution without seeking permission from the RSC, provided that any such republication is accompanied by an acknowledgement in the form: (Original citation) – Reproduced by permission of the Royal Society of Chemistry.

© The Royal Society of Chemistry 2005. Apart from fair dealing for the purposes of research or private study for non-commercial purposes, or criticism or review, as permitted under the Copyright, Designs and Patents Act 1988 and the Copyright and Related Rights Regulations 2003, this publication may only be reproduced, stored or transmitted, in any form or by any means, with the prior permission in writing of the Publishers or in the case of reprographic reproduction in accordance with the terms of

licences issued by the Copyright Licensing Agency in the UK. US copyright law is applicable to users in the USA.

The Royal Society of Chemistry takes reasonable care in the preparation of this publication but does not accept liability for the consequences of any errors or omissions.

Ⓢ The paper used in this publication meets the requirements of ANSI/NISO Z39.48-1992 (Permanence of Paper).

Royal Society of Chemistry: Registered Charity No. 207890

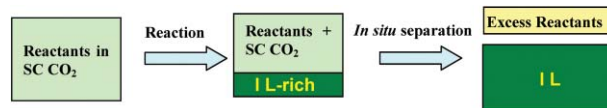
COMMUNICATIONS

701

A green and effective method to synthesize ionic liquids: supercritical CO₂ route

Weize Wu,* Wenjing Li, Buxing Han,* Zhaofu Zhang, Tao Jiang and Zhimin Liu

Ionic liquids (ILs) can be synthesized in supercritical (sc) CO₂. The product and the excess reactant can be separated *in situ* by scCO₂ without any cross-contamination, and the yield can reach 100%. The whole process is green, simple and highly efficient.

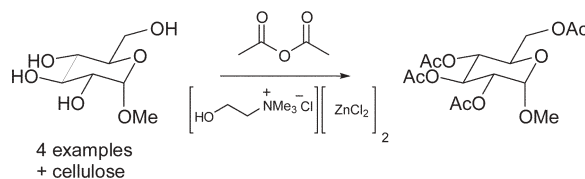


705

O-Acetylation of cellulose and monosaccharides using a zinc based ionic liquid

Andrew P. Abbott, Thomas J. Bell, Sandeep Handa* and Barry Stoddart

The efficient *O*-acetylation of monosaccharides and cellulose is demonstrated using a Lewis acidic ionic liquid based on choline chloride and zinc chloride.

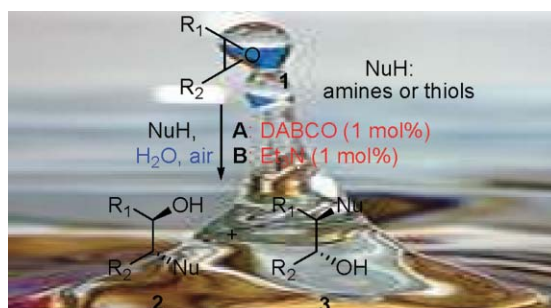


708

Tertiary amines as highly efficient catalysts in the ring-opening reactions of epoxides with amines or thiols in H₂O: expeditious approach to β-amino alcohols and β-aminothioethers

Jie Wu* and Hong-Guang Xia

Ring-opening of epoxides with various amines or thiols catalyzed by DABCO or Et₃N (1 mol%) in water afforded the corresponding products in good to excellent yields under mild reaction conditions.



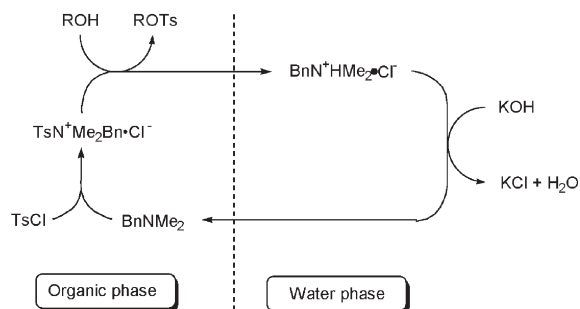
PAPERS

711

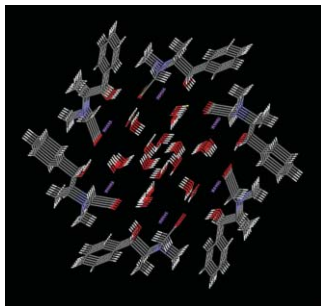
Water-solvent method for tosylation and mesylation of primary alcohols promoted by KOH and catalytic amines

Jun-ichi Morita, Hidefumi Nakatsuji, Tomonori Misaki and Yoo Tanabe*

We have developed an efficient water-solvent method for *p*-toluenesulfonylation (tosylation) and methanesulfonylation (mesylation) of primary alcohols using *p*-toluenesulfonyl chloride and methanesulfonyl chloride, respectively, promoted by KOH and catalytic amines.



716

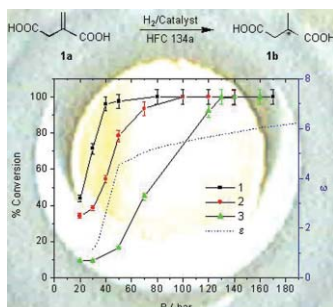


Strecker intermediates as non-pollutant scavengers for cyanides

Fernando Godinez-Salomon, Jose M. Hallen-Lopez, Herbert Höpfl, Adela Morales-Pacheco, Hiram I. Beltrán* and Luis S. Zamudio-Rivera*

Using a series of five bis(aminomethyl)ethers, a fast and efficient transformation of sodium cyanide to sodium *N*-2-hydroxyethylglycinates is reported, where the starting materials are prototypes for application in the mining and oil industries to diminish the pollution of the tailings derived from their processes.

721

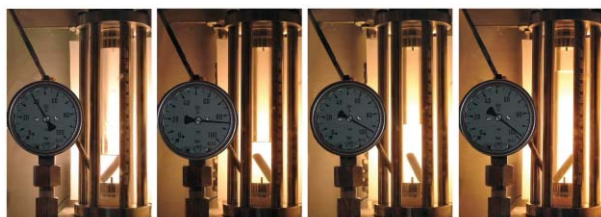


Hydrogenation in supercritical 1,1,1,2 tetrafluoroethane (HFC 134a)

Andrew P. Abbott, Wayne Eltringham, Eric G. Hope* and Mazin Nicola

Supercritical HFC 134a offers reactivities and enantioselectivities comparable to those achievable in conventional organic media in the asymmetric hydrogenation of a series of substrates using a rhodium(I)/MonoPhos catalyst generated *in situ*.

726



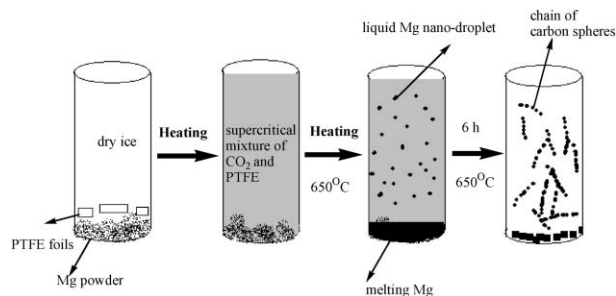
CO₂ - expanded liquid

Biphasic hydrogenation of α -pinene in high-pressure carbon dioxide

Anna Milewska, Anna M. Banet Osuna, Isabel M. Fonseca and Manuel Nunes da Ponte*

High pressure carbon dioxide expands liquid α -pinene so that hydrogenations can be carried out in a biphasic system, at lower pressure, in a safer and more economical way.

733



Formation of carbon micro-sphere chains by defluorination of PTFE in a magnesium and supercritical carbon dioxide system

Qiang Wang, Fangyu Cao and Qianwang Chen*

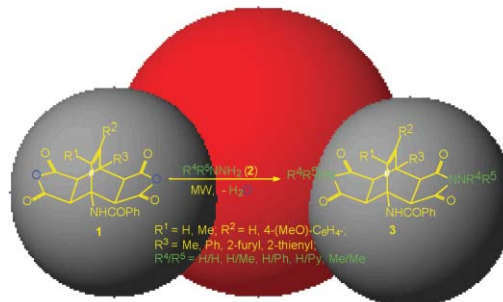
Well-crystallized carbon micro-spheres at the sub-micrometer scale, assembled in the shape of string, were prepared by defluorination of polytetrafluoroethylene (PTFE) with metallic magnesium in supercritical carbon dioxide at 650 °C for 6 h.

737

An efficient microwave-assisted green transformation of fused succinic anhydrides into *N*-aminosuccinimide derivatives of bicyclo[2.2.2]octene in water

Mitja Martelanc, Krištof Kranjc, Slovenko Polanc and Marijan Kočevar*

Elimination of water in water: the first efficient microwave accelerated green transformation of fused succinic anhydrides into *N*-aminosuccinimide derivatives of bicyclo[2.2.2]octene in water is presented.

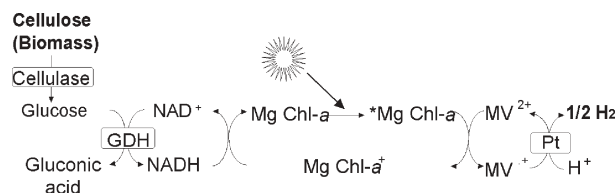


742

Green process for hydrogen production from cellulose derivative using visible light-harvesting function of Mg chlorophyll-*a*

Noriko Himeshima and Yutaka Amao*

A green process for hydrogen production, coupling cellulose derivative, methylcellulose (MC_n) hydrolysis and platinum colloid as a catalyst using the visible light-harvesting function of Mg chlorophyll-*a* has been developed.

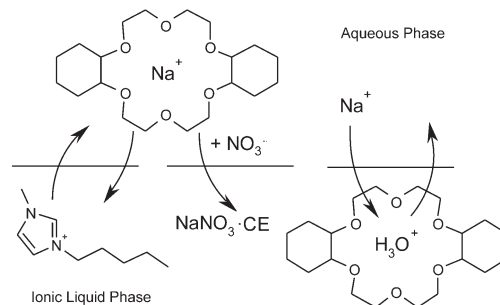


747

A ternary mechanism for the facilitated transfer of metal ions into room-temperature ionic liquids (RTILs): implications for the “greenness” of RTILs as extraction solvents

Mark L. Dietz* and Dominique C. Stepinski

Sodium ion extraction from aqueous nitrate media by DCH18C6 in 1-alkyl-3-methylimidazolium bis[(trifluoromethyl)sulfonyl]imides occurs *via* a complex, three-path mechanism, an observation shown to have negative implications for the “greenness” of ILs as extraction solvents.




AUTHOR INDEX

- | | | | |
|-----------------------------|--------------------------------|-----------------------------|------------------------------|
| Abbott, Andrew P., 705, 721 | Godinez-Salomon, Fernando, 716 | Li, Wenjing, 701 | Stepinski, Dominique C., 747 |
| Amao, Yutaka, 742 | Hallen-Lopez, Jose M., 716 | Liu, Zhimin, 701 | Stoddart, Barry, 705 |
| Bell, Thomas J., 705 | Han, Buxing, 701 | Martelanc, Mitja, 737 | Tanabe, Yoo, 711 |
| Beltrán, Hiram I., 716 | Handa, Sandeep, 705 | Milewska, Anna, 726 | Wang, Qiang, 733 |
| Cao, Fangyu, 733 | Himeshima, Noriko, 742 | Misaki, Tomonori, 711 | Wu, Jie, 708 |
| Chen, Qianwang, 733 | Hope, Eric G., 721 | Morales-Pacheco, Adela, 716 | Wu, Weize, 701 |
| da Ponte, Manuel Nunes, 726 | Höpfel, Herbert, 716 | Morita, Jun-ichi, 711 | Xia, Hong-Guang, 708 |
| Dietz, Mark L., 747 | Jiang, Tao, 701 | Nakatsuji, Hidefumi, 711 | Zamudio-Rivera, Luis S., 716 |
| Eltringham, Wayne, 721 | Kočevar, Marijan, 737 | Nicola, Mazin, 721 | Zhang, Zhaofu, 701 |
| Fonseca, Isabel M., 726 | Kranjc, Krištof, 737 | Osuna, Anna M. Banet, 726 | |
| | | Polanc, Slovenko, 737 | |

FREE E-MAIL ALERTS

Contents lists in advance of publication are available on the web *via* www.rsc.org/greenchem - or take advantage of our free e-mail alerting service (www.rsc.org/ej_alert) to receive notification each time a new list becomes available.

* Indicates the author for correspondence: see article for details.

 Electronic supplementary information (ESI) is available *via* the online article (see <http://www.rsc.org/esi> for general information about ESI).

ADVANCE ARTICLES AND ELECTRONIC JOURNAL

Free site-wide access to Advance Articles and the electronic form of this journal is provided with a full-rate institutional subscription. See www.rsc.org/ejs for more information.

ReSource

Lighting your way through the publication process

A website designed to provide user-friendly, rapid access to an extensive range of online services for authors and referees.

ReSource enables **authors** to:

- Submit manuscripts electronically
- Track their manuscript through the peer review and publication process
- Collect their free PDF reprints
- View the history of articles previously submitted

ReSource enables **referees** to:

- Download and report on articles
- Monitor outcome of articles previously reviewed
- Check and update their research profile

Register today!

RSCPublishing

www.rsc.org/resource

02030508

Materials Chemistry Books from the Royal Society of Chemistry

Introduction to Glass Science and Technology

2nd Edition

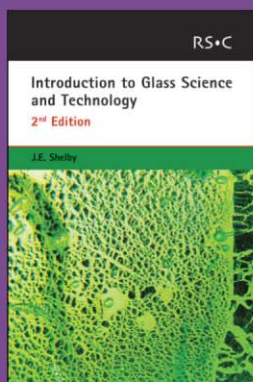
J E Shelby

Presents the fundamental topics in glass science and technology including glass formation, crystallisation and phase separation.

New chapters on:

- compositions and properties of commercial glasses
- thermal analysis of glasses and melts

Ideal for undergraduates in materials science, ceramics or inorganic chemistry. Also of great value to the engineer or scientist seeking basic knowledge of the formation, properties and production of glass.



Softcover | 0 85404 639 9 | 292 pages | £27.95 |
RSC member price £18.00

www.rsc.org/books/6399

The Chemistry and Physics of Coatings

2nd Edition

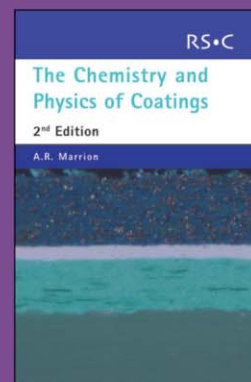
A R Marrion

Provides an introduction to the science underpinning the paint industry.

New features:

- separate chapters on binders for high solids and solvent-free coatings, inorganic and hybrid coatings and coatings formulation
- new section on coatings additives

Ideal for undergraduates and lecturers. This book will also be valuable to graduates of materials and polymer sciences and related areas, and those in the paint industry.



Hardcover | 0 85404 604 6 | 382 pages | £39.95 |
RSC member price £25.75

www.rsc.org/books/6046



JEM

Journal of Environmental Monitoring

Comprehensive, high quality coverage of multidisciplinary, international research relating to the measurement, pathways, impact and management of contaminants in all environments.

- Dedicated to the analytical measurement of environmental pollution
- Assessing exposure and associated health risks
- Fast times to publication
- Impact factor: 1.366
- High visibility - cited in MEDLINE



RSC Publishing

www.rsc.org/jem

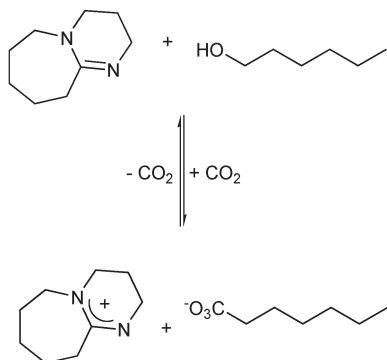
Highlights

DOI: 10.1039/b512282c

Markus Hölscher reviews some of the recent literature in green chemistry

Conversion of a liquid into an ionic liquid—and *vice versa*—by adding/removing compressed CO₂

Using a liquid as a solvent in one state of a chemical process has been an established technique for decades. Removing the liquid and adding another one to meet the desired solvent properties of a later step in a complex chemical procedure is the usual way of carrying a set of reactants through the whole process while they are transformed to products. If instead the properties of the solvent of the first step could easily be changed significantly and rationally in such a way, that the novel solvent properties are useful for the subsequent reaction/workup step, the solvent would not have to be removed each time one reaction step is completed. In addition to resulting in elegant chemical syntheses this procedure would add enormously to the economic efficiency of synthetic procedures. Impossible? Not at all! Jessop and coworkers from Queen's University and GeorgiaTech have recently made this fascinating idea come true.¹ A 1 : 1 mixture of 1,8-diazabicyclo-[5.4.0]-undec-7-ene (DBU) and 1-hexanol is a liquid with a polarity comparable to dimethylformamide or propanoic acid.

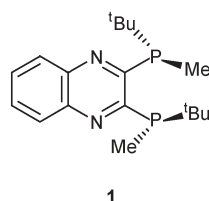


Upon the addition of CO₂ (1 atm, room temperature) the DBU molecule is protonated while the alcoholate anion binds one CO₂ molecule forming a carbonate species. This is an ionic

liquid (IL), which is as nonpolar as chloroform. When N₂ or argon is bubbled through the viscous IL, reversal of the reaction recreates DBU and 1-hexanol. As a test, the solubility of decane, which is a nonpolar compound, was tested in both solvent states. It could be shown that it dissolves in the liquid but not in the ionic liquid. Switchable solvent polarity could in the future help in improving environmentally benign chemical production, as the need for various different solvents might become obsolete when this new concept has been developed further.

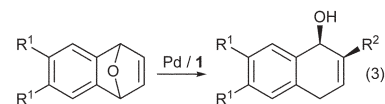
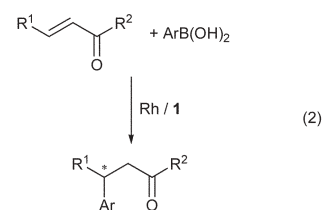
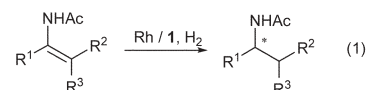
Highly enantioselective Rh- and Pd-catalyzed reactions with an air stable P-chiral phosphine ligand

Despite being very efficient and selective ligands for homogeneous transition metal catalysts, many phosphines suffer from the disadvantage of being fairly unstable in air. To both increase ligand stability and search for novel structures, Imamoto *et al.* from Chiba University developed the new phosphine ligand **1** in which the phosphorus centre is attached to a strongly electron withdrawing quinoxaline backbone.² As a result the electron density at the phosphorus centre is reduced rendering the P-atom less sensitive to oxidation by air.



The authors tested the new ligand in different reactions. At first they found the asymmetric hydrogenation of dehydroamino acid esters and enamides to be accomplished with ee-values ranging between 99.2 and 99.9% (1). Fortunately both (*E*)- and (*Z*)-β-(acetyl-amino)acrylates could be reduced with

high enantioselectivities. Interestingly Rh-catalyzed C–C bond forming reactions were also possible, with the asymmetric 1,4-addition of arylboronic acids to α,β-unsaturated carbonyl compounds proceeding with enantioselectivities ranging between 93.9 and 99.4% with yields ranging above 90% (2). Thirdly asymmetric alkylative ring opening reactions also proceeded with ee's above 95% and yields between 88 and 90% (3). As a result the ligand is air stable and versatile, which is a good starting point for further developments in this class of ligands.



Efficient and simple destruction of trichlorophenol by NaNO₂-O₂

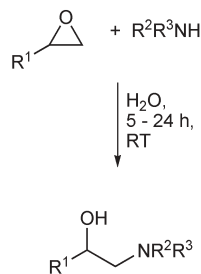
Polychlorinated phenols (PCPs) are toxic compounds that result for instance from lignin chlorination by chlorine-based bleaching processes. They are highly persistent and present in significant quantities in the environment. The US Environmental Protection Agency has classified these compounds as priority pollutants. A simple and efficient procedure to destroy these compounds and convert them into nontoxic and biodegradable products would enable industries to contribute to a major extent to environmental safety and public health.

The many different approaches to tackle the problem have by and large resulted in only limited success, due to a number of reasons. Microorganisms for example, which were intended to degrade PCPs, do the job, however in some cases they convert the PCPs into even more toxic and persistent pollutants. Catalytic reductive dechlorination is an alternative, but the noble metals used in this process would probably be deactivated by complex pollutants. Liang, Liu and Hu and coworkers from the Dalian Institute of Chemical Physics now report on a novel and highly efficient way to convert PCPs into comparably harmless material by reduction with $\text{NaNO}_2\text{-O}_2$.³ At moderate reaction temperatures of 150 °C $\text{NaNO}_2\text{-O}_2$ (NaNO_2 stoichiometric; O_2 pressure 0.5 MPa) converts 99% of the trichlorophenol (TCP) used as a model compound for the PCP family of compounds, with the TCP bound chlorine transformed to inorganic chlorides (91%). When NaNO_2 was used in catalytic amounts, TCP degradation was 25% and chlorine mineralization amounted to 11%. The major organic compounds of the degradation process are CO_2 and/or CO together with a small fraction of biodegradable organic compounds with a high conversion rate. As this $\text{NaNO}_2\text{-O}_2$ catalyst system, which also works successfully when O_2 is replaced by air and in scale-up experiments, avoids secondary pollution it might be well suited for practical applications.

Chemoselective β -aminoalcohol synthesis in water

Carrying out organic reactions in water has become highly desirable in recent years to meet environmental considerations. One novel example is the chemoselective addition of amines to epoxides forming β -aminoalcohols which are compounds of considerable interest in medicinal chemistry or for the production of amino acids as well as chiral auxiliaries. One of the current drawbacks of this reaction is the use of

moisture-sensitive catalysts and organic solvents. Very recently Azizi and Saidi from Sharif University of Technology showed that the reaction of aliphatic epoxides and aliphatic amines is possible in water with moderate to high yields and good regioselectivities and without the need to add any catalysts or organic solvents.⁴



Some products precipitated from the reaction mixture, others were extracted using diethyl ether. The regioselectivities for a broad variety of substrates reach values of up to 97% and are the highest reported to date for nucleophilic ring opening of epoxides with amines. Aromatic amines don't react as well as aliphatic, introducing chemoselectivity into the process. In a mixture of cyclohexene oxide, aniline and piperidine only piperidine is transformed while aniline does not react. Though an $\text{S}_\text{N}2$ -mechanism is proposed by the authors the reaction is to a major extent far from being understood.

Recent developments in BASF's contributions to sustainability

Adding to their long standing devotion to sustainable production BASF has introduced worldwide an interesting mix of strategies, ideas and products lately, strengthening the close relationship between economic competence and environmental/social responsibility.

As one prominent example, the company was awarded the 2005 Presidential Green Chemistry Challenge Award by the US Environmental Protection Agency for a novel UV-curable primer designed for use in automotive refinishing coatings.

An eco-efficiency analysis confirms high cost effectiveness and environmentally beneficial performance, which is made available by the new coating curing 10 times faster than conventional thermally cured products. The new product is simply irradiated with UV light making heating ovens obsolete and reducing energy consumption by approximately 80%.

1-Methylimidazole is the core of the new BASIL[™]-process by BASF used for scavenging acids during chemical syntheses of phosphorus compounds. Relative to the conventionally used amines the BASIL[™]-process is more cost efficient and also more environmentally friendly as it increases stability and reduces work expenses. The BASIL[™]-process is the first industrial process in which ionic liquids are employed.

Other than products, general strategies to save on energy and raw materials consumption are continuously put into practice. BASF has set up the so called Verbund-concept in which production and energy needs are combined in such a way, that the use of primary energy carriers in terms of raw materials and for power and steam generation is reduced. Figures for 2003 prove that the Verbund system resulted in a saving of ca. 1.4 million metric tons of fossil and substitute fuels for the whole BASF group. In Ludwigshafen, BASF's largest Verbund site, the steam requirements have declined by 49% since the 1970's while production has risen by 45% during the same period. In Antwert the volume of fossil fuels for the generation of steam was even reduced by 79% while the production rate increased by more than 400%.

References

- 1 P. G. Jessop, D. J. Heldebrant, X. Li, Ch. A. Eckert and Ch. L. Liotta, *Nature*, 2005, **436**, 1102.
- 2 T. Imamoto, K. Sugita and K. Yoshida, *J. Am. Chem. Soc.*, 2005, **127**, 11934–11935.
- 3 X. Liang, D. Fu, R. Liu, Q. Zhang, T. Y. Zhang and X. Hu, *Angew. Chem.*, 2005, **117**, 5656–5659.
- 4 N. Azizi and M. R. Saidi, *Org. Lett.*, 2005, **7**, 3649–3651.

A green and effective method to synthesize ionic liquids: supercritical CO₂ route

Weize Wu,* Wenjing Li, Buxing Han,* Zhaofu Zhang, Tao Jiang and Zhimin Liu

Received 3rd June 2005, Accepted 4th August 2005

First published as an Advance Article on the web 12th August 2005

DOI: 10.1039/b507845h

Many room temperature ionic liquids (ILs) are nonvolatile solvents which have huge potential applications in various chemical processes. However, the synthesis of ILs usually uses different kinds of volatile organic solvents in the reaction and subsequent separation process. In this work, supercritical (sc) CO₂, an environmentally benign solvent, has been utilized as the medium to synthesize ILs, 1-butyl-3-methylimidazolium bromide ([bmim]Br) and 1,3-dimethylimidazolium trifluoromethanesulfonate ([Me₂Im]TfO). The results show that ILs can be synthesized in scCO₂ with 100% yield and the excess reactants added can be extracted *in situ* by scCO₂ without any cross-contamination. The whole process is green and very effective.

Introduction

Chemical and industrial processes use huge amounts of volatile organic solvents. It is estimated that about 20 million tons of volatile organic solvents, one of the major contributors to air pollution, are released to the atmosphere each year.¹ Hence, many scientists have been dedicated to finding solutions to this problem.

Room temperature ionic liquids (ILs), which are organic salts and are liquids at ambient temperatures, possess many unusual properties,² such as extremely low vapor pressure, high thermal stability and chemical stability, and excellent solvent power for organic and inorganic compounds. They are regarded as a class of alternatives to organic solvents for a range of industrially important chemical processes, such as separations,³ reactions,^{2,4} material synthesis,⁵ *etc.* Therefore, studies on the fundamental properties and applications of ILs have attracted much attention recently.

While ILs are nonvolatile solvents, the processes to synthesize ILs usually use many volatile organic solvents,⁶ such as acetonitrile, methanol, ethanol, benzene, ethyl acetate, dichloromethane, and 1,1,1-trichloroethane. These organic solvents are used in both the reaction and subsequent separation processes. Utilization of these volatile solvents causes environmental pollution. At the same time, the commonly used organic solvents can usually dissolve all the substances in the reaction mixtures after the reaction. Therefore, cross-contamination is unavoidable in the subsequent separation and/or purification processes. This not only reduces the yield and efficiency, but also results in chemical and/or energy waste. Obviously, how to synthesize ILs using green, simple, and effective routes is very important to widen applications

of ILs and environmental protection, but this is a challenging prospect.

Supercritical (sc) CO₂, an environmentally benign solvent, has received much attention⁷ because it is nontoxic, nonflammable, inexpensive, readily available in large quantities, and has moderate critical temperature and pressure (31.1 °C and 7.38 MPa). ScCO₂ has been utilized in many chemical processes, such as extraction and fractionation,⁸ chemical reactions,⁹ and material processing.¹⁰

Brennecke and co-workers performed elegant studies on the phase behaviors of some scCO₂/IL systems.¹¹ They discovered that the unique feature of the phase behavior was that scCO₂ was soluble in the ILs, while the solubility of the ILs in scCO₂ was not detectable. The special and advantageous phase behavior of scCO₂/IL systems has been successfully used to recover organic substances from ILs without any cross-contamination,^{11a,12} and some scCO₂/IL mixed solvents have been used to carry out biphasic reactions.¹³

1-Butyl-3-methylimidazolium bromide ([bmim]Br) and 1,3-dimethylimidazolium trifluoromethanesulfonate ([Me₂Im]TfO) have been synthesized in organic solvents by other authors.^{6a,14} In this work, we synthesized these ILs using scCO₂ as the solvent. After reaction, the excess reactant in the IL was removed *in situ* by scCO₂ extraction, leaving pure IL in the reactor, and the extracted reactant was collected and can be recycled. This new route has some unique advantages. For example, the whole process is environmentally benign, simple, and the yield can reach 100%. We believe that this green and effective route can be used to synthesize many other ILs with similar advantages.

Experimental

Materials

Methylimidazole (99%), bromobutane (99%) and methyl trifluoromethanesulfonate (96%) were purchased from Acros Organics. CO₂ (99.95%) was provided by Beijing Analytical Instrument Factory. The chemicals were used as received.

Apparatus and measurements

The apparatus was similar to that used previously to determine the phase behaviours of mixtures at high pressures,¹⁵ and its schematic diagram is shown in Fig. 1. It consisted mainly of a CO₂ cylinder, a computer-controlled syringe pump, a constant temperature water bath, a pressure gauge, a view cell of 55 mL, a magnetic stirrer, and a cold trap. The water bath was maintained within ± 0.1 °C of the desired temperature by using a Haake D8 temperature controller. The pressure gauge was composed of a pressure transducer (FOXBORO/ICT, Model 93) and an indicator, which was accurate to ± 0.025 MPa.

Center for Molecular Science, Institute of Chemistry, Chinese Academy of Sciences, Beijing 100080, China. E-mail: wzwu@iccas.ac.cn; hanbx@iccas.ac.cn.; Fax: +86-10-62559397; Tel: +86-10-62562821

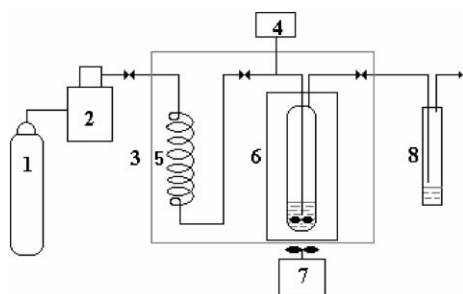


Fig. 1 Schematic diagram of the apparatus used for synthesis of the ILs and *in situ* separation. 1—CO₂ reservoir; 2—computer-controlled metering syringe pump; 3—constant temperature water bath; 4—pressure gauge; 5—pre-heater; 6—view cell; 7—magnetic stirrer; 8—cold trap.

We only describe the procedures to synthesize [bmim]Br because those to prepare [Me₂Im]TfO were similar. In an experiment, suitable amounts of methylimidazole and bromobutane were loaded into the view cell. Then the cell was placed in the constant-temperature water bath. CO₂ was compressed into the cell up to 15.0 MPa. The stirrer in the cell was started and the product precipitated to form an IL-rich phase. After a desired reaction time, the unreacted reactants in the cell were extracted *in situ* by scCO₂ at 15.0 MPa and 50.0 °C and condensed in the cold trap after depression, leaving the IL (the product in this work) in the cell due to the insoluble nature of ILs in scCO₂.^{11,16} The principle of the extraction was similar to that for separation of organic compounds from ILs using scCO₂.^{11a,12} The extracted reactants condensed in the cold trap can be recycled. In this work, it was very important to remove all the unreacted reactants in the product in order to get an accurate yield. Our experiments demonstrated that the reactants in the products could be removed completely after the extraction with 100 g of CO₂ at a flow rate of 30 g h⁻¹ CO₂. This was confirmed in two ways. The first was gas chromatography (Agilent 4890D) analysis. Second, we collected most of the product in a small beaker which was dried under vacuum at 50 °C for 24 h, and the mass of the product before and after drying was the same. To obtain the total amount of the product, the IL on the wall of the reactor was washed into another small beaker by diethyl ether. The diethyl ether was then removed under vacuum and 50 °C until the mass was independent of drying time. A balance (OHAUS) with a resolution of 0.1 mg was used to determine the masses in this work. The yield of the product was easily calculated from the masses of the product and the added reactants.

The ILs synthesized was characterized by ¹H-NMR (Bruker A V 400) and FT-IR (Bruker Tensor 27).

Results and discussion

In this work, we synthesized [bmim]Br from methylimidazole and bromobutane and [Me₂Im]TfO from methylimidazole and methyl trifluoromethanesulfonate in scCO₂. These two ILs have been synthesized in organic solvents by other authors.^{6a,14}

Synthesis of [bmim]Br

Methylimidazole is more expensive than bromobutane, with a higher and more desirable conversion. Therefore, the molar

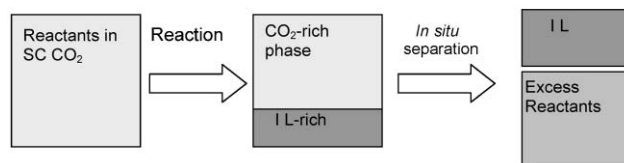


Fig. 2 Synthesis of IL using scCO₂.

concentration of bromobutane should be reasonably larger than that of methylimidazole in the feed.^{14,17} In this work the molar concentration of bromobutane was 20% larger than that of methylimidazole, and the original concentrations of methylimidazole and bromobutane in the reaction cell were 0.180 mol L⁻¹ and 0.216 mol L⁻¹, respectively.

The whole process can be illustrated simply in Fig. 2. At the beginning of the reaction, the mixture was homogenous, indicating that the reactants were soluble in scCO₂. As the reaction proceeded, an IL-rich liquid phase and a scCO₂-rich phase in the reactor were observed. The amount of the IL in the CO₂-rich phase was negligible, and therefore, after reaction, the IL and the excess reactants could be separated *in situ* by scCO₂ without any cross-contamination.

Fig. 3 illustrates the yield based on methylimidazole as a function of reaction time. The yield reaches 100% within 48 h at 70 °C, as can be known from Fig. 3. It indicates that all the methylimidazole can be reacted and all the product can be collected. This was further confirmed by the fact that there was no methylimidazole in the extract for the reactions with a reaction time of 48 h or longer, as was determined by GC. A yield of 100% cannot be achieved as organic solvents are used in the reaction and separation processes. Bonhôte *et al.*^{6a} used the same reactants to synthesize [bmim]Br with a yield of 64%, and 1,1,1-trichloroethane was used as reaction medium and separation solvent. Srinivas *et al.*¹⁴ also synthesized the same ionic liquid in a yield of 94% using diethyl ether as solvent to remove unreacted reactant. Several ILs have been synthesized using organic solvents in our laboratory, and the yields are generally in the range of 70–90%. There may be three main reasons for the high yield when scCO₂ is used as the solvent. First, scCO₂ has a much lower viscosity and higher diffusion coefficient than liquids^{7,9} and hence the reaction rate is faster. Second, the IL produced precipitates automatically from the scCO₂ phase, which is favorable to enhancing the reaction rate. Third, the loss of the IL was negligible in the separation process

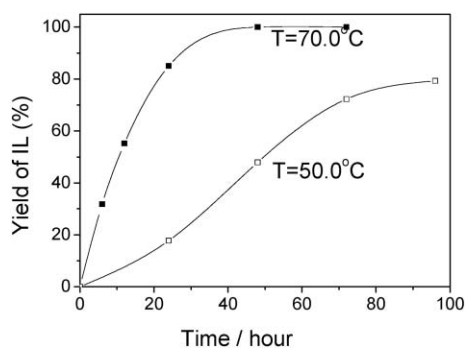


Fig. 3 Effect of reaction time on the yield for the synthesis of [bmim]Br in scCO₂ at 15.0 MPa and different temperatures.

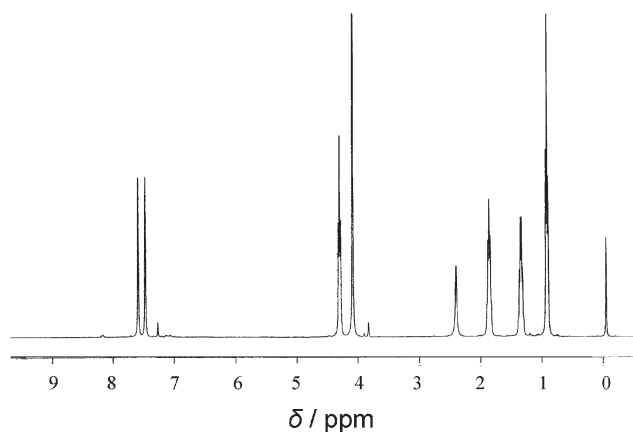


Fig. 4 $^1\text{H-NMR}$ spectrum of [bmim]Br (chloroform-d, δ/ppm relative to TMS).

because the IL is not soluble in scCO_2 .^{11,16} As discussed above, after the reaction the excess reactant was extracted and collected *in situ* by scCO_2 extraction, leaving the pure IL in the reaction cell. Therefore, the whole process is green, simple, effective, and there is no cross-contamination. It is well known that when a liquid organic solvent is used as a medium for a reaction, cross-contamination usually inevitably occurs, which results in the losses of both product and unreacted reactants.

The ILs synthesized in scCO_2 were characterized by $^1\text{H-NMR}$ and FT-IR. As examples, Fig. 4 and Fig. 5 give the NMR and FTIR spectra of the IL synthesized at $70.0\text{ }^\circ\text{C}$ and 15.0 MPa with a reaction time of 48 h, consistent with those reported by Bonhôte *et al.*^{6a} and Srinivas *et al.*¹⁴

Synthesis of [Me₂Im]TfO

Using scCO_2 as reaction medium and with the same procedures as above, we also synthesized [Me₂Im]TfO from methylimidazole and methyl trifluoromethanesulfonate at $32.0\text{ }^\circ\text{C}$ and 10.0 MPa . The same as the synthesis of [bmim]Br, the reaction system was homogenous at the beginning of the reaction. The IL synthesized was characterized by $^1\text{H-NMR}$, and the spectrum of the IL obtained with a reaction time of 2 h is shown in Fig. 6, which is consistent with that reported in the literature.^{6a} The FT-IR spectrum of the IL determined in this work is shown in Fig. 7. It further confirms that the product is [Me₂Im]TfO. The dependence of the yield on reaction time is shown in Fig. 8. It demonstrates

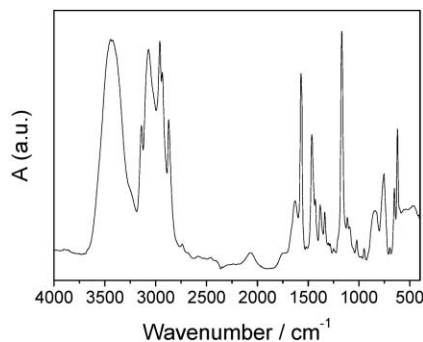


Fig. 5 FT-IR spectrum of [bmim]Br.

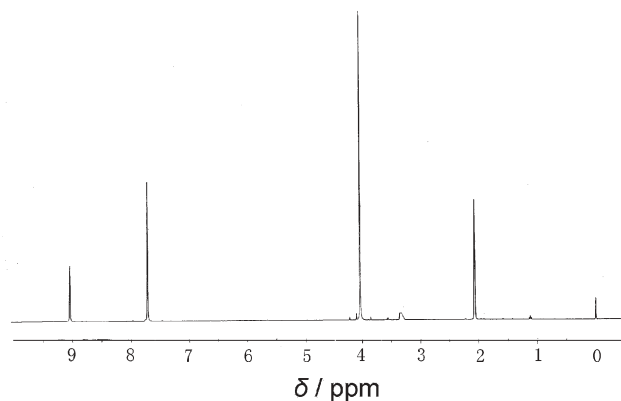


Fig. 6 $^1\text{H-NMR}$ spectrum of [Me₂Im]TfO synthesized at $32.0\text{ }^\circ\text{C}$ and 10.0 MPa with a reaction time of 2 h (acetone-d, δ/ppm relative to TMS).

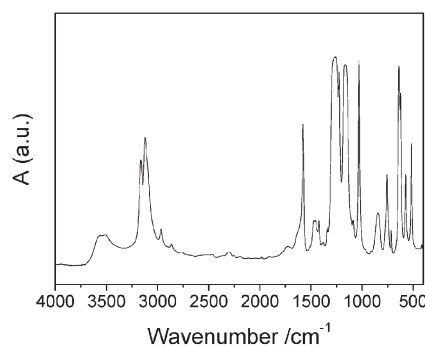


Fig. 7 FT-IR spectrum of [Me₂Im]TfO synthesized at $32.0\text{ }^\circ\text{C}$ and 10.0 MPa with a reaction time of 2 h.

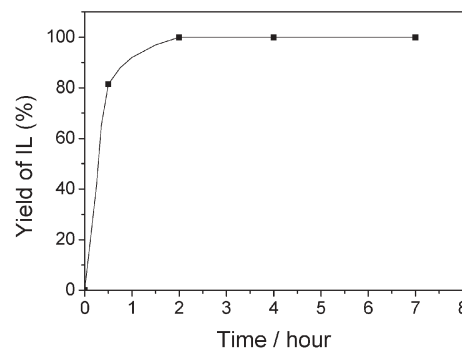


Fig. 8 Effect of reaction time on the yield for the synthesis of [Me₂Im]TfO in scCO_2 at 10.0 MPa and $32.0\text{ }^\circ\text{C}$. The initial concentrations of methylimidazole and methyl trifluoromethanesulfonate are 0.262 mol L^{-1} and 0.293 mol L^{-1} , respectively.

that a yield of 100% was reached after a reaction time of 2 h. This method has the same advantages as synthesizing [bmim]Br.

Conclusions

ILs, [bmim]Br and [Me₂Im]TfO, can be synthesized in scCO_2 , and the yields can reach 100%. The products and the excess reactant added can be separated *in situ* by scCO_2 extraction without any cross-contamination. The whole process is green and simple with high efficiency. We believe this green and effective route can be

used to synthesize many other ILs with similar features. These advantages are highly favorable for producing large amount of ILs without waste and with minimum pollution.

Acknowledgements

This work was financially supported by the National Natural Science Foundation of China (20473105, 20332030) and the National Key Basic Research Project of China (G2000048010).

References

- 1 J. F. Brennecke and E. J. Maginn, *AIChE J.*, 2001, **47**, 2384–2389.
- 2 (a) R. D. Rogers and K. R. Seddon, *Science*, 2003, **302**, 792–793; (b) P. Wasserscheid and W. Keim, *Angew. Chem. Int. Ed.*, 2000, **39**, 3772–3789; (c) J. Dupont, R. F. de Souza and P. A. Z. Suarez, *Chem. Rev.*, 2002, **102**, 3667–3691.
- 3 (a) E. D. Bates, R. D. Mayton, I. Ntai and J. H. Davis, Jr., *J. Am. Chem. Soc.*, 2002, **124**, 926–927; (b) W. Z. Wu, B. X. Han, H. X. Gao, Z. M. Liu, T. Jiang and J. Huang, *Angew. Chem. Int. Ed.*, 2004, **43**, 2415–2417; (c) K. R. Seddon, A. Stark and M. J. Torres, *Pure Appl. Chem.*, 2000, **72**, 2275–2287.
- 4 (a) D. J. Cole-Hamilton, *Science*, 2003, **299**, 1702–1706; M. J. Earle, P. B. McCormac and K. R. Sedden, *Chem. Commun.*, 1998, 2245–2246; (b) T. Welton, *Chem. Rev.*, 1999, **99**, 2071–2084; (c) C. Baudequin, J. Baudoux, J. Levillain, D. Cahard, A. C. Gaumont and J. C. Plaquevent, *Tetrahedron Asymm.*, 2003, **14**, 3081–3093.
- 5 E. R. Cooper, C. D. Andrews, P. S. Wheatley, P. B. Webb, P. Wormald and R. E. Morris, *Nature*, 2004, **430**, 1012–1016.
- 6 (a) P. Bonhôte, A. P. Dias, N. Papageorgiou, K. Kalyanasundaram and M. Grätzel, *Inorg. Chem.*, 1996, **35**, 1168–1178; (b) J. S. Wilkes, J. A. Levisky, R. A. Wilson and C. L. Hussey, *Inorg. Chem.*, 1982, **21**, 1263–1264; (c) J. G. Huddleston, H. D. Willauer, R. P. Swatloski, A. E. Visser and R. D. Rogers, *Chem. Commun.*, 1998, 1765–1766; (d) J. D. Holbrey, W. M. Reichert, R. P. Swatloski, G. A. Broker, W. R. Pitner, K. R. Seddon and R. D. Rogers, *Green Chem.*, 2002, **4**, 407–413.
- 7 M. Poliakoff, J. M. Fitzpatrick, T. R. Farren and P. T. Anastas, *Science*, 2002, **297**, 807–810.
- 8 K. Zosel, *Angew. Chem. Int. Ed.*, 1978, **17**, 702–709.
- 9 (a) J. A. Darr and M. Poliakoff, *Chem. Rev.*, 1999, **99**, 495–542; (b) W. Leitner, *Acc. Chem. Res.*, 2002, **35**, 746–756.
- 10 (a) K. P. Johnston and P. S. Shah, *Science*, 2004, **303**, 482–483; (b) R. A. Pai, R. Humayun, M. T. Schulberg, A. Sengupta, J. N. Sun and J. J. Watkins, *Science*, 2004, **303**, 507–510.
- 11 (a) L. A. Blanchard, D. Hancu, E. J. Bechman and J. F. Brennecke, *Nature*, 1999, **399**, 28–29; (b) L. A. Blanchard, Z. Gu and J. F. Brennecke, *J. Phys. Chem. B*, 2001, **105**, 2437–2444.
- 12 L. A. Blanchard and J. F. Brennecke, *Ind. Eng. Chem. Res.*, 2001, **40**, 287–292.
- 13 (a) S. V. Dzyuba and R. A. Bartsch, *Angew. Chem. Int. Ed.*, 2003, **42**, 148–150; (b) P. B. Webb, M. F. Sellin, T. E. Kunene, S. Williamson, A. M. Z. Slawin and D. J. Cole-Hamilton, *J. Am. Chem. Soc.*, 2003, **125**, 15577–15588; (c) V. Najdanovic-Visak, A. Serbanovic, J. M. S. S. Esperanca, H. J. R. Guedes, L. P. N. Rebelo and M. Nunes da Ponte, *Chem. Phys. Chem.*, 2003, **4**, 520–522.
- 14 K. A. Srinivas, A. Kumar and S. M. S. Chauhan, *Chem. Commun.*, 2002, 2456–2457.
- 15 Z. S. Hou, B. X. Han, X. G. Zhang, H. F. Zhang and Z. M. Liu, *J. Phys. Chem. B*, 2001, **105**, 4510–4513.
- 16 W. Z. Wu, J. M. Zhang, B. X. Han, J. W. Chen, Z. M. Liu, T. Jiang, J. He and W. J. Li, *Chem. Commun.*, 2003, 1412–1413.
- 17 C. P. Fredlake, J. M. Crosthwaite, D. G. Hert, S. N. V. K. Aki and J. F. Brennecke, *J. Chem. Eng. Data*, 2004, **49**, 954–964.

O-Acylation of cellulose and monosaccharides using a zinc based ionic liquid†

Andrew P. Abbott,^a Thomas J. Bell,^a Sandeep Handa*^a and Barry Stoddart^b

Received 16th August 2005, Accepted 18th August 2005

First published as an Advance Article on the web 5th September 2005

DOI: 10.1039/b511691k

The efficient *O*-acylation of monosaccharides and cellulose is demonstrated using a Lewis acidic ionic liquid based on choline chloride and zinc chloride.

Introduction

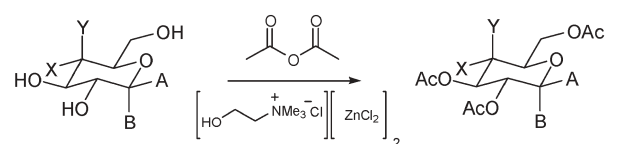
The application of ionic liquids as environmentally benign reaction solvents for synthesis and catalysis has received extensive recent attention.^{1–4} In this regard we have developed ionic liquids based on the cheap and readily available components choline chloride (ChCl; HOCH₂CH₂N(Me)₃·Cl) and zinc chloride as alternatives to the more commonly employed alkyl imidazolium-aluminium chloride mixtures.⁵ In an analogous manner to the chloroaluminate systems, we have shown that these zinc based liquids form complex anions of the form ZnCl₃[−] and Zn₂Cl₅[−]. Although these species are less Lewis acidic than their aluminium counterparts the ChCl–ZnCl₂ ionic liquids are water insensitive and zinc is environmentally more benign. These Lewis acidic solvents have been successfully employed for a variety of reactions including Diels–Alder, Fisher indole synthesis and polymerisations.^{6,7} In this current study we report that *O*-acylation of sugars and cellulose can effectively be carried out using chlorozincate ionic liquids.

The *O*-acylation of carbohydrates is widely employed not only for the protection of hydroxy groups but also for the purification and structural elucidation of natural products. Per-*O*-acylation is most frequently achieved using excess acetic anhydride together with a wide variety of catalysts including, amongst others, pyridine⁸ (and its derivatives),⁹ sodium acetate,¹⁰ FeCl₃,¹¹ metal triflates,¹² and ZnCl₂.¹⁰ The reaction has also been carried out in ionic liquids although only imidazolium based salts have been employed to date. Thus, the acetylation of carbohydrates has been demonstrated in imidazolium systems containing dicyanamide¹³ or benzoate¹⁴ anions and in both cases the ionic liquid acted as both solvent and catalyst for the reaction. In addition ionic liquids have also recently been employed as media for the enzymatic acylation of glycosides.¹⁵

Results and discussion

To test the efficacy of Lewis acidic ChCl-based mixtures for the acetylation of carbohydrates the compounds **1–4** were reacted with acetic anhydride in the ionic liquid for 3 h at 90 °C (Scheme 1).† Substrates **1–4** were completely soluble under the reaction conditions and the mixtures were worked up by the addition of water followed by extraction with ethyl acetate to give in each case only the per-*O*-acetylated product **1a–4a**. Table 1 summarises the results of these reactions. It can be seen (entries 1–4) that the [ChCl][ZnCl₂]₂ ionic liquid can be successfully employed as both solvent and catalyst for the acetylation of simple monosaccharides. The yields for these conversions are remarkable considering the potential side reaction involving acetylation of choline (present in *ca.* 20 mole equivalents to the substrate). In fact reaction of **1** using an acetylcholine chloride (AcChCl)–zinc chloride mixture (entry 5) gave a similar yield of **1a** suggesting that the potential side reaction does not significantly affect the process. The reaction is also successful with the less Lewis acidic [ChCl][SnCl₂]₂ ionic liquid (entry 6) albeit with a slightly reduced yield. However, a eutectic mixture of [ChCl][Urea]₂ (which forms an ionic liquid analogue but has no Lewis acidity)¹⁶ gave no significant reaction (entry 7). In addition to acetylation the [ChCl][ZnCl₂]₂ system also supported reaction of **1** with propionic and isobutyric anhydrides to give, under the same reaction conditions, only the corresponding per-*O*-acylated products in 65% and 33% yield respectively (unoptimised yields, data not shown).

The most intriguing result is from the reaction of **1** with only 1 equivalent of acetic anhydride (entry 8). The *only* product isolated from this reaction was **1a** (96% yield based on Ac₂O) with no evidence for any partially acetylated intermediates. This result compares favorably with our observations for the reaction of **1** with 1 equivalent of acetic anhydride under conventional conditions in either pyridine (giving a complex mixture of partially acetylated intermediates) or ZnCl₂ in THF (giving predominately **1a** together with significant amounts (*ca.* 20–30%) of partially



- 1: X=OH, Y=H; A=H, B=OMe
 2: X=H, Y=OH; A=H, B=OMe
 3: X=H, Y=OH; A=OMe, B=H
 4: X=OH, Y=H; A=H, B=OH

- 1a: X=OAc, Y=H; A=H, B=OMe
 2a: X=H, Y=OAc; A=H, B=OMe
 3a: X=H, Y=OAc; A=OMe, B=H
 4a: X=OAc, Y=H; A, B = H, OAc

Scheme 1 Acetylation of monosaccharides in ChCl-based ionic liquids.

^aDepartment of Chemistry, University of Leicester, Leicester, UK LE1 7RH. E-mail: s.handa@le.ac.uk; Fax: +44 (0)116 252 3789; Tel: +44 (0)116 252 2128

^bP&G Technical Centres, Whitley Road, Longbenton, Newcastle Upon Tyne, UK NE12 9TS

† Electronic supplementary information (ESI) available: Experimental procedures and IR calibration plot. See <http://dx.doi.org/10.1039/b511691k>

Table 1 Acetylation reactions of monosaccharides in ChCl-based ionic liquids at 90 °C for 3 h

Entry	Substrate	Solvent	Ac ₂ O (eq.)	Yield (%) ^a
1	1	[ChCl][ZnCl ₂] ₂	5	78
2	2	[ChCl][ZnCl ₂] ₂	5	81
3	3	[ChCl][ZnCl ₂] ₂	5	78
4	4	[ChCl][ZnCl ₂] ₂	5	79 ^b
5	1	[AcChCl][ZnCl ₂] ₂	5	66
6	1	[ChCl][SnCl ₂] ₂	5	68
7	1	[ChCl][urea] ₂	5	<5
8	1	[ChCl][ZnCl ₂] ₂	1	96 ^c

^a Isolated yield of per-*O*-acetylated product. ^b 3 : 1 mixture of α : β anomers. ^c Yield based on Ac₂O.

acetylated intermediates). The reason(s) for the selective formation of only **1a** in the ionic liquid is not entirely clear. However, this novel finding is also observed in the reaction of **1** with 1 mole equivalent of propionic and isobutyric anhydrides (giving only per-acetylated products in 88 and 68% respectively (based on anhydride)) and we believe that this may prove an effective method for producing per-acetylated derivatives from synthetically or commercially valuable anhydrides.

In seeking to explore the potential environmental benefits of our system we next examined solvent recycling. Recovery of the solvent from the acetylation reactions was possible by employing a non-aqueous work up (involving simple extraction of the [ChCl][ZnCl₂]₂ with ethyl acetate) followed by removal of any volatiles (presumably acetic acid) from the ionic liquid *in vacuo*. Pleasingly ionic liquid recovered in this way could be employed for the repeated acetylation of **1** without any reduction in the reaction yield (run 1—72%, run 2—67%, run 3—71%, run 4—72%). However, it should be noted that failure to remove volatiles from the recovered ionic liquid led to an appreciable decrease in the yields for subsequent reactions. Significantly the ionic liquid could also be re-used for different reactions with very low levels of cross contamination. Thus **4** was converted to **4a** (75%, 3 : 1 mixture of α : β anomers) and the recovered ionic liquid was subsequently used for the acetylation of **1** to give the product **1a** in good yield (80%) and with <1% (by ¹H NMR) contamination by **4a**. This finding appreciably increases the potential scope for these ionic liquid reactions.

Having successfully demonstrated the acylation of monosaccharides we turned our attention to the acetylation of cellulose using the [ChCl][ZnCl₂]₂ ionic liquid. Cellulose is traditionally acetylated using acetic anhydride, acetic acid and a sulfuric acid catalyst. The process gives a product in which all three OH groups are acetylated and which has relatively poor mechanical properties. Of more importance is the diacetate (generally termed cellulose acetate) which is obtained from the partial hydrolysis of the triacetate. Acetic anhydride and zinc chloride have also been used for the acetylation of cellulose, both neat and with a variety of solvents but this also gives exclusively the triacetylated product.¹⁷ Rogers and colleagues recently showed that cellulose was partially soluble in a variety of allylimidazolium based ionic liquids and that those containing strong hydrogen bond acceptors (*e.g.* Cl⁻) were the most effective solvents especially when combined with microwave heating.¹⁸ Subsequent studies suggest that the polymer is disordered in these solutions.¹⁹ The first example of the acetylation of cellulose in an ionic liquid has recently been

reported by Zhang and co-workers.²⁰ The authors employed a novel allylimidazolium based ionic liquid and intriguingly the process was reported to occur under homogeneous conditions and in the absence of any catalyst. Cellulose acetates having a degree of substitution (DS) value of between 0.64–2.74 (corresponding to 21–91% acetylation) were produced using this system.

Using microwave heating as reported by Rogers we found that microcrystalline cellulose (*ex. Sigma-Aldrich, DP ca. 200*) was slightly soluble (<3 wt%) in [ChCl][ZnCl₂]₂. However, microwave conditions were not required for acetylation reactions which were carried out with 100 mg of cellulose in 3 ml of ionic liquid for 3 h at 90 °C (traditional heating) and with varying equivalents of acetic anhydride. At the end of the experiments water was added to the reaction mixture, precipitating the product which was centrifuged, filtered, washed with water and freeze dried. The resulting samples were initially analysed using infrared spectroscopy and the degree of acetylation estimated from the ratio of peak areas in the regions 3000–3500 (OH) and 1730–1750 (C=O) wavenumber and comparison to a calibration plot for different cellulose and cellulose acetate standard mixtures (see ESI†). Table 2 shows a clear trend in that the degree of acetylation increases with the mole equivalents of acetic anhydride.

The functionalisation seen in these experiments could be due to per-acetylation of a fraction of the polymer chains or partial acetylation of all the chains. Since low molecular weight cellulose triacetate is soluble in acetone the samples were extracted with this solvent and only a small fraction was found to be soluble (*ca.* 1–10 wt%). IR analysis of this soluble material showed negligible absorbance at 3000–3500 cm⁻¹ confirming it to be the triacetate and gel permeation chromatography (GPC) indicated a *M_n* of between 2470–2580. We assume that this small amount of low molecular weight polymer is either present in the starting cellulose and/or is produced by glycoside hydrolysis under the reaction conditions. If the low molecular weight material is fully soluble in the ionic liquid then the per-acetylation is in accordance with the results seen with the monosaccharides described above.

The vast majority (>90 wt%) of the material isolated from the acetylation reactions was insoluble in acetone. IR analysis of this insoluble fraction indicated that a significant proportion was acetylated and that the degree of acetylation increased with the equivalents of acetic anhydride used (Table 2). This finding raises the possibility of controlled synthesis of partially substituted cellulose acetates. The greater degree of functionalisation observed on increasing the equivalents of acetic anhydride is similar to the results reported by Zhang with their allylimidazolium based ionic liquid.²⁰ However, it should be noted that these authors observed an unexplained drop in functionalisation when >6.5 equivalents of acetic anhydride were employed whereas the system reported here

Table 2 Acetylation of OH groups on cellulose with various mole equivalents of acetic anhydride in [ChCl][ZnCl₂]₂ at 90 °C for 3 h

Entry	Ac ₂ O (eq.)	Acetylated groups (%) ^{a,b}	Acetylated groups (%) ^{a,c}
1	1	15	14
2	7.5	17	14
3	10	26	21
4	20	47	31

^a Estimated by IR analysis. ^b Analysis of total isolated material. ^c Analysis of acetone insoluble fraction.

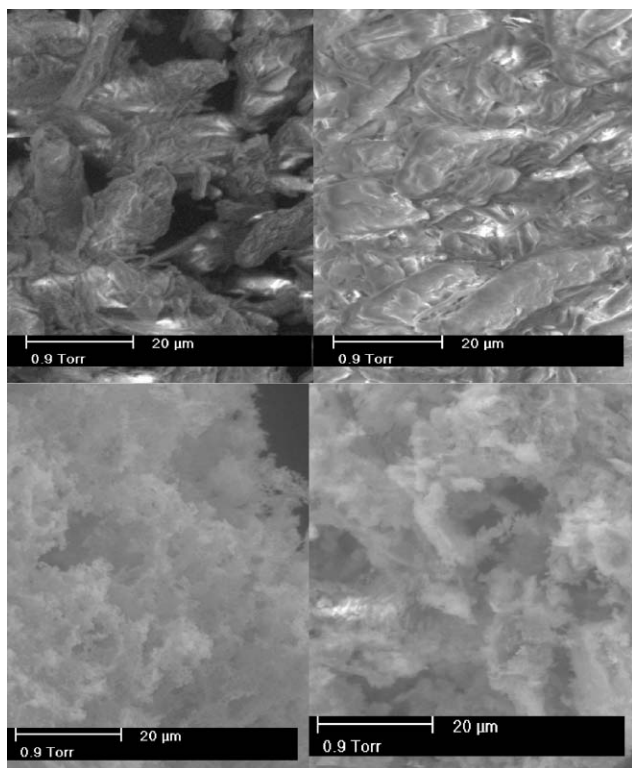


Fig. 1 SEM images of cellulose (top left), partially acetylated cellulose (top right), cellulose after dissolution in ionic liquid and regeneration with water (bottom left) and acetone soluble cellulose triacetate (bottom right).

shows increasing levels of derivatisation up to 20 equivalents of acetic anhydride used. Additionally, our $[\text{ChCl}][\text{ZnCl}_2]$ system also allows access to cellulose acetate having low levels of functionalisation (*i.e.* <20% acetylation).

Assuming that the hydroxyl groups can only react if they are wetted by the ionic liquid then this must involve significant restructuring of the polymer. Fig. 1 shows scanning electron microscopy (SEM) images of starting cellulose, partially acetylated cellulose, cellulose that has been dissolved in the ionic liquid and regenerated by the addition of water and low molecular weight cellulose triacetate. It can be seen that dissolution of the cellulose in the ionic liquid gives material having a homogeneous morphology which is consistent with the results of Rogers¹⁸ who found that the structure of cellulose was opened upon contact with the imidazolium based ionic liquids. The partially acetylated sample (top right) has a structure that is intermediary between crystalline starting cellulose and amorphous regenerated material suggesting

that only a small fraction of the polymer chains have been opened up by the ionic liquid.

Conclusion

In summary this work has shown that ionic liquids based on ZnCl_2 and ChCl are effective at carrying out *O*-acetylation reactions on a number of monosaccharides and cellulose. Per-*O*-acetylation is exclusively observed with monosaccharides and for low molecular weight polymer. Partial acetylation of cellulose is also possible with some control over the degree of modification.

Acknowledgements

The authors would like to acknowledge EPSRC (GR/R 39771), the Crystal Faraday Partnership and Procter and Gamble for funding this work.

References

- 1 P. Wasserscheid and T. Welton, *Ionic Liquids in Synthesis*, Wiley-VCH Verlag, Weinheim, Germany, 2003.
- 2 T. Welton, *Coord. Chem. Rev.*, 2004, **248**, 2459.
- 3 T. Welton, *Chem. Rev.*, 1999, **99**, 2071.
- 4 P. Wasserscheid and W. Keim, *Angew. Chem. Int. Ed.*, 2000, **39**, 3772.
- 5 A. P. Abbott, G. Capper, D. L. Davies and R. K. Rasheed, *Inorg. Chem.*, 2004, **43**, 3447.
- 6 A. P. Abbott, G. Capper, D. L. Davies, R. Rasheed and V. Tambyrajah, *Green Chem.*, 2002, **4**, 24.
- 7 R. C. Morales, V. Tambyrajah, P. R. Jenkins, D. L. Davies and A. P. Abbott, *Chem. Commun.*, 2004, 158.
- 8 H. H. Schulubach and K. Repenning, *Angew. Chem.*, 1959, **71**, 193.
- 9 G. Hoeffle and W. Steglich, *Synthesis*, 1972, 619.
- 10 A. I. Vogel, *Vogel's Textbook of Practical Organic Chemistry*, Wiley, New York, 5th edn, 1989, p. 644.
- 11 F. Dasgupta, P. P. Singh and H. C. Srivastava, *Carbohydr. Res.*, 1980, **80**, 346.
- 12 C-A. Tai, S. S. Kulkarni and S-C. Hung, *J. Org. Chem.*, 2003, **68**, 8719.
- 13 S. A. Forsyth, D. R. MacFarlane, R. J. Thomson and M. von Itzstein, *Chem. Commun.*, 2002, 714.
- 14 S. Murugasen, N. Karst, T. Islam, J. M. Weincek and R. J. Linhardt, *Synlett*, 2003, 1283.
- 15 M-J. Kim, M. Y. Choi, J. K. Lee and Y. Ahn, *J. Mol. Catal. B*, 2003, **26**, 115.
- 16 A. P. Abbott, G. Capper, D. L. Davies, R. Rasheed and V. Tambyrajah, *Chem. Commun.*, 2003, 70.
- 17 B. Philipp, B. Lukanoff, H. Schleicher and W. Wagenknecht, *Z. Chem.*, 1986, **26**, 50.
- 18 R. P. Swatloski, S. K. Spear, J. D. Holbrey and R. D. Rogers, *J. Am. Chem. Soc.*, 2002, **124**, 4974.
- 19 J. S. Moulthrop, R. P. Swatloski, G. Moyna and R. D. Rogers, *Chem. Commun.*, 2005, 1557.
- 20 J. Wu, J. Zhang, H. Zhang, J. He, Q. Ren and M. Guo, *Biomacromolecules*, 2004, **5**, 266.

Tertiary amines as highly efficient catalysts in the ring-opening reactions of epoxides with amines or thiols in H₂O: expeditious approach to β -amino alcohols and β -aminothioethers

Jie Wu*^{ab} and Hong-Guang Xia^a

Received 30th June 2005, Accepted 19th August 2005

First published as an Advance Article on the web 31st August 2005

DOI: 10.1039/b509288d

Ring-opening of epoxides with various amines or thiols catalyzed by DABCO (1,4-diazabicyclo[2,2,2]octane) or Et₃N (1 mol%) in water afforded the corresponding products in good to excellent yields under mild reaction conditions.

Interest in the field of organocatalysis has increased spectacularly in the last few years as a result of both the novelty of the concept and, more importantly, the fact that the efficiency and selectivity of many organocatalytic reactions meet the standards of established organic reactions. The diverse examples show that in recent years organocatalysis has developed within organic chemistry into its own subdiscipline, whose ‘‘Golden Age’’ has already dawned.¹ The pinpointing of ‘‘privileged’’ catalyst classes (such as L-proline in aldol and Mannich reactions) showing general superiority for many reaction types is undoubtedly one of the most intriguing aspects and may have a considerable impact on the development of new catalytic systems.^{2,3} Catalysts of the same class may promote similar reactions or less closely related reactions. For example, chiral thiourea derivatives and their analogues catalyze the hydrocyanation of imines (Strecker reaction) as well as asymmetric Mannich reactions.⁴ Tertiary amines are another example of a privileged catalyst class. They are able to mediate an astonishingly wide variety of transformations.^{5,6} For instance, DABCO (1,4-diazabicyclo[2,2,2]octane) and its analogues show high efficiency in Morita–Baylis–Hillman reactions⁶ as well as cyanation of ketones.⁷ Recently, we found that tertiary amines are also efficient as catalysts in the ring-opening reactions of epoxides with amines or thiols in water, which is disclosed herein.

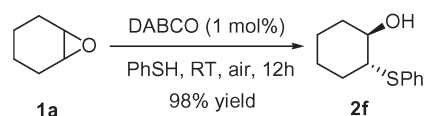
Ring-opening reactions of epoxides with nucleophiles provide a useful protocol in organic synthesis, and many reagents have been developed to realize the opening of the epoxide ring.⁸ However, most of these suffered from the fact that a Lewis acid or strong base was necessary to effect the reaction. Only a few examples were reported by employing small organic molecules as catalyst. Recently, Fan and Hou developed nonmetallic catalyzed ring-opening reactions of epoxides with nucleophiles by utilizing tributylphosphine as catalyst, which opens the way to a variety of 1,2-bifunctional products.⁹ However, the catalyst, Bu₃P, is not stable and easily oxidized in the air. Furthermore, a high loading catalyst (at least 10%) had to be utilized in order to achieve the

respective yields. The yield and rate was dramatically decreased if catalyst loading was reduced.^{9b}

In view of the stability and nucleophilic similarity, DABCO should be a very attractive alternative due to its unique characteristics. Initial studies were performed by using DABCO (5 mol%) as catalyst in the reaction of compound **1a** with thiophenol in different solvents (THF, toluene, MeCN, CH₂Cl₂, DMF, H₂O) at room temperature. To our delight, we observed the formation of the corresponding product **2f**. Complete conversion and 98% isolated yield was obtained after 12 h when the reaction was performed *in water* (only 15% yield of **2f** was afforded in the absence of catalyst). It is interesting since water is environmentally benign and potential advantages of using water as a solvent are its low cost, safety, and ease of use. Further studies showed that the catalyst loading of 1 mol% was substantially efficient for this reaction (12 h, RT, 98% yield) and the reaction could be adequately carried out in the air with the same excellent yield (Scheme 1). The *anti*-stereochemistry of the product **2f** was confirmed by the coupling constant for two cyclic methine hydrogens at the *trans*-positions.¹⁰

Further studies show Et₃N (1 mol%) was also highly efficient in this reaction (98% yield, 12 h, RT) after screening a series of tertiary amines. Furthermore, it was found that aniline was also a good nucleophile for the reaction of **1a** described above (DABCO: 64% yield; Et₃N: 93% yield; without catalyst: 25% yield). To demonstrate the generality of this method, we next investigated the scope of this reaction and the results are summarized in Table 1. The operation is simple: nucleophile amine or thiol (1.1 equiv.) was added to a solution of epoxide **1** (0.25 mmol) and DABCO (Method A) or Et₃N (Method B) (1 mol%) in water (2.0 mL) under air. The reaction mixture was stirred at room temperature and was separated directly by a flash chromatography column (silica gel) to afford the corresponding product after the reaction was completed as monitored by TLC.

The conditions have proved to be useful for coupling a range of epoxides **1** with an array of amines and thiols (Table 1). For reactions of compounds **1a–e**, various thiophenols and anilines are suitable substrates. The reactions were very clean and the desired products were afforded in good to excellent isolated yields.



Scheme 1

^aDepartment of Chemistry, Fudan University, 220 Handan Road, Shanghai, 200433, P. R. China. E-mail: jie_wu@fudan.edu.cn; Fax: +86 21 6510 2412; Tel: +86 21 5566 4619

^bState Key Laboratory of Organometallic Chemistry, Shanghai Institute of Organic Chemistry, Chinese Academy of Sciences, 354 Fenglin Road, Shanghai, 200032, P. R. China

Table 1 Ring-opening reactions of epoxides with amines or thiols in water catalysed by DABCO or Et₃N (1 mol%)

NuH: amines or thiols

Entry	Epoxide	NuH	Product	Yield (%) ^a		
				A ^b	B ^c	C ^d
1		C ₆ H ₅ NH ₂	2a	64	93	25
2	—	C ₆ H ₅ NH ₂	2a	96 ^e	—	—
3	—	4-OMe-C ₆ H ₄ NH ₂	2b	92 ^e	96	—
4	—	4-Cl-C ₆ H ₄ NH ₂	2c	14	68	—
5	—	BnNH ₂	2d	68	53	39
6	—	^t PrNH ₂	2e	—	—	—
7	—	C ₆ H ₅ SH	2f	98	98	15
8	—	4-OMe-C ₆ H ₄ SH	2g	98	99	—
9	—	4-Cl-C ₆ H ₄ SH	2h	92	96	—
10	—	BnSH	2i	53	61	—
11	—	^t BuSH	2j	—	—	—
12		C ₆ H ₅ NH ₂	2k	53	88	26
13	—	C ₆ H ₅ SH	2l	91	96	16
14		C ₆ H ₅ NH ₂	2m	98	98	—
15	—	C ₆ H ₅ SH	2n	98	98	—
16		C ₆ H ₅ NH ₂	2o	92	93	—
17	—	C ₆ H ₅ SH	2p	96	96	—
18		C ₆ H ₅ NH ₂	2q/3q (R ¹ = H, R ² = Ph)	93 (94/6)	91 (93/7)	—
19	—	C ₆ H ₅ SH	2r/3r (R ¹ = H, R ² = Ph)	98 (85/15)	98 (75/25)	41(80/20)

^a Isolated yields. ^b DABCO (1 mol%) as catalyst. ^c Et₃N (1 mol%) as catalyst. ^d Without catalyst. ^e The reaction was performed at 40 °C.

However, aromatic nucleophiles had higher reactivity than aliphatic ones. For example, DABCO-catalyzed reaction of **1a** with benzyl mercaptan afforded the corresponding product in 53% yield, and only trace amounts of product were detected when BuSH was employed as the nucleophile. In the case of unsymmetrically substituted epoxides **1c** and **1d**, complete regioselectivity with the attack of nucleophile on the less substituted epoxide carbon was observed. For the substrate **1e**, it is reasonable that regioselectivity is not as specific as others since the benzyl position of epoxide **1e** is more positive and easy to be attacked by nucleophiles. Although the mechanism of the observed rate enhancements by using water as solvent is not clear, a hydrophobic effect may play a role in accelerating this reaction.¹¹

In summary, we have discovered DABCO or Et₃N is an efficient catalyst in the reactions of epoxides with amines or thiols, which provides a general and convenient way to prepare a variety of β-amino alcohol and β-aminothioethers. The advantages of this

method include good substrate generality, low catalyst loading, the use of air-stable, inexpensive DABCO or Et₃N as catalyst in water under mild conditions, which offers the potential of being both economical and environmentally benign, and experimental operational ease. Mechanistic studies and desymmetrization of *meso*-epoxides with various nucleophiles by using chiral tertiary amines as catalysts are under investigation in our laboratory.†

Acknowledgements

Financial support from Fudan University is gratefully acknowledged.

Notes and references

† General procedure: nucleophile amine or thiol (1.1 equiv.) was added to a solution of epoxide **1** (0.25 mmol) and DABCO (Method A) or Et₃N (Method B) (1 mol%) in water (2.0 mL) under air. The reaction mixture

was stirred at room temperature. After the reaction was completed as monitored by TLC, the mixture was separated directly using a flash chromatography column (silica gel) to afford the corresponding product. (All the products are known compounds. The characterizations of these compounds are identical with the literature reports.)

- 1 P. I. Dalko and L. Moisan, *Angew. Chem., Int. Ed.*, 2004, **43**, 5138.
- 2 T. P. Yoon and E. N. Jacobsen, *Science*, 2003, **299**, 1691.
- 3 The term was coined in analogy with pharmaceutical compound classes that are active against a number of different biological targets.
- 4 (a) M. S. Sigman and E. N. Jacobsen, *J. Am. Chem. Soc.*, 1998, **120**, 4901; (b) M. S. Sigman, P. Vachal and E. N. Jacobsen, *Angew. Chem., Int. Ed.*, 2000, **39**, 1279; (c) P. Vachal and E. N. Jacobsen, *J. Am. Chem. Soc.*, 2002, **124**, 10012; (d) P. Vachal and E. N. Jacobsen, *Org. Lett.*, 2000, **2**, 867; (e) J. T. Su, P. Vachal and E. N. Jacobsen, *Adv. Synth. Catal.*, 2001, **343**, 197; (f) A. G. Wenzel and E. N. Jacobsen, *J. Am. Chem. Soc.*, 2001, **124**, 12964; (g) A. G. Wenzel, M. P. Lalonde and E. N. Jacobsen, *Synlett*, 2003, 1919; (h) G. D. Joly and E. N. Jacobsen, *J. Am. Chem. Soc.*, 2004, **126**, 4102; (i) M. S. Taylor and E. N. Jacobsen, *J. Am. Chem. Soc.*, 2004, **126**, 10558.
- 5 S.-K. Tian, Y. Chen, J. Hang, L. Tang, P. McDaid and L. Deng, *Acc. Chem. Res.*, 2004, **37**, 621.
- 6 D. Basavaiah, A. J. Rao and T. Satyanarayana, *Chem. Rev.*, 2003, **103**, 811.
- 7 S.-K. Tian, R. Hong and L. Deng, *J. Am. Chem. Soc.*, 2003, **125**, 9900.
- 8 For reactions of epoxides, see reviews: (a) G. Pattenden, in *Comprehensive Organic Synthesis*, ed. B. M. Trost and I. Fleming, Pergamon, Oxford, UK, 1991, vol. 3, p. 223; (b) D. M. Hodgson, A. R. Gibbs and G. P. Lee, *Tetrahedron*, 1996, **52**, 14361; (c) E. N. Jacobsen and M. H. Wu, in *Comprehensive Asymmetric Catalysis*, ed. E. N. Jacobsen, A. Pfaltz and H. Yamamoto, Springer, New York, 1999; (d) M. C. Willis, *J. Chem. Soc., Perkin. Trans. 1*, 1999, 1765.
- 9 (a) R.-H. Fan and X.-L. Hou, *J. Org. Chem.*, 2003, **68**, 726; (b) R.-H. Fan, PhD Thesis, Shanghai Institute of Organic Chemistry, Chinese Academy of Sciences, 2003.
- 10 G. Sekar and V. K. Singh, *J. Org. Chem.*, 1999, **64**, 2537 and references cited therein.
- 11 C. J. Li and T. H. Chang, *Organic Reactions in Aqueous Media*, Wiley, New York, 1997.

Water-solvent method for tosylation and mesylation of primary alcohols promoted by KOH and catalytic amines

Jun-ichi Morita, Hidefumi Nakatsuji, Tomonori Misaki and Yoo Tanabe*

Received 15th April 2005, Accepted 11th August 2005

First published as an Advance Article on the web 26th August 2005

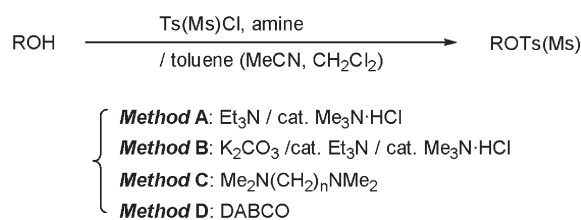
DOI: 10.1039/b505345e

We have developed an efficient water-solvent method for *p*-toluenesulfonylation (tosylation) and methanesulfonylation (mesylation) of primary alcohols using *p*-toluenesulfonyl chloride and methanesulfonyl chloride, respectively, promoted by KOH and catalytic amines. The reaction was performed by maintaining the pH at around 10 using a pH controller to prevent the undesirable decomposition of sulfonyl chlorides. Several primary alcohols were smoothly sulfonylated in excellent yield. The choice of the amine catalyst (0.1 equiv.) was important: *N,N*-dimethylbenzylamine, a sterically unhindered and lipophilic tertiary amine, was effective for the tosylation, whereas *N,N*-dimethylbutylamine and triethylamine were effective for the mesylation. The present Schotten–Baumann-type method is the first example of catalytic sulfonylation using sulfonyl chlorides, and is a green chemical process due to the use of water as the solvent.

Introduction

The *p*-toluenesulfonylation (tosylation) and methanesulfonylation (mesylation) of alcohols are well recognized as fundamental processes in various fields of organic syntheses.¹ Traditional tosylation using TsCl/Py (Ts = *p*-toluenesulfonyl, Py = pyridine) reagent requires over *ca.* 10 equiv. of pyridine and careful conditions to prevent undesirable side substitution from ROTs to RCl. The pyridine-free method^{2,3} is a useful alternative to sulfonylation to resolve these problems (Scheme 1). This protocol has been utilized for the syntheses of complex natural products and fine chemicals both on laboratory and industrial scales; for example, (+)-vinblastine (Fukuyama, Tokuyama and coworkers),⁴ fluorescence amino acid derivatives (Nau and coworkers),⁵ and flumioxadine (Sumitomo Chemical group).⁶ We extended this protocol to develop effective methods for the esterification, thioesterification and amide formation.⁷

Organic reactions in water solvent has recently attracted much attention from the standpoint of green chemistry.⁸ We report herein an effective Schotten–Baumann-type method⁹ for the tosylation and mesylation of alcohols in water solvent utilizing catalytic amines.



Scheme 1 Pyridine-free sulfonylation of alcohols in organic solvents.

Department of Chemistry, School of Science and Technology, Kwansai Gakuin University, 2-1 Gakuen, Sanda, Hyogo, 669-1337, Japan.
E-mail: tanabe@kwansai.ac.jp; Fax: +81-795-65-9077;
Tel: +81-795-65-8394

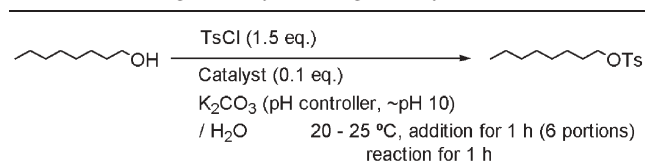
Results and discussion

The use of sterically unhindered *N,N*-dimethylamines (RNMe₂) accelerates the sulfonylation of alcohols² and mixed anhydride formation of carboxylic acids,^{6a,b} because these amines form reactive sulfonylammonium salts (R'SO₂N⁺Me₂R·Cl⁻) with sulfonyl chlorides (R'SO₂Cl). In addition, the ion pair (RN⁺HMe₂·Cl⁻), a main byproduct, is so tight that side chlorination (from ROTs to RCl) is considerably reduced, even in cases in which labile allylic and propargylic alcohols are used.

The major problem of the present method is the hydrolysis of sulfonyl chlorides by water. To prevent this problem, pH control of the reaction system was examined. First, we checked the stability of TsCl in water solvent at 20–25 °C in the absence of amine catalysts and alcohols: when the pH was maintained at around 10, the hydrolysis of TsCl was sufficiently prevented. Additionally, 1-octyl tosylate, a desired product, was not hydrolyzed under the same conditions.

The initial screening of amine catalysts was guided by the tosylation of 1-octanol. TsCl (1.5 equiv.) was added in 6 portions over 1 h, while the water solvent was maintained at pH 10 with continuous addition of KOH (1.5 equiv.) aqueous solution using a pH controller apparatus (Table 1). Without the catalyst, the reaction did not proceed. The use of catalysts (0.1 equiv.) such as Me₃N·HCl and TMEDA, which were effective for sulfonylation in organic solvents,² failed to promote the reaction. Et₃N (the most familiar tertiary amine), DMAP (a super acylation catalyst), and benzyltriethylammonium chloride, (a representative phase-transfer catalyst) also produced disappointing results. In clear contrast, *N,N*-dimethylbenzylamine (BnNMe₂) had a dramatic effect (93%).

A plausible reaction mechanism of the present method is illustrated in Scheme 2. In the organic phase, BnNMe₂ forms the reactive sulfonylammonium salt (TsN⁺Me₂Bn·Cl⁻) with TsCl, which in turn reacts with an alcohol to give the desired

Table 1 Screening of catalysts during the tosylation of 1-octanol


Catalyst	Yield (%)	Catalyst	Yield (%)
None	Trace	DMAP	Trace
Me ₃ N ⁺ HCl	Trace	BTEAC ^a	Trace
TMEDA	Trace	BnNMe ₂	93
Et ₃ N	33		

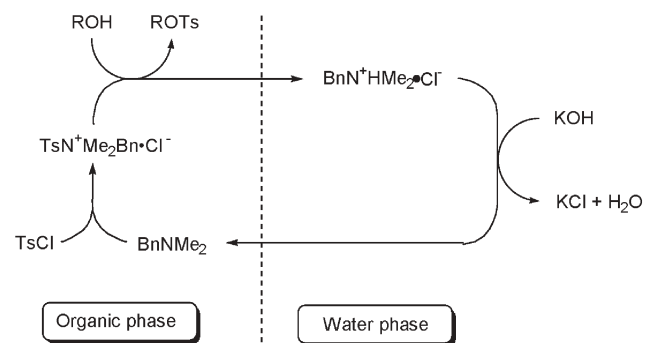
^a Benzyltriethylammonium chloride.



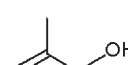
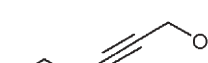



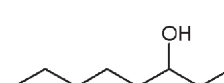
tosylate with the production of BnN⁺HMe₂·Cl⁻ in the water phase. Finally, BnN⁺HMe₂·Cl⁻ is neutralized by KOH to regenerate BnNMe₂, which moves into the organic phase. ¹H NMR measurement (400 MHz) supported this speculation with regard to the formation of TsN⁺Me₂Bn·Cl⁻; BnNMe₂ [δ = 2.23 (6H, s), 3.42 (2H, s), 7.22–7.32 (5H, m)] and a 1 : 1 mixture of TsCl and BnNMe₂ [δ = 2.32 (6H, s), 2.49 (3H, s), 3.53 (2H, s), 7.24–7.32 (5H, m), 7.38–7.44 (2H, m), 7.90–7.95 (2H, m)]. The proton chemical profiles of dimethyl (6H) and benzylic (2H) adjacent to the nitrogen were significantly shifted downfield by the formation of the sulfonylammonium salt. These results coincide with the precedent study.^{2b}

We attribute the failure of Me₃N⁺HCl and TMEDA catalysts to their high solubility in water; these amines cannot sufficiently dissolve in the organic phase.

Table 2 lists the results of the tosylation using several alcohols. Primary alcohols underwent tosylation in excellent yields (entries 1, 4–9). The use of 4-bromobenzenesulfonyl chloride and benzenesulfonyl chloride in the place of TsCl also afforded good results (entries 2, 3). Due to the mild reaction conditions, an allylic and a propargylic alcohol successfully afforded the corresponding labile tosylates (entries 5, 6). The reaction using 3-octanol, however, a secondary alcohol, resulted in low yield (entry 9).

Next, we investigated the mesylation utilizing the present protocol. Taking into account the higher reactivity of MsCl (Ms = methanesulfonyl), an initial screening of amine catalysts was guided using a less reactive 3-octanol (Table 3). Because MsCl is liquid and less stable than TsCl in basic aqueous solution, MsCl was added to the reaction mixture over 1 h,

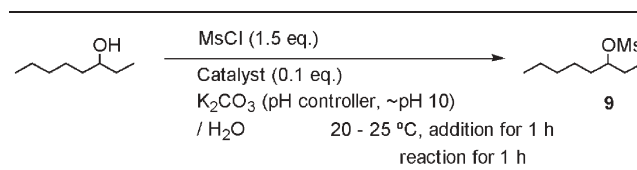
**Scheme 2** Plausible reaction mechanism.**Table 2** Tosylation of several alcohols in water solvent using TsCl/cat. BnNMe₂ and KOH

Entry	ROH	TsCl (equiv.)	Product	Yield (%)
1		1.5	1a	93
2		1.8	1b^a	93
3		1.8	1c^b	92
4		1.8	2	95
5		1.5	3	95
6		1.5	4	93
7		1.8	5	92
8		1.8	6	96
9		3.0	7	95 ^c
10		1.5	8	27

^a 4-Bromobenzenesulfonyl chloride was used instead of TsCl. ^b Benzenesulfonyl chloride was used instead of TsCl. ^c Bis(tosylate) was obtained using 0.2 equiv. of BnNMe₂.

using a microfeeder apparatus equipped with a syringe (Fig. 1). KOH aqueous solution was simultaneously added to the mixture using another microfeeder apparatus equipped with a syringe to more strictly maintain the pH at 10; the pH controller was used to adjust the timing of the addition of MsCl.

In contrast to the tosylation, *n*-BuNMe₂ and Et₃N had a higher reactivity than BnNMe₂. We hypothesize that the mesylation mechanism is considerably different from that of tosylation. The tosylation proceeds through the reactive sulfonylammonium salt, as mentioned above, whereas mesylation proceeds through the sulfene formation pathway.^{10,7b} The latter pathway is considered to depend less on the steric bulkiness of the amine. Table 4 lists the successful results of the mesylation using several primary alcohols. All examples

Table 3 Screening of amines in water solvent during the mesylation of 3-octanol


Catalyst	Yield (%)
BnNMe ₂	25
Et ₃ N	37
Bu ₃ N	20
<i>n</i> -BuNMe ₂	59

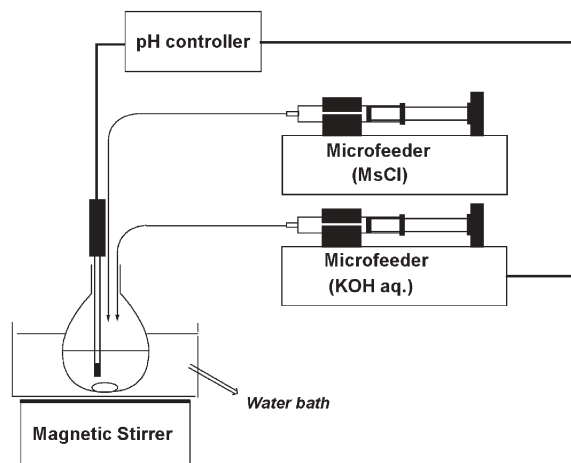


Fig. 1 Mesylation system using dual microfeeder equipped with pH controller.

examined using both Et_3N and BuNMe_2 catalysts were successfully performed in excellent yield (entries 1–8).

Conclusions

We achieved efficient tosylation and mesylation of primary alcohols in water solvent using the combined bases, catalytic $\text{BuNMe}_2/\text{KOH}$ and Et_3N or $n\text{-BuNMe}_2/\text{KOH}$, respectively. The present method is environmentally benign from a green chemical standpoint, and is a new candidate especially for industrial scale production of methane and *p*-toluene sulfonates.

Experiment

Commercial TsCl was recrystallized from EtOAc prior to use. Commercial MsCl was purified by distillation. Additions of MsCl and aqueous KOH were performed using a microfeeder apparatus (Furue Science JP-S-W2 and JP-S5, respectively). The control pH was performed using a pH controller apparatus (Toko Chemical Laboratoried Co., Ltd. TDP-200 L). Melting points were determined on a hot stage

Table 4 Mesylation of several alcohols in water using $\text{MsCl}/\text{cat. amines}$ and KOH

Entry	ROH	MsCl (equiv.)	Catalyst	Product	Yield (%)
1		1.5	Et_3N	10	98
2		1.5	$n\text{-BuNMe}_2$	11	98
3			Et_3N		97
4		1.5	$n\text{-BuNMe}_2$	12	97
5			Et_3N		97
6		1.8	$n\text{-BuNMe}_2$	13	94
7			Et_3N		94
8			$n\text{-BuNMe}_2$		94

microscope apparatus (Yanagimoto) and were uncorrected. NMR spectra were recorded on a JEOL ALPHA400 spectrometer, operating at 400 MHz for ^1H NMR and 100 MHz for ^{13}C NMR. Chemical shifts (δ/ppm) were reported downfield from tetramethylsilane (0 ppm) for ^1H NMR and were reported in the scale relative to CDCl_3 (77.00 ppm) for ^{13}C NMR. IR spectra were recorded on JASCO FT/IR-8000 and/or FT/IR-5300 spectrophotometer.

General procedure for tosylation

TsCl (2.86–3.43 g, 15.0–18.0 mmol) was added over 1 h (6 portions, every 10 min) to a stirred suspension of alcohol (10.0 mmol), BuNMe_2 (135 mg, 1.0 mmol) and K_2CO_3 (2.07 g, 15.0 mmol) in water (20.0 mL) at 20–25 °C. Using a microfeeder, 1 M KOH (ca. 15.0–18.0 mL) aqueous solution was continuously added to the reaction mixture, while the water solvent was maintained at pH 10 with the use of a pH controller apparatus. The mixture was stirred at the same temperature for an additional 1 h. To decompose an excess TsCl , *N,N*-dimethylethylenediamine (ca. 1.3 g) was added to the mixture, which was stirred for 10 min. Water was added to the mixture, which was extracted with EtOAc . The organic phase was washed with water, brine, dried (Na_2SO_4), and concentrated. The obtained crude tosylate was sufficiently pure. If necessary, it was purified by silica-gel column chromatography (hexane : ether = 40 : 1–10 : 1).

1-Octyl *p*-toluenesulfonate (**1a**)^{2b}

Colorless oil; ^1H NMR (400 MHz, CDCl_3) δ 0.87 (3H, t, $J = 7.2$ Hz), 1.08–1.82 (12H, m), 2.44 (3H, s), 4.03 (2H, t, $J = 6.9$ Hz), 7.24–7.49 (2H, m), 7.72–7.91 (2H, m); ν_{max} (neat)/ cm^{-1} 2928, 2857, 1599, 1466, 1362, 1177, 1098, 949, 910.

1-Octyl 4-bromobenzenesulfonate (**1b**)¹¹

Colorless crystals; mp 27.5–28.5 °C; ^1H NMR (400 MHz, CDCl_3) δ 0.87 (3H, t, $J = 6.8$ Hz), 1.17–1.35 (10H, m), 1.65 (2H, m), 4.06 (2H, t, $J = 6.5$ Hz), 7.70 (2H, m), 7.78 (2H, m); ν_{max} (KBr)/ cm^{-1} 2957, 2857, 1576, 1472, 1391, 1111, 740.

1-Octyl benzenesulfonate (**1c**)¹²

Colorless oil; ^1H NMR (400 MHz, CDCl_3) δ 0.86 (3H, t, $J = 7.0$ Hz), 1.15–1.34 (10H, m), 1.64 (2H, m), 4.05 (2H, t, $J = 6.5$ Hz), 7.57 (2H, m), 7.65 (1H, m), 7.92 (2H, m); ν_{max} (neat)/ cm^{-1} 2928, 2857, 1449, 1362, 1188, 1098, 949.

9-Decene-1-yl *p*-toluenesulfonate (**2**)^{2b}

Colorless oil; ^1H NMR (400 MHz, CDCl_3) δ 0.78–2.18 (14H, m), 2.44 (3H, s), 4.02 (2H, t, $J = 7.7$ Hz), 4.81–5.12 (2H, m), 5.58–6.04 (1H, m), 7.22–7.44 (2H, m), 7.72–7.91 (2H, m); ν_{max} (neat)/ cm^{-1} 2928, 1639, 1599, 1362, 1177, 937.

2-methyl-2-propenyl *p*-toluenesulfonate (**3**)^{2a}

Colorless oil; ^1H NMR (400 MHz, CDCl_3) δ 1.70 (3H, s), 2.45 (3H, s), 4.45 (2H, s), 4.89–5.06 (2H, m), 7.21–7.47 (2H, m), 7.70–7.91 (2H, m); ν_{max} (neat)/ cm^{-1} 2980, 2949, 1599, 1360, 1171, 934, 816.

2-Hexyn-1-yl *p*-toluenesulfonate (4)^{2b}

Colorless oil; ¹H NMR (400 MHz, CDCl₃) δ 0.90 (3H, t, *J* = 7.0 Hz), 1.20–1.65 (2H, m), 1.90–2.30 (2H, m), 2.45 (3H, s), 4.70 (2H, s), 7.20–7.45 (2H, m), 7.70–7.90 (2H, m); *v*_{max} (neat)/cm⁻¹ 2967, 2240, 1364, 1175, 1098.

2-Phenylethyl *p*-toluenesulfonate (5)¹³

Colorless crystals; mp 35.0–36.0 °C; ¹H NMR (400 MHz, CDCl₃) δ 2.42 (3H, s), 2.94 (2H, t, *J* = 7.1 Hz), 4.20 (2H, t, *J* = 7.1 Hz), 7.10 (2H, m), 7.17–7.30 (5H, m), 7.67 (2H, m); *v*_{max} (KBr)/cm⁻¹ 2959, 1599, 1456, 1360, 1177, 1098, 965.

6-Chlorohexyl *p*-toluenesulfonate (6)¹⁴

Colorless crystals; mp 37.0–38.0 °C; ¹H NMR (400 MHz, CDCl₃) δ 1.29–1.44 (4H, m), 1.60–1.78 (4H, m), 2.45 (3H, s), 3.49 (2H, t, *J* = 6.6 Hz), 4.03 (2H, t, *J* = 6.5 Hz), 7.35 (2H, m), 7.79 (2H, m); *v*_{max} (KBr)/cm⁻¹ 2940, 1599, 1458, 1360, 1211, 1098, 816.

Hexamethylene di(*p*-toluenesulfonate) (7)¹⁵

Colorless crystals; mp 64.5–65.5 °C; ¹H NMR (400 MHz, CDCl₃) δ 1.27 (4H, m), 1.60 (4H, m), 2.45 (6H, m), 3.98 (4H, t, *J* = 6.4 Hz), 7.36 (4H, m), 7.77 (4H, m); *v*_{max} (KBr)/cm⁻¹ 2955, 1597, 1456, 1352, 1188, 1096, 953.

3-Octyl *p*-toluenesulfonate (8)^{2b}

Colorless oil; ¹H NMR (400 MHz, CDCl₃) δ 0.80 (3H, t, *J* = 7.7 Hz), 1.01–1.82 (13H, m), 2.42 (3H, s), 4.38–4.62 (1H, m), 7.22–7.48 (2H, m), 7.71–7.89 (2H, m); *v*_{max} (neat)/cm⁻¹ 2957, 2934, 2864, 1597, 1460, 1364, 1188, 1177, 1098, 910.

General procedure for mesylation

(See Fig. 1) Using a microfeeder, MsCl (1.72–2.06 g, 15.0–18.0 mmol) was added over 1 h to a stirred suspension of alcohol (10.0 mmol), *n*-BuNMe₂ or Et₃N (1.0 mmol) and K₂CO₃ (2.07 g, 15.0 mmol) in water (20.0 mL) at 20–25 °C. 5–7 M KOH aqueous solution (*ca.* 2.1–3.6 mL) was simultaneously added to the mixture using another microfeeder apparatus to strictly maintain the pH at 10; the pH controller was used to adjust the timing of the addition of MsCl.

The mixture was stirred at the same temperature for an additional 1–2 h. Water was added to the mixture, which was extracted with EtOAc. The organic phase was washed with water, brine, dried (Na₂SO₄), and concentrated. The obtained crude mesylate was sufficiently pure. If necessary, it was purified by distillation or silica-gel column chromatography (hexane : ether = 30 : 1–10 : 1).

3-Octyl methanesulfonate (9)^{2b}

Colorless oil; ¹H NMR (400 MHz, CDCl₃) δ 0.90 (3H, t, *J* = 6.8 Hz), 0.98 (3H, t, *J* = 7.4 Hz) 1.25–1.46 (6H, m), 1.61–1.80 (4H, m), 3.00 (3H, s), 4.63–4.69 (1H, m); ¹³C NMR (100 MHz, CDCl₃) δ 9.18, 13.89, 22.40, 24.57, 27.33, 31.47, 33.82, 38.59, 85.30.

1-Octyl methanesulfonate (10)¹¹

Bp 75–80 °C/0.2 mmHg. colorless oil; ¹H NMR (400 MHz, CDCl₃) δ 0.89 (3H, t, *J* = 7.0 Hz), 1.19–1.44 (10H, m), 1.71–1.78 (2H, m), 3.00 (3H, s), 4.22 (2H, t, *J* = 6.6 Hz); ¹³C NMR (100 MHz, CDCl₃) δ 14.01, 22.55, 25.37, 28.94, 29.02, 29.08, 31.66, 37.31, 70.18.

9-Decene-1-yl methanesulfonate (11)¹⁸

Colorless oil; ¹H NMR (400 MHz, CDCl₃) δ 1.26–1.44 (10H, m), 1.71–1.78 (2H, m), 2.01–2.07 (2H, m), 3.00 (3H, s), 4.22 (2H, t, *J* = 6.6 Hz), 4.92–5.02 (2H, m), 5.76–5.86 (1H, m); ¹³C NMR (100 MHz, CDCl₃) δ 25.32, 28.76, 28.88, 29.04, 29.16, 33.66, 37.27, 70.12, 114.16, 139.03.

2-Phenylethyl methanesulfonate (12)¹⁶

Colorless oil; ¹H NMR (400 MHz, CDCl₃) δ 2.83 (3H, s), 3.06 (2H, t, *J* = 6.8 Hz), 4.42 (2H, t, *J* = 7.0 Hz), 7.22–7.35 (5H, m); ¹³C NMR (100 MHz, CDCl₃) δ 35.55, 37.21, 70.29, 127.01, 128.65, 128.93, 136.29.

6-Chlorohexyl methanesulfonate (13)¹⁷

Colorless oil; ¹H NMR (400 MHz, CDCl₃) δ 1.41–1.54 (4H, m), 1.74–1.83 (4H, m), 3.01 (3H, s), 3.54 (2H, t, *J* = 6.6 Hz), 4.24 (2H, t, *J* = 6.2 Hz); ¹³C NMR (100 MHz, CDCl₃) δ 24.68, 26.16, 28.89, 32.20, 37.26, 44.74, 69.79.

References

- (a) M. B. Smith and J. March, *Advanced Organic Chemistry*, Wiley, New York, 5th edn, 2001, p. 576; (b) L. F. Fieser and M. Fieser, *Reagent for Organic Synthesis*, Wiley, New York, 1967, vol. 1, p. 1179. For representative examples; (c) V. C. Sekera and C. S. Marvel, *J. Am. Chem. Soc.*, 1933, **55**, 345; (d) R. S. Tipson, *J. Org. Chem.*, 1944, **9**, 235; (e) R. K. Crossland and K. L. Servis, *J. Org. Chem.*, 1970, **35**, 3195; (f) G. W. Kabalka, M. Varma, R. S. Varma, P. C. Srivastava and F. F. Knapp, Jr., *J. Org. Chem.*, 1986, **51**, 2386.
- (a) Y. Tanabe, H. Yamamoto, Y. Yoshida, T. Miyawaki and N. Utsumi, *Bull. Chem. Soc. Jpn.*, 1995, **68**, 297; (b) Y. Yoshida, Y. Sakakura, N. Aso, S. Okada and Y. Tanabe, *Tetrahedron*, 1999, **55**, 2183; (c) Y. Yoshida, K. Shimonishi, Y. Sakakura, S. Okada, N. Aso and Y. Tanabe, *Synthesis*, 1999, 1633.
- J. Hartung, S. Hunig, R. Kneuer, M. Schwarz and H. Wenner, *Synthesis*, 1997, 1433.
- S. Yokoshima, T. Ueda, S. Kobayashi, A. Sato, T. Kuboyama, H. Tokuyama and T. Fukuyama, *J. Am. Chem. Soc.*, 2002, **124**, 2137.
- R. P. Hudgins, F. Huang, G. Gramlich and W. M. Nau, *J. Am. Chem. Soc.*, 2002, **124**, 556.
- R. Yoshida, M. Sakai, R. Sato, T. Haga, E. Nagano, H. Oshio and K. Kamoshita, *Brighton Crop Protection Conference—Weeds*, 1991, p. 69.
- (a) K. Wakasugi, A. Nakamura and Y. Tanabe, *Tetrahedron Lett.*, 2001, **42**, 7427; (b) K. Wakasugi, A. Nakamura, A. Iida, Y. Nishii, N. Nakatani, S. Fukushima and Y. Tanabe, *Tetrahedron*, 2003, **59**, 5337; (c) K. Wakasugi, A. Iida, T. Misaki, Y. Nishii and Y. Tanabe, *Adv. Synth. Catal.*, 2003, **345**, 1209.
- (a) C.-J. Li and T.-H. Chan, *Organic Reactions in Aqueous Media*, Wiley, New York, 1997; (b) *Organic Reactions in Water*, ed. P. Grieco, Blackie Academic & Professional, London, 1998; (c) *Modern Solvents In Organic Synthesis*, (Topics In Current Chemistry, 206), ed. P. Knochel, K. N. Houk, H. Kessler, Springer, Berlin, 1999; (d) C.-J. Li, *Chem. Rev.*, 1993, **93**, 2023; (e) S. Kobayashi, *Adv. Synth. Catal.*, 2002, **344**, 219.

-
- 9 (a) C. Schottenn, *Ber.*, 1884, **17**, 2544; (b) E. Baumann, *Ber.*, 1884, **19**, 3218; (c) M. B. Smith and J. March, *Advanced Organic Chemistry*, Wiley, New York, 5th edn, 2001, p. 482.
- 10 G. Opitz, T. Ehliis and K. Rieth, *Chem. Ber.*, 1990, **123**, 1989.
- 11 C. H. Snyder and A. R. Soto, *J. Org. Chem.*, 1964, **29**, 742.
- 12 D. Reisdorf and H. Normant, *Organomet. Chem. Synth.*, 1972, **1**, 375–391.
- 13 D. Klamann, *Monatsh. Chem.*, 1953, **84**, 54.
- 14 W. J. Gensler, R. S. Prasad, A. P. Chaudhuri and I. Alam, *J. Org. Chem.*, 1979, **44**, 3643.
- 15 F. Drahowzal and D. Klamann, *Monatsh. Chem.*, 1951, **82**, 460.
- 16 W. F. Beech, *J. Chem. Soc. C*, 1968, 1869.
- 17 G. Radivoy, F. Alonso and M. Yus, *Tetrahedron*, 1999, **55**, 14479.
- 18 T. H. Jones, M. S. Blum, A. N. Andersen, M. Henry and P. Escoubas, *J. Chem. Ecol.*, 1988, **14**, 35.

Strecker intermediates as non-pollutant scavengers for cyanides

Fernando Godínez-Salomon,^{ab} Jose M. Hallen-Lopez,^b Herbert Höpfl,^c Adela Morales-Pacheco,^a Hiram I. Beltrán^{*a} and Luis S. Zamudio-Rivera^{*a}

Received 4th April 2005, Accepted 15th August 2005

First published as an Advance Article on the web 30th August 2005

DOI: 10.1039/b504406e

Using a series of five bis(aminomethyl)ethers, a fast and efficient transformation of sodium cyanide to sodium *N*-2-hydroxyethylglycinates is reported, where the starting materials are prototypes for application in the mining and oil industries to diminish the pollution of the tailings derived from their processes.

Introduction

For the petroleum industry, hydrogen sulfide and metal cyanides are among the most common corrosive pollutants in crude oil.^{1,2} Of these two reagents cyanide ions are especially problematic, since their damage is twofold: firstly, the H₂S induced corrosion is enhanced by ⁻CN ions through the interaction they have with iron sulfide; and secondly, cyanide pollution affects the petroleum feedstock for further processes.^{2,3} On the other hand, the cyanide process of gold recovery enables a higher percentage of not only gold but silver to be extracted from hard rock, making many operations viable that would otherwise have had to close.^{4,5} During the ore extraction, environmental harm is caused through the tailings, which have unavoidably high amounts of cyanide ions.^{4,5}

Tailings, also called gangue, are the rejected material from mining and screening operations. These tailings are the uneconomic remainders from mining; as mining techniques

and the price of minerals improve it is not unusual for tailings to be reprocessed, mainly to recover minerals other than those originally mined.

One of the strategies to solve these problems is to diminish the concentration of the pollutants, which in industrial application is commonly achieved by the addition of scavenger molecules.^{1–3,6} Characteristics required for a good scavenger are (i) that the scavenging reaction takes place under the industrial process conditions, (ii) that the product derived from the scavenging reaction is no longer contaminating and/or does not interfere in such a process, and (iii) that the resulting compounds can be reused within the industrial facilities or used for other important side applications.

So far, only a few scavengers that are selective towards cyanide ions are known; among them are hydroxocobalamin,⁷ dicyano-cobalt(III)-porphyrins⁸ and other vitamin B12 analogues,⁸ metallophthalocyanines⁸ and the hexahydrated dichloride compounds of cobalt(II) and nickel(II), which have shown good performance, but are rather toxic.⁸

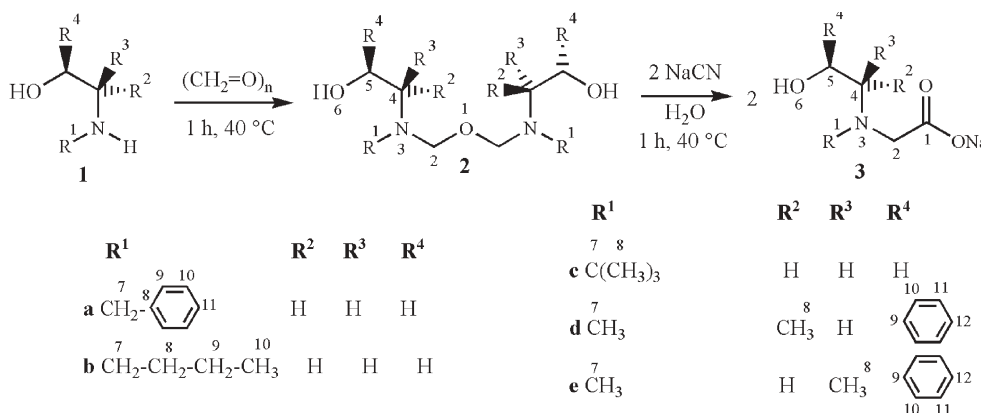
^aPrograma de Ingeniería Molecular, Instituto Mexicano del Petróleo, Eje Central Lázaro Cárdenas 152, Col. San Bartolo Atepehuacan, México D.F. E-mail: lzamudio@imp.mx, hbeltran@imp.mx; Fax: +52 5591756239; Tel: +52 5591757399

^bDepartamento de Ingeniería Metalúrgica, Escuela Superior de Ingeniería Química e Industrias Extractivas, I.P.N. Unidad Profesional Adolfo López Mateos, México D.F.

^cCentro de Investigaciones Químicas, U.A.E.M., Av. Universidad 1001, C. P. 62210 Cuernavaca, Morelos, México

Results and discussion

One pot reactions between the β-aminoalcohols **1a–1e** and paraformaldehyde (Scheme 1) led to five cyanide scavengers **2a–2e** in yields ranging from 80 to 99%. The title compounds are isolated intermediates of the well known Strecker synthesis.⁹ Because of ecological reasons the reactions were



Scheme 1 Reaction for the preparation and scavenger activity of bis(semiaminals) **2a–2e** for sodium cyanide.

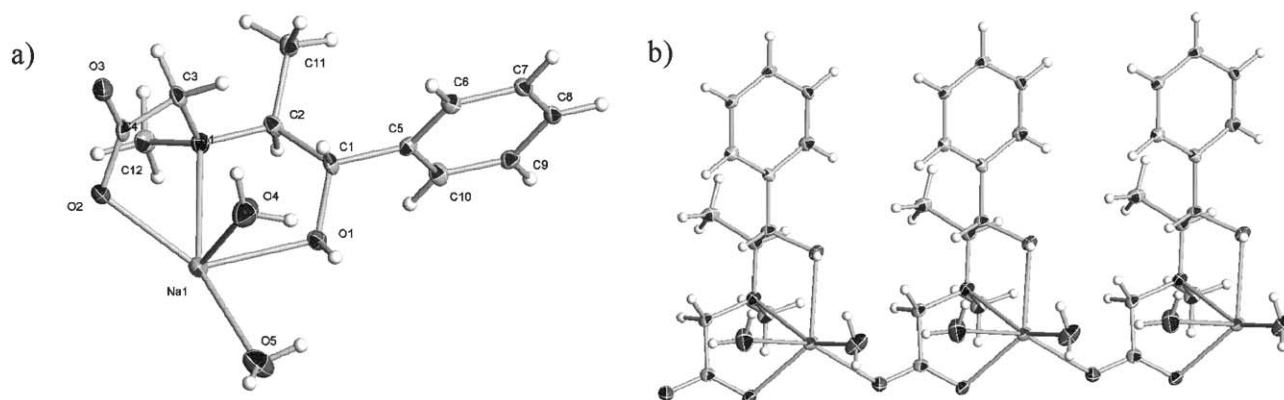


Fig. 1 (a) The crystal lattice of **3d** contains six molecular units, one of which is shown here. (b) Fragment of one of the linear coordination polymers, showing the octahedral coordination geometry of the sodium ions.

carried out in the absence of any solvent. When compounds **2a–2e** were treated with two equivalents of sodium cyanide and heated in water or different water/solvent mixtures to a temperature of 40 °C, the expected cyanide induced hydrolysis reaction took place, giving the *N*-substituted *N*-2-hydroxyethylglycine sodium salts **3a–3e** (Scheme 1) in yields between 66 and 94%.¹⁰ It was noticeable that the *n*-butyl, **2b** (66%), and *tert*-butyl, **2c** (80%), Strecker scavengers were the less efficient for the scavenging action. It is also worth mentioning that in the mining industry, most of the washing operations are carriers of harmful ions, where the water molecules physically scavenge the cyanide counterparts. For that reason, the present scavengers imply an important chemical strategy since they take their action in the presence of water. In order to evaluate the potential of compounds **2a–2e** for an application directed to the petroleum industry, the reactions outlined in Scheme 1 have also been successfully carried out in 50 : 1 heptane–water and in a second trial in 50 : 1 chloroform–water solvent mixtures. For application purposes, the temperature required for the transportation and general processing of crude oil is sufficient to reach the activation energy required for the scavenger reaction that is fast and easily accomplished at 40 °C. The application of compounds **2a–2e** in real petroleum currents is under study and a patent development with a large number of derivatives for these means is being carried out.

Compounds **3a–3e** were isolated in yields ranging from 56 to 94% by filtration of the precipitates that were formed after slow addition of acetone to the reaction mixture. All products were completely characterized by IR, ¹H, ¹³C and 2D NMR spectroscopic methods and elemental analyses, certifying the formation of the scavenger molecules as well as the corresponding sodium salts.

As an insight into the supramolecular architectures formed by these chemical products, further structural evidence was provided by the X-ray diffraction analysis of compound **3d**.^{†11–14} Two solutions were obtained for the collected data in different space groups, trigonal, *P*3₂, and hexagonal, *P*6₂; both of them were refined resulting in better statistical values for the latter[†] which hence was used for the forthcoming discussion. Moreover, an incoming problem was the possibility of a crystal as a racemic twin, since the Flack parameter was 0.4(10) as well as the thermal ellipsoids for the water molecules and the

final *R* indices were high in both pseudosymmetric solutions when the collection was carried out at room temperature due to the disorder present in the uncoordinated water moiety. Attempts to refine as a racemic twin were unsuccessful.¹⁵ Finally, the collection of X-ray data at 100 K led to a congruent Flack parameter near to zero and an uncoordinated water moiety was easily situated. Fig. 1a shows one of the independent molecular fragments present in the crystal lattice of **3d**, which is the repeating unit of a linear coordination polymer (similar to transition metal coordination polymers) as shown in Fig. 1b. Each sodium is coordinated to the three donor atoms of the chelating tridentate ligand in a meridional fashion, and furthermore to two water molecules and the carbonyl group of a neighbouring complex molecule, giving rise to a coordination polymer along *c*. The sodium ions possess distorted octahedral coordination geometries; the Na–N bond length is 2.572 Å, the Na–O bond lengths are: for Na–OH, 2.414, for Na–OOC_{intramol}, 2.320 Å, for Na–OH₂, 2.391, 2.604 Å, and for Na–OOC_{intermol}, 2.335 Å. Due to the coordination of the tridentate ligand towards the sodium ion, a five-five-membered rings fused structure is constructed. The O(2)–C(4)–C(3)–N(1)–Na(1) five-membered ring has an envelope conformation, where the C(1) atom is placed away from the plane due to the presence of the phenyl moiety. In the crystal lattice, the two independent linear polymers form double chains through three different hydrogen-bonding interactions.

Six molecular slabs of the infinite chain were selected to mimic the supramolecular structure organized through further hydrogen-bonding interactions (two per individual complex molecule) around a crystallographic *c*₂ symmetry axis to give a chiral tubular structure as shown in Fig. 2. The hydrogen

[†] Crystal data and experimental details for **3d**. Empirical formula: C₂₄H₄₄N₂Na₂O₁₂, formula weight, 598.6, crystal colour, colourless, cryst. dim. [mm³], 0.02 × 0.02 × 0.05, lattice parameters, *a* [Å], 21.1806 (15), *c* [Å], 5.6912 (6), volume [Å³], 2211.1 (3), crystal system, hexagonal, space group, *P*6₂, *Z*, 3, ρ_{calc} [mg m⁻³], 1.349, μ [mm⁻¹], 0.131, θ_{range} [°], 1.92 to 24.98, coll. refl., 21426, indep. refls [*R*_{int}], 1441, data/restr/param, 1441/26/248, GOOF, 1.112, *R* indices [*I* > 2 σ (*I*)], 0.0553, *R* indices (all data), 0.1364, $\Delta\rho_{\text{min}}$ [e Å⁻³], -0.53, $\Delta\rho_{\text{max}}$ [e Å⁻³], 0.74. CCDC reference number 255743. See <http://dx.doi.org/10.1039/b504406e> for crystallographic data in CIF or other electronic format.

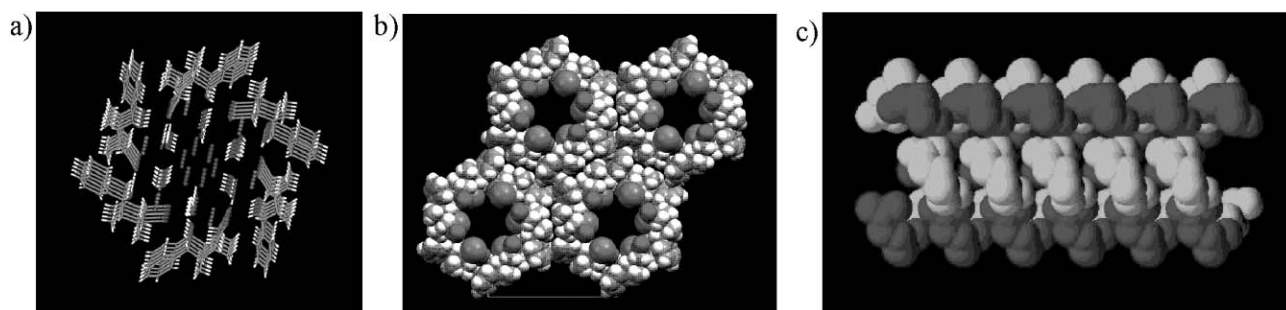


Fig. 2 (a) Perspective view of the crystal lattice of compound **3d** along *c*, showing one of the chiral tubes. (b) Hexagonal arrangement of the tubes shown before; special attention should be paid to the hydrophobic outer-sphere and the hydrophilic core (for clarity, the sodium-coordinated and uncoordinated water molecules have been omitted). (c) Lateral view of the chiral assembly of the two independent (dark and light grey) coordination polymers present in the supramolecular structure.

bonds are formed between the sodium-coordinated water molecules, the hydroxyl groups of the β -aminoalcohol fragments in the ligands and the carboxylate groups ($O \cdots O = 2.72$ – 2.83 Å) as well as with the uncoordinated water molecules. The nano-sized tubes have overall diameters of 22.9 Å and are organized in a pseudosymmetric hexagonal honeycomb-like arrangement (Fig. 2b). They possess a hydrophobic outer-sphere formed by the phenyl and methyl groups of the β -aminoalcohol fragments and contain hydrophilic channels. The distance between opposite sodium ions is 10.3 Å. The pores, whose hydrophilic interior is formed by the sodium-coordinated water molecules, extend throughout the whole crystal lattice and are filled by uncoordinated water molecules; the water molecules mainly govern this type of architectures.¹⁶ A search of the CCDC database¹⁷ revealed that there are only very few structurally characterized sodium complexes containing tridentate ligands of the NO_2 type.

Since the Strecker intermediates, **2a–2e**, and the resulting ligands, **3a–3e**, are going to be tested as anthropogenic chemicals, they might be evaluated as environment-friendly compounds. Following a well established protocol,^{3,18–19} fast screening toxicity tests were performed for compounds **2a–2e** and **3a–3e**.^{18–19} The EC_{50} values measured at incubation times of 5 and 15 min range from 416–1127 ppm (Table 1), so that

Table 1 Yields and acute toxicity^a tests for compounds **2a–2e** and **3a–3e**

Compound	Yield (%)	EC_{50} (ppm)	
		5 min	15 min
2a	99	681	420
2c	97	660	499
2b	86	551	416
2e	80	646	659
2d	85	794	455
3a	91	959	744
3c	66	1127	841
3b	80	596	463
3e	92	659	583
3d	94	863	636
NaCN	—	0.017	0.011

^a Concentration range in ppm, classification, category: 0.01–0.10, 5, extremely toxic; 0.1–1.0, 4, highly toxic; 0.1–10, 3, moderately toxic; 0.10–100, 2, slightly toxic; 0.100–1000, particularly non toxic, more than 1000, 0, non toxic. See ref. 3 and 17 for further details.‡

these chemicals can be classified as only slightly toxic, in comparison to the high toxicity in the case of sodium cyanide and other cyanide derivatives.

Conclusions

The Strecker intermediates described herein can be prepared in fast and efficient one-step reactions without the requirement of a solvent. They can function as scavengers for sodium cyanide in water and solvent mixtures that have a composition similar to crude oil and the tailings derived from the mining processes. The Strecker intermediates themselves and the resulting tridentate ligands coordinated with sodium are environment-friendly and water-soluble compounds. These ligands coordinate to sodium ions through their carboxylate, hydroxyl and amino functional groups, thus giving insight into the coordination chemistry of aminoalcohol and aminoacid derivatives, which indeed construct interesting nano-rod motifs.

Experimental

Paraformaldehyde and β -aminoalcohols were purchased from Aldrich Co. The acetone, chloroform and heptanes solvents were purchased as reagent grade from Fermont Co. All reactions and operations were carried out under atmospheric conditions.

Instrumentation

NMR experiments were performed on a VARIAN Mercury 200-BB spectrometer. 1H and ^{13}C chemical shifts [ppm] are relative to internal $SiMe_4$ (TMS). Coupling constants are quoted in Hz. The IR spectra were recorded in the range of 4000 – 400 cm^{-1} on a Bruker Tensor-27 FT-IR spectrometer by

‡ In the test, a vial of the *Photobacterium phosphoreum* culture was reconstituted in 1 mL of solution and maintained at 3 °C in an incubator well on the analyzer. For each test, a serial dilution of the compounds was prepared in 2% brine. In addition, a series of brine solutions containing approximately 106 colony forming units of *P. phosphoreum* were prepared in glass cuvettes by pipetting 10 μL of the suspension into 500 μL of 2% brine. As a bacterial population control, these solutions were incubated in temperature controlled wells (6 °C) over 15 min and measured. The activity of compounds was recorded after 5 and 15 min of exposure. The results of the Microtox[®] tests are expressed in terms of the EC_{50} value.

using KBr pellets or the ATR technique. The X-ray structure determination was performed in a BRUKER-AXS APEX diffractometer with a CCD area detector ($\lambda_{\text{Mo K}\alpha} = 0.71073 \text{ \AA}$, monochromator: graphite).

General method for the preparation of compounds 2a–2e and 3a–3e

The 2a–2e and 3a–3e series of compounds have each been prepared by analogous methods, therefore, only the preparation of compounds 2c and 3c is described in detail: 2.00 g (8.50 mmol) of 1c and 0.51 g (8.50 mmol) of paraformaldehyde were heated to 40 °C for 1 h without using a solvent. The water formed during the condensation reaction was removed at reduced pressure giving 2c as a light greenish liquid in a yield of 86%. Then, 1.80 g of 2c (6.47 mmol) and 0.64 g of sodium cyanide (13.03 mmol) were heated to 40 °C for 1 h in 30 mL of bidistilled water. When the reaction time was accomplished, the solvent was partially removed at reduced pressure and 3c was precipitated by addition of 30 mL of acetone. The resulting beige powder was filtered and identified as 3c (yield: 59%).

Characterization and spectroscopic data

2a: Yield 99%. IR (ν/cm^{-1}) 3465, 3062, 3028, 2878, 1494, 1453, 1154, 733, 697. $^1\text{H NMR}$ (δ/ppm , J/Hz): 7.33–7.31 (m, 10H, H-9, 10, 11), 4.10 (s, 4H, H-2), 3.85 (t, $J = 6.8$, 4H, H-5), 3.71 (s, 4H, H-7), 2.93 (t, 4H, $J = 6.8$, H-4). $^{13}\text{C NMR}$ (δ/ppm): 138.2 (C-8), 128.3–126.6 (C-9, 10, 11), 86.3 (C-2), 63.2 (C-5), 58.0 (C-7), 52.1 (C-4).

3a: Yield 91%, mp 85–87 °C. IR (ν/cm^{-1}) 3062, 2878, 1612, 1406, 1000, 733, 697. $^1\text{H NMR}$ (δ/ppm , J/Hz): 7.24 (m, 5H, H-9, 10, 11), 3.61 (s, 2H, H-7), 3.48 (t, 2H, $J = 6.0$, H-5), 2.82 (s, 2H, H-2), 2.58 (t, 2H, $J = 6.0$, H-4). $^{13}\text{C NMR}$ (δ/ppm): 179.5 (C-1), 137.7 (C-8) 137.2–127.7 (C-9, 10, 11), 59.0 (C-5), 58.4 (C-2), 57.5 (C-7), 55.3 (C-4).

2b: Yield 97%. IR (ν/cm^{-1}) 3446, 2932, 2872, 1460, 1021, 738. $^1\text{H NMR}$ (δ/ppm , J/Hz): 4.16 (s, 4H, H-2), 3.67 (t, 4H, $J = 7.6$, H-5), 2.83 (t, 4H, $J = 7.6$, H-4), 2.41 (t, 4H, $J = 7.4$, H-7), 1.33 (m, 8H, H-8,9), 0.83 (t, 6H, $J = 7.6$, H-10). $^{13}\text{C NMR}$ (δ/ppm): 86.4 (C-2), 63.4 (C-5), 53.8 (C-4), 52.3 (C-7), 31.7 (C-8), 30.7 (C-9), 14.3 (C-10).

3b: Yield 66%, mp > 400 °C. IR (ν/cm^{-1}) 3446, 2932, 2872, 1596, 1460, 1021, 738. $^1\text{H NMR}$ (δ/ppm , J/Hz): 3.33 (t, 2H, $J = 5.2$, H-5), 2.80 (s, 2H, H-2), 2.44 (t, 2H, $J = 5.2$, H-4), 2.42 (t, 2H, $J = 4.6$, H-7), 1.27 (m, 4H, H-8,9), 0.83 (t, 3H, H-10). $^{13}\text{C NMR}$ (δ/ppm): 176.2 (C-1), 60.8 (C-5), 60.4 (C-2), 59.5 (C-4), 55.2 (C-7), 29.3 (C-8), 20.8 (C-9), 14.7 (C-10).

2c: Yield 86%. IR (ν/cm^{-1}) 2970, 1657, 1470, 1393, 1091. $^1\text{H NMR}$ (δ/ppm , J/Hz): 4.34 (s, 4H, H-2), 3.78 (t, 4H, $J = 6.6$, H-5), 2.89 (t, 4H, $J = 6.6$, H-4), 1.06 (s, 18H, H-8). $^{13}\text{C NMR}$ (δ/ppm): 80.6 (C-2), 66.1 (C-5), 52.4 (C-4), 45.1 (C-7), 26.9 (C-8).

3c: Yield 59%, mp 171–172 °C. IR (ν/cm^{-1}) 3255, 2971, 2813, 1602, 1408, 1359, 1084. $^1\text{H NMR}$ (δ/ppm , J/Hz): 4.65 (s, 1H, H-6), 3.42 (t, 2H, $J = 6.0$, H-5), 3.02 (s, 2H, H-2), 2.89 (t, 2H, $J = 6.0$, H-4), 1.06 (s, 9H, H-8). $^{13}\text{C NMR}$ (δ/ppm): 182.0 (C-1), 60.8 (C-5), 55.6 (C-2), 52.3 (C-7), 51.8 (C-4), 25.7 (C-8).

2d: Yield 80%. IR (ν/cm^{-1}) 3032, 2968, 2875, 1674, 1494, 1053, 810, 750. $^1\text{H NMR}$ (δ/ppm , J/Hz , 200 MHz): 7.34 (bs, 10H, H-10,11,12), 4.75 (d, 2H, $J = 3.3$, H-2a), 4.48 (d, 2H, $J = 8.2$, H-5), 4.29 (d, 2H, $J = 3.3$, H-2b), 2.43 (dq, 2H, $J = 6.2$, 2.0, H-4), 2.36 (s, 6H, H-7), 1.17 (d, 6H, $J = 6.2$, H-8). $^{13}\text{C NMR}$ (δ/ppm): 140.4 (C-9), 128.2–126.0 (C-10, 11, 12), 88.6 (C-5), 85.8 (C-2), 68.0 (C-4), 36.8 (C-7), 14.2 (C-8).

3d: Yield 92%, mp = 172–173 °C. IR (ν/cm^{-1}) 3356, 3031, 1731, 1572, 1494, 1043, 763, 700. $^1\text{H NMR}$ (δ/ppm , J/Hz): 7.25 (bs, 5H, H-10,11,12), 4.19 (d, 2H, $J = 3.2$, H-5), 2.98 (d, 1H, $J = 16.2$, H-2a), 2.97 (d, 1H, $J = 16.2$, H-2b), 2.69 (dq, 1H, $J = 6.7$, 3.2, H-4), 2.12 (s, 3H, H-7), 0.49 (d, 3H, $J = 6.7$, H-8). $^{13}\text{C NMR}$ (δ/ppm): 180.1 (C-1), 140.1 (C-9), 128.7–127.7 (C-10,11,12), 72.3 (C-5), 64.2 (C-2), 57.5 (C-7), 39.9 (C-4), 7.8 (C-8).

2e: Yield 85%. IR (ν/cm^{-1}): 3064, 3028, 2786, 1604, 1493, 1454, 1224, 751, 698. $^1\text{H NMR}$ (δ/ppm , J/Hz): 7.29 (bs, 10H, H-10,11,12), 5.11 (d, 2H, $J = 7$, H-5), 4.88 (bs, 2H, H-2a), 4.06 (bs, 2H, H-2b), 2.87 (t, 2H, $J = 6.6$, H-4), 2.37 (s, 6H, H-7), 0.67 (d, 6H, $J = 6.4$, H-8). $^{13}\text{C NMR}$ (δ/ppm): 139.8 (C-9), 127.8–126.8 (C-10,11,12), 88.1 (C-2), 81.8 (C-5), 63.3 (C-4), 37.6 (C-7), 14.2 (C-8).

3e: Yield 94%, mp > 172 °C (dec.). IR (ν/cm^{-1}) 3250, 2952, 2834, 1888, 1581, 1017, 760, 694. $^1\text{H NMR}$ (δ/ppm , J/Hz): 7.25 (bs, 5H, H-10, 11, 12), 3.46–3.35 (m, 2H, H-2a, H-5), 2.99 (bs, 1H, H-2b), 2.65 (bs, 1H, H-4), 2.23 (s, 3H, H-7), 0.71 (bs, 3H, H-8). $^{13}\text{C NMR}$ (δ/ppm): 177.5 (C-1), 145.2 (C-9), 128.6–126.7 (C-10, 11, 12), 72.4 (C-5), 64.7 (C-2), 59.6 (C-7), 40.8 (C-4), 10.5 (C-8).

The 8 eV EI mass spectra of compounds 2a–2e do not show the molecular ion peak; all show a C–O bond rupture leading to iminium fragments.

X-ray crystallography

An X-ray diffraction study of 3d was carried out on a BRUKER-AXS APEX diffractometer with a CCD area detector ($\lambda_{\text{Mo K}\alpha} = 0.71073 \text{ \AA}$, monochromator: graphite). Frames were collected at $T = 100 \text{ K}$ or 298 K via ω - and ϕ -rotation at 10 s per frame (SMART¹¹). The measured intensities were reduced to F^2 and corrected for absorption with SADABS (SAINT-NT¹²). Structure solution, refinement, and data output were carried out with the SHELXTL-NT,¹³ SHELXS-97,¹⁴ and SHELXL-97¹⁴ programs. Non-hydrogen atoms were refined anisotropically. All data were corrected for Lorentz and polarization effects. All additional treatments were done through the WIN-GX²⁰ program set with the PARST²¹ utility; the corresponding molecular graphs were prepared with the ORTEP 3²² and Mercury 1.2²³ programs.

Acknowledgements

The present study was supported by Instituto Mexicano del Petróleo, Programa de Ingeniería Molecular with project number D.00178.

References

- 1 D. Brodel, R. Edwards, A. Hayman, D. Hill, S. Mehta and T. Semerad, *Oilfield Rev.*, 1994, **35**, 4.
- 2 L. A. C. J. Garcia, C. J. B. M. Joia, E. M. Cardoso and O. R. Mattos, *Electrochim. Acta*, 2001, **46**, 3879; D. Urban, S. Frisbie and S. Croce, *Environ. Prog.*, 1997, **16**, 171.
- 3 G. F. Whale and T. S. Whitham, *Soc. Pet. Eng.*, 1991, **23357**, 355.

- 4 M. R. Ally, J. B. Berry, L. R. Dole, J. J. Ferrada and J. W. Van Dyke, *Economical Recovery of by-Products in the Mining Industry*, ORNL/TM-2001/225, Oak Ridge National Laboratory, Oak Ridge Tennessee, 37831-6285, UT-Batelle LLC & U.S. Department of Energy, 2001, p. 33. Web page: www.dole.nu/lesdole/TM225.pdf.
- 5 A. Smith and T. Mudder, *The Chemistry and Treatment of Cyanidation Wastes*, Mining J. Books Ltd. Pub., London, 1991.
- 6 L. S. Zamudio-Rivera, A. Estrada-Martinez, A. Morales-Pacheco, J. L. R. Benitez-Aguilar, R. Roldan-Perez, J. L. Yañez-Ayuso, J. Marin-Cruz and M. G. Guzman-Pruneda, *Mex. Pat. Req.*, 2002Pa/a/2002/006434.
- 7 S. W. Sauer and M. E. Keim, *Ann. Emerg. Med.*, 2001, **37**, 635.
- 8 S. Mosseri, P. Neta, A. Harriman and P. Hambright, *J. Inorg. Biochem.*, 1990, **39**, 2, 93; R. Rahimi and P. Hambright, *J. Porphyrins Phthalocyanines*, 1998, **2**, 493.
- 9 A. Strecker, *Liebigs. Ann. Chem.*, 1850, **75**, 27; D. Enders and J. P. Shilcock, *Chem. Soc. Rev.*, 2000, **29**, 359.
- 10 N. Farfan, L. Cuellar, J. M. Aceves and R. Contreras, *Synthesis*, 1987, **10**, 927.
- 11 Bruker Analytical X-ray Systems, *SMART: Bruker Molecular Analysis Research Tool*, version 5.618, 2000.
- 12 Bruker Analytical X-ray Systems, *SAINTE+NT*, version 6.04, 2001.
- 13 Bruker Analytical X-ray Systems, *SHELXTLNT*, version 6.10, 2000.
- 14 G. M. Sheldrick, *SHELX-97, Program for Crystal Structure Solution*, University of Göttingen, Germany, 1993.
- 15 R. I. Cooper, R. O. Gould, S. Parsons and D. J. Watkin, *J. Appl. Crystallogr.*, 2002, **35**, 168; ROTAX program.
- 16 P. Román-Bravo, M. López-Cardoso, P. García y García, H. Höpfl and R. Cea-Olivares, *Chem. Commun.*, 2004, 1940.
- 17 CSD version 5.25, November 2003, <http://www.ccdc.cam.ac.uk>; F. M. Allen, *Acta Crystallogr., Sect. B*, 2002, **58**, 380; I. J. Bruno, J. C. Cole, P. R. Edington, M. Kessler, C. F. Macrae, P. McCabe, J. Pearson and R. Taylor, *Acta Crystallogr., Sect. B*, 2002, **58**, 389.
- 18 A. E. Lindsay, A. R. Greenbaum and D. O'Hare, *Anal. Chim. Acta*, 2004, **511**, 185.
- 19 G. Mannaioni, A. Vannacci, C. Marzocca, A. M. Zorn, S. Peruzzi and F. Moroni, *J. Toxicol. Clin. Toxicol.*, 2002, **40**, 181.
- 20 L. J. Farrugia, *J. Appl. Crystallogr.*, 1999, **32**, 837–838; Win GX program set.
- 21 M. Nardelli, *J. Appl. Crystallogr.*, 1995, **28**, 659–660; PARST program, release Nov. 1999.
- 22 L. J. Farrugia, *J. Appl. Crystallogr.*, 1997, **30**, 565–566; ORTEP 3 program.
- 23 Mercury 1.1.2, Copyright CCDC 2001–2002, All rights reserved. For more information about this application, please contact User Support by e-mail at: support@ccdc.cam.ac.uk, or at the www site <http://www.ccdc.cam.ac.uk/mercury/>.

Hydrogenation in supercritical 1,1,1,2 tetrafluoroethane (HFC 134a)

Andrew P. Abbott,^a Wayne Eltringham,^a Eric G. Hope*^a and Mazin Nicola^b

Received 27th May 2005, Accepted 11th August 2005

First published as an Advance Article on the web 2nd September 2005

DOI: 10.1039/b507554h

Conventional, unmodified, transition metal catalysts, substrates and reagents have sufficient solubility in sc HFC134a for organic synthesis. Reactivities (100% conversion in 2 h) and enantioselectivities (*ca.* 90%), comparable to those achievable in conventional organic solvents, are obtained in the asymmetric hydrogenation of a series of substrates in this alternative reaction medium using a rhodium(I)/MonoPhos catalyst.

Introduction

Supercritical fluids (SCFs) have received a huge amount of attention, in both academia and industry, as alternative reaction media for more environmentally friendly chemical processes.^{1–4} The key advantages of SCFs arise from their tuneable polarity, high mass transport rates and environmental compatibility. Most studies have concentrated on scCO₂ because of the easily accessible critical constants, cost and low toxicity, exemplified by the recent launch of a scCO₂-based commercial hydrogenation process by Thomas Swan.⁵ Whilst the range of reactions evaluated in SCFs is large, the number of examples of asymmetric induction are few^{1–4} and these are virtually all restricted to scCO₂. Asymmetric hydrogenation of α,β -unsaturated carboxylic acids by [Ru(OAc)₂(BINAP)] in scCO₂ was reported to afford low conversions and low enantioselectivities, although both the conversion and ee's could be improved when the ligand was made more CO₂-philic by saturating two of the naphthyl rings.⁶ Solubility in scCO₂ can also be enhanced by the introduction of perfluoroalkyl substituents, for example in the 6,6'-positions of the BINAP ligand.^{7,8} However, we observed poor reactivity and enantioselectivity in the hydrogenation of dimethyl itaconate in scCO₂, which we have ascribed to the apolarity of the solvent.⁸ We,⁸ and others,^{6,9} have observed enhanced conversions and improved enantioselectivities for such ruthenium-catalysed asymmetric hydrogenations in scCO₂ by the addition of polar additives, such as methanol. However, here we add a note of caution since, under carefully controlled conditions, in our work it appears that the reaction is essentially finished *before* the conditions for scCO₂ had been reached.⁸ Asymmetric hydrogenation of α -enamides with a cationic Rh-DuPHOS catalyst has been made possible by using a highly fluorinated, CO₂-philic anion,¹⁰ and a similar approach has been adopted for the enantioselective hydrogenation of an imine with a cationic iridium catalyst.¹¹ We have also shown that the addition of a highly fluorinated anion offers improvements in both reactivity and asymmetric induction in the asymmetric hydrogenation of dimethylitaconate with cationic rhodium complexes containing perfluoroalkylated monodentate

phosphinite, phosphite and phosphoramidite ligands, but the results are, at best, modest.¹²

These studies suggest that, for asymmetric hydrogenation at least, the apolarity of scCO₂ is a significant issue. However, we have previously shown that some hydrofluorocarbon (HFC) fluids such as difluoromethane and 1,1,1,2 tetrafluoroethane (HFC 134a) are relatively polar solvents,^{13–15} even in the sc state, and this allows them to be used as efficient extraction solvents either on their own or in conjunction with CO₂.^{16,17} Furthermore, these solvents are also readily available and non-toxic. They have easily accessible critical constants (HFC 134a $T_c = 374.1$ K; $p_c = 40.6$ bar and CH₂F₂ $T_c = 351.1$ K; $p_c = 57.8$ bar), gaseous dipole moments of about 2 D¹⁵ and very high densities in the sc state. HFCs have been proposed as useful solvents for synthesis in the sc state and we have recently shown the first examples of the use of CH₂F₂ for the radical polymerisation of methylmethacrylate,¹⁸ the Friedel Crafts alkylation of anisole¹⁹ and the esterification of benzoic acid.²⁰ Here, we report our results using sc HFC 134a as a convenient, environmentally benign solvent, for enantioselective hydrogenation.

Results and discussion

The study took two parts. Initially, Wilkinson's catalyst was used for the homogeneous hydrogenation of styrene, as a test reaction, to establish catalytic protocols and the viability of HFC 134a as a solvent for hydrogenation. Subsequently, enantioselective hydrogenation in HFC 134a was evaluated using a rhodium/MonoPhos catalyst generated *in situ*.

Wilkinson's catalysts have often been used as model systems for the homogeneous hydrogenation of alkenes in liquid solvents^{21–23} and hence it was initially used for the hydrogenation of styrene in sc HFC 134a. Although the solubility of [RhCl(PPh₃)₃] in HFC 134a could not be measured quantitatively, a visual inspection using the cell shown in Fig. 1 showed that fully homogeneous solutions of Wilkinson's catalyst in HFC 134a up to 3×10^{-3} M, at 383 K in the pressure range of 50–280 bar, could be readily prepared. In marked contrast, a similar experiment using 1.3×10^{-3} mol dm⁻³ [RhCl(PPh₃)₃] in CO₂ at 313 K in the pressure range 50–120 bar did not show any evidence of catalyst dissolution. This is a significant observation indicating that HFCs can be used as reaction media for homogeneous catalysis without the need for

^aChemistry Department, University of Leicester, Leicester, UK LE1 7RH. E-mail: egh1@le.ac.uk; Fax: +44 116 252 3789

^bAdvanced Photonics Ltd, Olway Works, Healey Road, Ossett, West Yorkshire, UK WF5 8LT

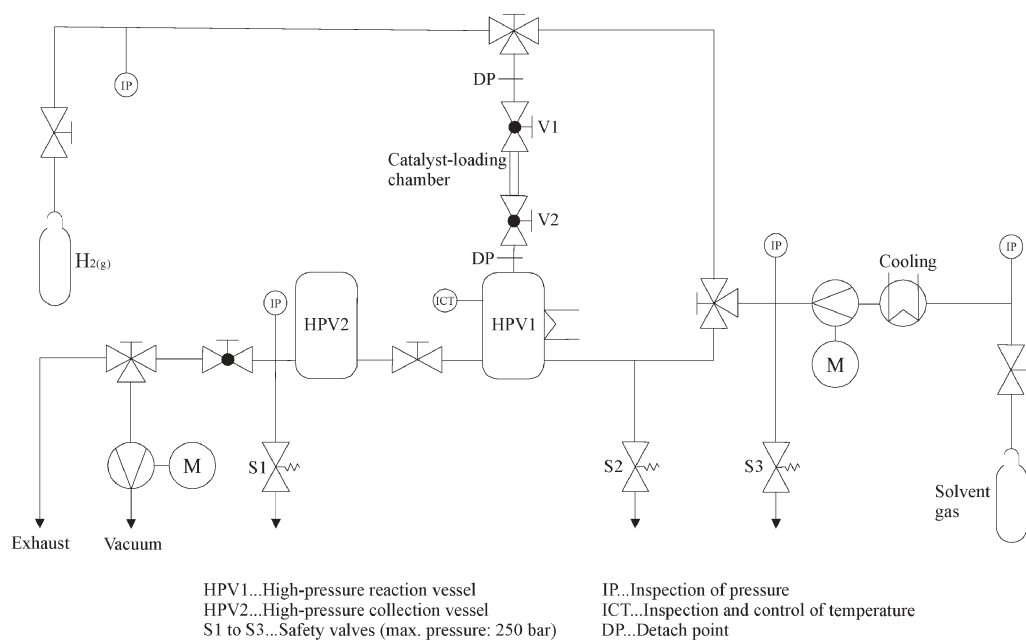


Fig. 1 Schematic diagram of the high-pressure apparatus used in this work.

co-solvents or modification of catalytic species, such as the addition of perfluoroalkyl-ponytails, which is often a requirement for homogeneous catalytic reactions in $scCO_2$.¹

Firstly, the time dependency of the hydrogenation of styrene ($6.56 \times 10^{-3} \text{ mol dm}^{-3}$) in sc HFC 134a, using $2.20 \times 10^{-6} \text{ mol dm}^{-3}$ of $[RhCl(PPh_3)_3]$ and 0.57 mol dm^{-3} of hydrogen at 383 K and 100 bar total pressure, was investigated. The results are shown in Fig. 2. It can be seen that the reaction reached maximum conversion after 1.75 h and, therefore, subsequent hydrogenation reactions were carried out for 2 h to ensure that the reaction had gone to completion. The time dependency results are generally the average of at least two determinations and a reproducibility of $\pm 3\%$ was obtained. Analysis of the data in Fig. 2 yields a reaction rate of $167 \pm 5 \text{ mmol dm}^{-1} \text{ h}^{-1}$ which is comparable to that reported for the hydrogenation of styrene in toluene.²³

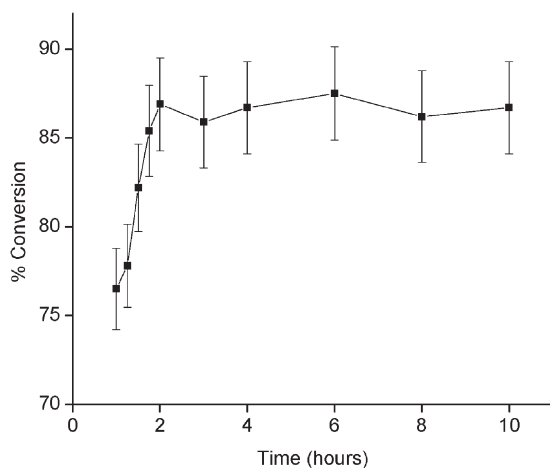


Fig. 2 Time dependency of the hydrogenation of styrene in HFC 134 using $2.20 \times 10^{-6} \text{ mol dm}^{-3}$ of $[RhCl(PPh_3)_3]$ and 0.57 mol dm^{-3} of hydrogen at 383 K and 100 bar total pressure.

The pressure dependency of the hydrogenation of styrene at 383 K was also investigated and the results are shown in Fig. 3. The results had a reproducibility of $\pm 3\%$ and the change in dielectric constant with pressure for the pure HFC 134a solvent at 383 K is also shown.¹⁵ Reactions were carried out at constant mole fraction in order to observe the effect of pressure on the % conversion and rule out the possibility of dilution effects as pressure is increased. The mole fractions used are the same as those used in the time dependency study at 383 K and 100 bar (Fig. 2). It can be seen that the % conversion increases with increasing pressure and this is attributed to the higher dielectric constant of HFC 134a at higher pressures. It was suggested by Wilkinson *et al.*^{21,22} that the rate determining step for the hydrogenation of olefins involves the formation of an activated complex, which has a greater dipole moment than the reacting species and that some charge separation is occurring during the formation of the

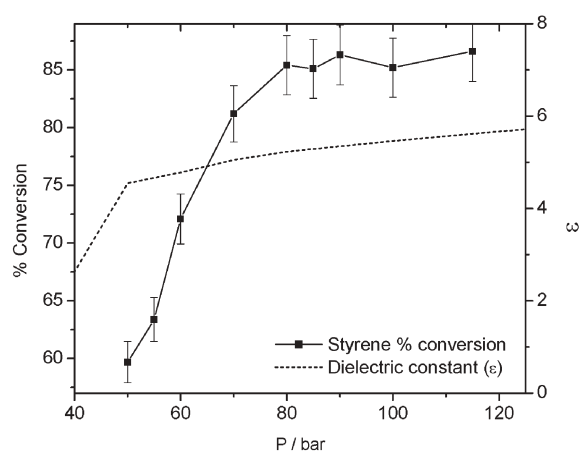


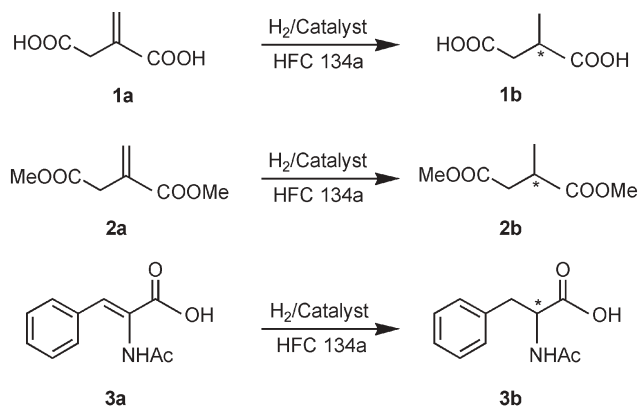
Fig. 3 Pressure dependency of the hydrogenation of styrene using $[RhCl(PPh_3)_3]$ in HFC 134a at constant mole fraction and 383 K.

activated intermediate. The formation of such an activated complex is likely to be more favourable in more polar solvents and is, therefore, more favourable in HFC 134a at higher pressures (higher dielectric constant).

This initial study, the first to use HFC 134a as a reaction medium, demonstrates that both catalytic species and substrates have sufficient solubilities without modification to afford homogeneous hydrogenation conditions, and that reactions rates comparable to those in liquid solvents can be obtained.

The asymmetric hydrogenation studies in sc HFC 134a were performed using $[\text{Rh}(\text{COD})_2\text{BF}_4]$ {bis(1,5-cyclo-octadiene)-rhodium(I) tetrafluoroborate} as the catalyst precursor and the monodentate (*R*)-MonoPhos ligand in a 1 : 2 ratio. MonoPhos, an air- and moisture-stable species, is easily prepared from readily available starting materials and it has been shown that it can facilitate highly enantioselective rhodium-catalysed hydrogenations in conventional solvent systems,^{24,25} whilst BF_4 electrolytes have been shown to be highly soluble and extensively dissociated in HFC 134a,^{26,27} making such a rhodium/MonoPhos catalyst ideal for investigating asymmetric hydrogenation in sc HFC 134a. Reactions were carried out using itaconic acid, dimethyl itaconate and (*Z*)- α -acetamido-cinnamic acid (**1a**, **2a** and **3a** respectively in Scheme 1) as model substrates. Prior to the catalytic studies in HFC 134a, we benchmarked the rhodium/(*R*)-MonoPhos catalytic system and our methodology in the hydrogenation of **1a–3a** in conventional organic solvents, where conversions and enantioselectivities very similar to those reported previously were obtained.²⁸

In HFC 134a hydrogenations were carried out at 383 K under a variety of pressures at constant mole fraction, so that dilution effects could be ruled out and the results are shown in Fig. 4 and 5. The results shown for the pressure dependency had a reproducibility of $\pm 4\%$ whereas those for the enantioselectivity have a larger error of $\pm 8\%$. It can be seen from Fig. 4 that the % conversion during the asymmetric hydrogenation reactions shows a similar dependence on pressure as those seen for styrene using $[\text{RhCl}(\text{PPh}_3)_3]$ in Fig. 3 and the same reasoning is offered to explain these trends. For conversions less than 100% it can be seen that the trend follows the order **1a** > **2a** > **3a** for a given pressure. One possible hypothesis for these observations is that there are two



Scheme 1 Reactions studied for asymmetric hydrogenation.

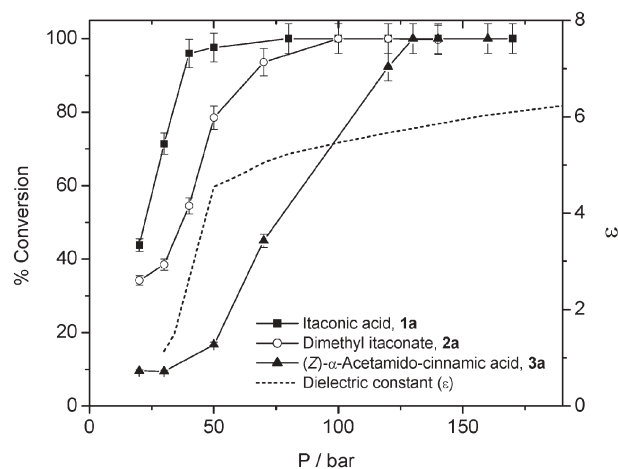


Fig. 4 Pressure dependency of % conversion for the asymmetric hydrogenation of substrates **1a–3a** in HFC 134a at 383 K.

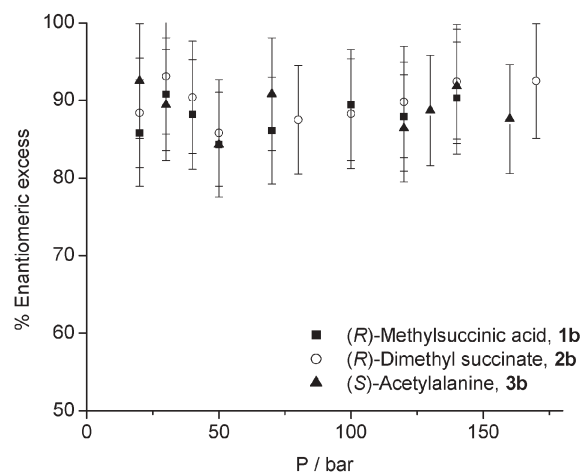


Fig. 5 Pressure dependency of enantiomeric excess for products **1b–3b** in HFC 134a at 383 K.

conflicting influences acting during the reaction; a negative steric effect and the positive effect of increasing dielectric constant. At lower pressures it is suggested that the reaction is under steric control and steric factors are hindering olefinic binding to the rhodium metal centre. The steric hindrance around the position of unsaturation for each substrate follows the trend **1a** < **2a** < **3a**. At higher pressures the dielectric constant becomes the influencing factor and the % conversion increases to its maximum value of 100%.

In contrast to our studies on asymmetric hydrogenation in scCO_2 ,⁸ the enantioselectivities for the hydrogenation of **1a–3a** in HFC 134a (Fig. 5) are comparable to some of those obtained in liquid solvents, which suggests that HFCs are promising alternative solvents for asymmetric hydrogenation of olefinic substrates. Within experimental error the enantioselectivities at constant mole fraction show no dependency on pressure and, therefore, no dependency on the dielectric constant of HFC 134a. These results are consistent with those of de Vries and co-workers²⁸ who carried out solvent screening studies with the rhodium/MonoPhos catalyst using the methyl ester of (*Z*)- α -acetamido-cinnamic acid and found that % ee

varied from 70 (methanol) to 95 (DCM) It was concluded that non-protic solvents lead to higher enantioselectivities than protic ones and that the effect of solvent polarity could be ruled out.

It is well known that the concentration of hydrogen can have an effect on the enantioselectivity during asymmetric hydrogenation.²⁹ Here, it was found that the % ee remained roughly constant at $89 \pm 2\%$, in the hydrogenation of **1a** at 383 K and 100 bar total, by varying the initial hydrogen pressure from 2 to 20 bar. These results complement those obtained using conventional organic solvents employing rhodium/MonoPhos^{24,25,28} and rhodium/MonoPhos-based³⁰ catalysts that have illustrated that the hydrogen pressure has no effect on enantioselectivity, and suggest that the mechanism of rhodium/MonoPhos catalysis is the same in sc fluids as in liquid solvents.

A study by Poliakoff *et al.*³¹ showed that the critical parameters of CO₂ were reduced during the hydrogenation of propane as the ratios of reagents to products changed. Here, α -acetamido-cinnamic acid was used as the substrate in a qualitative set of experiments to investigate the phase behaviour of the HFC 134a hydrogenation system. A windowed vessel was loaded with the same concentration amounts of **3a** and catalyst used for the asymmetric hydrogenation reactions and the system was pressurised with HFC 134a. This process was repeated twice more using the same concentration amount of catalytic material but with a 50/50 substrate/product mixture and with product alone (emulating the reaction going to completion). It was found from these investigations that, at 383 K, the lowest pressure at which multi-phase behaviour was observed was around 35–38 bar, which is a small reduction on the critical pressure of pure HFC 134a (40.59 bar). Above 38 bar and throughout the pressure dependency studies (Fig. 4) the system was in a single homogeneous phase.

Conclusion

This work has shown the first example of a reaction in sc HFC 134a. It has been demonstrated that homogeneous catalysts can be used for hydrogenation reactions without the need for co-solvents or fluorinated ponytails. The hydrogenation of styrene with Wilkinson's catalyst was used as a model system and it was found that reaction rates comparable to, and in some cases higher than, those in liquid solvents were obtained. The high reaction rates are attributed to the higher diffusivity of gaseous hydrogen in the supercritical media when compared to that in liquid solvents and the percentage conversion is dependent on the solvent dielectric constant, which can be tuned by manipulating the HFC 134a system pressure.

High conversions and enantioselectivities have been obtained for the asymmetric hydrogenation of a range of substrates using a rhodium-MonoPhos catalyst in HFC 134a, which suggests that HFCs are promising alternatives as reaction media for the industrially important asymmetric hydrogenation process. We have recently shown that methylsuccinic acid (**1b**) and itaconic acid (**1a**) have significantly different solubilities in HFC 134a and that this has been used to

develop an ideal supercritical fluid extraction process, for the separation of reagents and products, using a counter-current separating column.³² This, coupled with the high solubility of catalysts and reagents, suggests that HFC 134a is a useful alternative to CO₂ as solvent for reactions in the supercritical state.

Experimental

(*R*-)MonoPhos was prepared by the literature route,³³ and all other reagents/products were commercial samples and used as received.

The high-pressure cells were constructed from 316 stainless steel and were heated using 240 V, 250 W band heaters supplied by Walton Ltd. The temperature was controlled and maintained (± 0.5 K) using CAL 9900 heater/controllers fitted with an iron/constantan thermocouple, the tip of which was in contact with the solvent close to the centre of the cell. The high-pressure seals between the body of the cells and the cell tops were provided by Teflon[®] supported, standard nitrile o-rings. The cells had 3 cm thick walls, a maximum working pressure of 1 kbar and were rated to 1.5 kbar. Each high-pressure system was fitted with pressure relief valves set to 300 bar for safety. Pressure was applied using a Thar Technologies P-Series piston pump filled with polytetrafluoroethane (PTFE) composite seals in order to accommodate the use of hydrofluorocarbon (HFC) solvents.

The high-pressure system used for the hydrogenation work is shown schematically in Fig. 1. The catalyst-loading chamber is a 3×0.3 cm length of stainless steel pipe sealed at each end by a valve. V₁ is a two-way needle valve and V₂ is a two-way ball valve with a polychlorotrifluoroethylene (PCTFE) seat. The substrate was placed into the reaction vessel and the catalyst was loaded into the catalyst-loading chamber. In the case of air- and moisture-sensitive catalysts the chamber was loaded in a glove box and sealed under nitrogen using V₁ and V₂. The cell was heated to the desired temperature and evacuated to ensure the reaction vessel was air- and moisture-free. The vessel was charged with the required amount of hydrogen and then pressurised with the appropriate solvent using the P-Series piston pump. The solvent gas was passed through the catalyst-loading chamber, which flushed the catalyst into the reaction vessel, thus starting the reaction. When using HFC solvents, cooling was applied before the gas entered the pump because the pump is more efficient at pumping liquids. The reaction was left for the desired amount of time and the products/unreacted starting materials were collected by depressurisation into the larger volume collection vessel. The products were analysed using NMR (DPX 300), GC-MS (Perkin Elmer) and GC (Perkin Elmer Autosystem XL controlled by Turbochrom software). The enantiomeric excess values for the hydrogenation of dimethyl itaconate and α -acetamido-cinnamic acid were determined by GC using a ChiralDex B-DM column. The enantiomeric excess values for the hydrogenation of itaconic acid were determined using polarimetry. Absolute configurations for the itaconic acid and dimethyl itaconate hydrogenation products (methylsuccinic acid and dimethyl succinate) were determined by comparison with commercially available enantiomerically pure

products and that for acetylalanine, was determined using GC literature data.³⁴

The reagent amounts for the constant mole fraction asymmetric hydrogenation studies were 8.25×10^{-5} mol of substrate and MonoPhos, 4.13×10^{-7} mol of $\text{Rh}(\text{COD})_2\text{BF}_4$ and 1.65×10^{-4} mol of H_2 gas for reactions conditions of 100 bar and 383 K. All other reactions were based on these mole fraction values.

In a typical catalytic evaluation, small quantities of reagents were introduced into the cell by dissolving the solid in an appropriate organic solvent and transferring the solution using a Gilson pipette. The air-sensitive catalyst was dissolved in dried and degassed solvents and transferred into the catalyst-loading chamber in a glove box. The number of moles of hydrogen was converted to pressure values using data from the NIST Chemistry WebBook.³⁵

Acknowledgements

The authors would like to thank Advanced Phytonics Ltd and EPSRC (GR/R 05802) for funding this work.

References

- 1 P. G. Jessop, T. Ikariya and R. Noyori, *Chem. Rev.*, 1999, **99**, 475.
- 2 T. Kariy and Y. Kayaki, *Catal. Surv. Jpn.*, 2000, **4**, 39.
- 3 W. Leitner, *Acc. Chem. Res.*, 2002, **35**, 746.
- 4 E. J. Beckman, *J. Supercrit. Fluids*, 2004, **28**, 121.
- 5 S. K. Ritter, *Chem. Eng. News*, 2001, **79**, 27.
- 6 J. Xiao, S. C. A. Nefkens, P. G. Jessop, T. Ikariya and R. Noyori, *Tetrahedron Lett.*, 1996, **37**, 2813.
- 7 D. J. Birdsall, E. G. Hope, A. M. Stuart, W. Chen, Y. Hu and J. Xiao, *Tetrahedron Lett.*, 2001, **42**, 8551.
- 8 Y. Hu, D. J. Birdsall, A. M. Stuart, E. G. Hope and J. Xiao, *J. Mol. Catal. A*, 2004, **219**, 57.
- 9 X. Dong and C. Erkey, *J. Mol. Catal. A*, 2004, **211**, 73.
- 10 M. J. Burk, S. Feng, M. F. Gross and W. Tumas, *J. Am. Chem. Soc.*, 1995, **117**, 8277.
- 11 S. Kainz, A. Brinkmann, W. Leitner and A. Pfaltz, *J. Am. Chem. Soc.*, 1999, **121**, 1999.
- 12 D. J. Adams, W. Chen, E. G. Hope, A. J. West, J. Xiao and A. M. Stuart, *Green Chem.*, 2003, **5**, 118.
- 13 A. P. Abbott and C. A. Eardley, *J. Phys. Chem B*, 1998, **102**, 8574.
- 14 A. P. Abbott and C. A. Eardley, *J. Phys. Chem. B*, 1999, **103**, 2504.
- 15 A. P. Abbott, C. A. Eardley and R. Tooth, *J. Chem. Eng. Data*, 1999, **44**, 112.
- 16 A. P. Abbott, C. A. Eardley and J. E. Scheirer, *J. Phys. Chem., B*, 1999, **103**, 8790.
- 17 A. P. Abbott, C. A. Eardley and J. E. Scheirer, *Green Chem.*, 2000, **2**, 63.
- 18 A. P. Abbott, P. W. Dyer, E. G. Hope, S. Lange and S. Vukusic, *Green Chem.*, 2004, **6**, 81.
- 19 A. P. Abbott, N. E. Durling and E. G. Hope, *Chem. Phys. Chem.*, 2005, **6**, 466.
- 20 A. P. Abbott, N. E. Durling and E. G. Hope, *J. Phys. Chem. B*, 2004, **108**, 4922.
- 21 S. Montalatici, A. van der Ent, J. A. Osborn and G. Wilkinson, *J. Fluorine Chem.*, 1999, **99**, 197.
- 22 G. Wilkinson, R. D. Gillard and J. A. McCleverty, *Comprehensive Coordination Chemistry*, Pergamon Press, Oxford, 1987.
- 23 E. G. Hope, D. W. Kemmit, D. R. Paige and A. M. Stuart, *J. Fluorine Chem.*, 1999, **99**, 197.
- 24 X. Jia, R. Guo, X. Li, X. Yao and A. S. C. Chan, *Tetrahedron Lett.*, 2002, **43**, 5541.
- 25 A.-G. Hu, Y. Fu, J.-H. Xie, H. Zhou, L.-X. Wang and Q.-L. Zhou, *Angew. Chem. Int. Ed. Engl.*, 2002, **41**, 2348.
- 26 A. P. Abbott and C. A. Eardley, *J. Phys. Chem. B*, 2000, **104**, 9351.
- 27 A. P. Abbott, C. A. Eardley, J. C. Harper and E. G. Hope, *J. Electroanal. Chem.*, 1998, **457**, 1.
- 28 M. van den Berg, A. J. Minnaard, E. P. Schudde, J. van Esch, A. H. M. de Vries, J. G. de Vries and B. L. Feringa, *J. Am. Chem. Soc.*, 2000, **122**, 11539.
- 29 R. Noyori, *Asymmetric Catalysis in Organic Synthesis*, John Wiley and Sons, New York, 1994.
- 30 Q. Zeng, H. Liu, A. Mi, Y. Jiang, X. Li, M. C. K. Choi and A. S. C. Chan, *Tetrahedron*, 2002, **58**, 8799.
- 31 J. Ke, W. George, M. Poliakoff, B. Han and H. Yan, *J. Phys. Chem. B*, 2002, **106**, 4496.
- 32 A. P. Abbott, W. Eltringham, E. G. Hope and M. Nicola, *Green Chem.*, 2005, **7**, 210.
- 33 R. Hulst, N. Koen de Vries and B. L. Feringa, *Tetrahedron: Asymmetry*, 1994, **5**, 699.
- 34 α -Acetamido-cinnamic acid is a test substrate used by Chiraldex and the order of elution and separation conditions for the Chiraldex B-DM column are given in the Chiraldex handbook. Absolute configuration was determined using the handbook data.
- 35 <http://webbook.nist.gov/chemistry/>.

Biphasic hydrogenation of α -pinene in high-pressure carbon dioxide

Anna Milewska,^a Anna M. Banet Osuna,^a Isabel M. Fonseca^b and Manuel Nunes da Ponte^{*ab}

Received 26th April 2005, Accepted 9th August 2005

First published as an Advance Article on the web 31st August 2005

DOI: 10.1039/b505873b

Results on the kinetics of hydrogenation of α -pinene in high-pressure carbon dioxide, using Pt/C (1%) catalysts, are presented. Experiments were performed at different carbon dioxide pressures, so that the reaction mixture in contact with the solid catalyst would either be biphasic (liquid + gas) or a single supercritical phase. The technique involved the use of a high-pressure view cell, which allows direct visual observation of the number of phases in the reactor. The hydrogenations in biphasic conditions, at lower carbon dioxide pressures, are completed faster than in supercritical conditions. The results indicate that the pinene adsorption to the metal in the catalyst is the rate-controlling step.

1. Introduction

Reactions in supercritical fluids are an established field of research in the area of Green Chemistry.^{1–3} Carbon dioxide is by far the most studied supercritical fluid, due to its low price, its advantages as a “generally regarded as safe (GRAS)” solvent, and also due to its convenient critical temperature, which allows it to be used as a supercritical fluid just above room temperature.

Supercritical fluids are gases, and they mix completely with other gases, like hydrogen. Those fluids have consequently been regarded as potentially advantageous solvents for carrying out hydrogenation reactions, especially in the cases where the reactants to be hydrogenated are also soluble. In these situations, all reactants will be in a single fluid phase, and the access of hydrogen to the catalyst (either heterogeneous or homogeneous) will be easier than in the case of biphasic, liquid–gas reaction media. Härröd *et al.*,⁴ for instance, developed processes where the hydrogenation of fatty acid methyl esters is carried out in propane. This gas is a sufficiently good solvent of the esters to allow the reaction to be carried out in one single supercritical phase contacting the solid catalyst, and with enough hydrogen to ensure an extremely fast and selective reaction. Carbon dioxide was not chosen, because the solubilities of the esters in the supercritical gas are indeed too low.

The fact is, however, that at least some of the hydrogenations in carbon dioxide reported in the literature are clearly carried out in a biphasic, gas + liquid system. Striking examples are many of those described by Hitzler *et al.*,⁵ who managed to perform fast hydrogenations using a highly effective flow process, either at the laboratory level or at the large-scale pilot plants built at the Thomas Swan site.

These possibilities have been recently explained on the basis of the high solubility of carbon dioxide in many organic

liquids, even those that hardly dissolve at all in the gas phase. The high quantity of CO₂ in the liquid makes it an “expanded fluid”, as pointed out by Wei *et al.*,⁶ avoiding the need to generate a single phase of CO₂, reactants and products. In that situation, the solubility of gaseous reactants in the liquid phase increases, and transport limitations towards the catalyst are, at least, greatly minimised. Simply ensuring that a significant amount of CO₂ is present in the liquid phase may be sufficient to gain kinetic control over the reaction. Another advantage of this type of approach is that reactions can be carried out at lower (sometimes much lower) pressures than in truly supercritical conditions.

This focus on phase behaviour was already present in the review chapter of Darr and Poliakov,⁷ and it brought about the understanding that the densities of liquid mixtures close to the mixture critical line are sufficiently lower than those of a “classical” liquid exhibiting the same type of property values (lower viscosity, higher diffusivity, higher solubility of gases) that confer enhanced mass transfer capabilities to supercritical solvents.

Chouchi *et al.*⁸ carried out the hydrogenation of α -pinene in CO₂-containing mixtures. These mixtures can be easily turned either biphasic (liquid + gas) or single-phase (supercritical), by small changes in pressure, at moderate pressures—around 100 bar. Using a Pd catalyst, the hydrogenation of α -pinene was surprisingly faster in a two-phase system than when a single-phase contacts the catalyst. This was possibly the first study where a comparison was made using the same reactants and catalyst, but with different phase behaviour, with only small changes in the process parameters. Those authors interpreted their data based on the assumption that the rate was controlled by the adsorption of pinene, and not hydrogen, at the catalyst surface. As for many other liquids, CO₂ is highly soluble in pinene; at pressures close to the critical pressure, the liquid phase in a biphasic mixture can contain 80 mol% or more of CO₂. Hence, the liquid reactant is an “expanded liquid”, which can dissolve large quantities of hydrogen, thus significantly increasing its concentration in the vicinity of the solid catalyst, even when the system is biphasic. If the adsorption of pinene is related to the limiting rate step, a biphasic system will lead to higher rates, because pinene will be

^aInstituto de Tecnologia Química e Biológica, Universidade Nova de Lisboa, Apt. 127, 2781-901 Oeiras, Portugal.

E-mail: mnponde@itqb.unl.pt; Fax: +351 21 442 1161;

Tel: +351 21 446 9444

^bREQUIMTE, Departamento de Química, Faculdade de Ciências e Tecnologia, Universidade Nova de Lisboa, 2829-516 Caparica, Portugal

more concentrated in the liquid around the catalyst than when diluted in a single supercritical phase. The opposite will happen for catalysts where hydrogen adsorption controls the rate.

In order to check these assumptions, it was desirable to perform the same reaction using different catalysts. Herein we report studies of the catalytic hydrogenation of α -pinene in supercritical CO_2 using carbon-supported platinum catalysts. These catalysts were chosen because they could be prepared in different ways, in order to yield radically diverse types of distribution of metallic platinum on the surface of the support, allowing in principle very different conditions for adsorption of pinene, the reactant with the bulkier molecule. Although it is known that CO_2 itself can be reduced to CO by hydrogen in the presence of platinum,⁹ leading to the poisoning of catalysts, Bhanage *et al.*¹⁰ have managed to perform highly selective hydrogenations of aldehydes using Pt/ Al_2O_3 catalysts. These reactions were carried out in such pressure-temperature conditions that the reaction system was most probably biphasic. It was therefore interesting to check whether the lower carbon dioxide pressures used in the above-described “expanded-liquid” situation, coupled to lower availability of hydrogen to the catalyst, could protect it from poisoning.

Reaction rates were measured, either in biphasic or single-phase conditions, in a newly assembled apparatus, with some characteristics similar to the one described by Devetta *et al.*¹¹ in their study of the biphasic catalytic hydrogenation of an unsaturated ketone in CO_2 . The experiments were planned so that the results might elucidate the effect of pressure of H_2 and CO_2 on the rate and the selectivity of the reaction.

2. Experimental

2.1 Materials

The Pt/C (1%) catalysts were prepared using an impregnation method.^{12,13} 1 g of granular activated carbon Norit GAC 1240 was impregnated with 10 cm³ of aqueous solution of $\text{H}_2\text{PtCl}_6 \cdot 6\text{H}_2\text{O}$ with the appropriate concentration to obtain a Pt load of 1 wt%. Nitrogen was bubbled through the suspension up to the total vaporisation of the liquid, and the remaining solid was dried in an oven at 120 °C. The catalyst was first heated in nitrogen at 350 °C for 2 h and then reduced in hydrogen, for another 2 h, at increasing temperatures up to 480 °C. Textural characterisation was performed by N_2 adsorption at 77 K on an ASAP 2010 V1.01 B Micromeritics instrument. The samples were degassed at 423 K for 24 h prior to adsorption measurements.

Essentially two types of catalysts were prepared, one with well distributed platinum through the whole volume of the carbon support, and another one with the metal essentially accumulated at the outer surface. That difference was obtained by inducing different oxidation of the carbon support surfaces before impregnation. The activated carbon was divided in two samples, and one of them was treated in air at 300 °C. It is, in fact, well known that the oxygen surface groups on the carbon surface play an important role in the final Pt distribution.¹²

The BET apparent surface area (S_{BET}), the micropore volume (V_{mic}) and the total pore volume (V_{p}), were determined according to BET theory, and the t -plot method.

The Pt dispersion on the activated carbon was observed using an electronic transmission microscope (TEM) Jeol-JEM-2010 (2×10^{-5} , 200 kV). Samples were dispersed in acetone and spread over self perforated microgrids. Dispersion values were obtained on the basis of the calculated average particle diameter. Scanning electron microscopy (SEM) with a Hitachi S-2400 apparatus was also used to characterise the catalyst surface.

Hydrogen and carbon dioxide were supplied by Air Liquide, with a stated purity of 99.998 mol%. α -Pinene (purity: 99%) and *cis*-pinane (purity > 99%) were supplied by Fluka.

2.2 Experimental set-up

Experiments of the hydrogenation of α -pinene in high-pressure CO_2 were carried out at 50 °C, using 2 ml of α -pinene and about 0.4 g of catalyst, in a newly built apparatus. Fig. 1 is a schematic representation of the apparatus. It consists essentially of two cells connected by a pump. The first cell is a sapphire-windowed reactor (VC) (New Ways of Analytics) with an internal volume of approximately 50 cm³. This reactor is provided with a magnetically driven stirrer for efficient mixing of the components (max. speed: 2500 rpm), as well as a wide sapphire window (diameter: 36 mm, thickness: 16 mm). The temperature control is achieved by means of a PID controller (T) (Eurotherm 2216e) connected to a Pt-100 probe located in the reactor and two 100 W resistances inserted in the reactor walls. The pressure inside the reactor is measured with a pressure transducer (PT) (Setra C204).

The second cell is the actual chemical reactor (CR). It is a short tube, which encloses a catalyst bed. Electrical heating wire is wrapped around the tube, connected to a controller and a Pt 100 temperature sensor (T). The temperature in the reactor is kept at the same value as the temperature in the cell.

The reactants are continuously withdrawn from the bottom of the view cell by a high-pressure piston pump (PP), circulated through the catalyst bed, and sent back to the upper inlet of the first cell. The outlet of the sapphire-windowed cell is

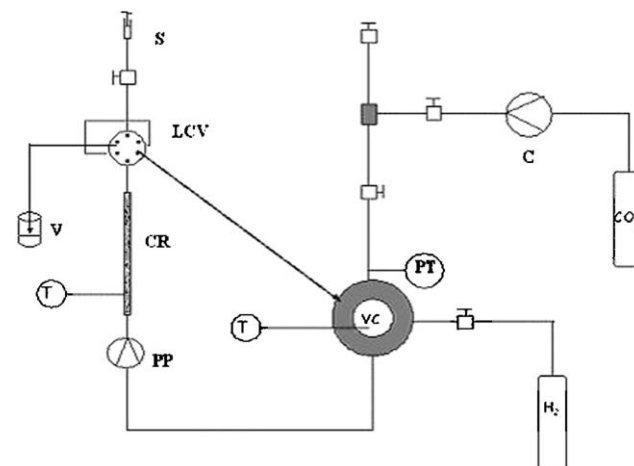


Fig. 1 Schematic representation of the apparatus for hydrogenation reactions at high pressure: (C) CO_2 compressor, (CR) reactor, (LCV) liquid chromatography valve, (PP) high-pressure piston pump, (PT) pressure transducer, (S) syringe, (T) temperature controller, (V) vial, (VC) view cell.

located at the bottom, so that, when the mixture in the cell is biphasic, it is the lower, liquid phase that is circulated through the catalyst bed. The nominal flow generated by the piston pump is 8 g min^{-1} .

A liquid chromatography switching valve (LCV) (Rheodyne 7000), equipped with a $100 \mu\text{l}$ loop connected on-line to the reactor outlet, was used to collect, at regular intervals, samples of the reaction mixture right after it passed through the catalyst. Samples were collected in a vial (V), and bubbled through a measured amount of hexane, which was used as solvent. The samples were subject to gas chromatography (Varian 3800 GC) analysis, with FID detector, equipped with a dimethylpolysiloxane column (CP-Sil 8 CB, 30 m long, 0.32 mm id, film thickness of 0.25 mm), working between 373 K and 473 K with a heating range of 15 K min^{-1} .

2.3 Reaction experiments

Reaction experiments were performed at $50 \text{ }^\circ\text{C}$, using 2 ml of α -pinene and about 0.4 g of catalyst. The reactor is first flushed with low-pressure CO_2 and then hydrogen at pressures between 10.0 MPa and 11.0 MPa was circulated through the catalyst cell during about 15 h before each reaction run. This was done in order to reactivate the catalyst, so that each experiment would start with the catalyst in identical conditions.

The actual experiment starts by venting hydrogen to the desired pressure. A measured amount of pinene is then loaded into the top valve above the cell (see Fig. 1), by means of a syringe, and through a thin tube that travels inside the outer tube, and ends past the cross connection below the valve. With this configuration, the liquid pinene sample is positioned so that incoming CO_2 flow, introduced by means of a compressor, pushes it into the cell. When the final desired total pressure is reached, the stirrer and the circulation pump are switched on.

During the reaction, samples are withdrawn from the reactor at regular intervals by means of a high-pressure switching valve, described in section 2.2. The content in the loop is then carefully depressurised to the atmosphere in a closed vial filled with hexane in order to trap the α -pinene and the pinane. Finally, the switching valve loop is washed twice with approximately 2 ml of hexane and flushed with N_2 . The hexane fractions are analysed by gas chromatography. The concentrations of α -pinene and of pinane in the collected samples are determined using dodecane as an internal standard (response factor for α -pinene: 0.90; response factor for pinane: 0.81; precision of the method: better than 10%). Pinane is actually composed of two isomers, *cis* and *trans*, which appear as two close, but separate peaks in the chromatographs. The *cis/trans* ratio could therefore be quantified.

3. Experimental results and discussion

3.1 Preliminary experiments with different catalysts

The influence on reaction rates of the distribution of platinum in the outer surface of the catalyst carbon support was studied. As mentioned in sub-chapter 2.1, two types of catalysts were prepared, one with well distributed platinum over the whole volume of the carbon support, and another one with the metal

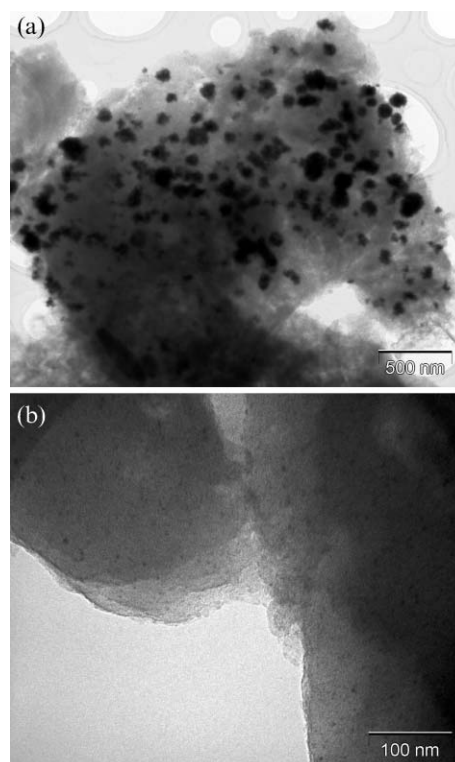


Fig. 2 Transition electron microscopy pictures of two different Pt/C (1%) catalysts. [a] Bad distribution (Pt is shown in large, black dots), [b] Good distribution (Pt corresponds to the small dots).

essentially accumulated at the outer surface. Transmission electron microscopy results are shown in Fig. 2. It is quite apparent in Fig. 2 (a) that the metal is accumulated in large particles, while Fig. 2 (b) shows a more uniform distribution, with the platinum particles corresponding to the small, darker dots. The dispersion of platinum was calculated, from the TEM micrographs, as the ratio between the number of surface metal atoms and the number of metal atoms present at the catalyst. The values obtained were: (a) 2.24% D; (b) 56.1%.

On the other hand, the SEM images have shown that catalyst (a) accumulated platinum on the surface, while in catalyst (b) the platinum was more distributed over the whole volume of support. A surface EDX analysis gave the following values for the weight surface platinum composition: (a) 70%; (b) 22%.

Table 1 gives the values of BET specific apparent surface area, volume of micropores and total pore volume. The adsorption–desorption isotherms of the carbon support are of type I, as defined by IUPAC, characteristic of microporous

Table 1 BET apparent surface area (S_{BET}), total pore volume (V_{p}), and micropore volume (V_{mic}) for the carbon support and for the two catalysts

Catalyst	$S_{\text{BET}}/\text{m}^2 \text{ g}^{-1}$	$V_{\text{p}}/\text{cm}^3 \text{ g}^{-1}$	$V_{\text{mic}}/\text{cm}^3 \text{ g}^{-1}$
Carbon	1008	0.57	0.50
Pt/C (1%) ^a	842	0.51	0.44
Pt/C (1%) ^b	795	0.50	0.30

^a Catalyst with Pt at the outer surface of the support. ^b Catalyst with well distributed Pt.

carbons, with a small type H4 hysteresis loop. Comparing the supported catalysts with the parent carbon, the sample with well-dispersed Pt shows a larger decrease in surface area, especially in the micropore volume. This result suggests that the metal is dispersed inside the porous structure, and it is consistent with the TEM photographs. In fact, the less platinum is on the surface, the more it should fill the carbon pores, decreasing the surface area, as well as the micropore volume.

Preliminary reaction experiments were carried out at 4 MPa hydrogen pressure plus either 8.5 or 12 MPa carbon dioxide pressures, corresponding to total pressures in the cell of 12.5 MPa (and a two-phase system) or 16 MPa (and a single phase regime), respectively. The reaction rates were highly dependent on the distribution of platinum on the carbon surface. When the platinum was mainly on the outer surface of the carbon, high reaction rates were obtained for the hydrogenation of α -pinene. In contrast, when the platinum was mainly inside the pores of the carbon (good dispersion), very low conversions were observed.

The observations with the two different types of catalyst are consistent with kinetics controlled by the adsorption of α -pinene to the catalyst active sites. In fact, as this is a bulky molecule, the mass transfer limitations to diffuse into the solid support are certainly much higher than for hydrogen.

The experimental results presented below were all obtained with the catalyst pictured in Fig. 2 (a).

3.2. The influence of carbon dioxide pressure on reaction rates

Pinene conversion rates were measured at a fixed initial pressure of hydrogen (4 MPa), with a range of different pressures of carbon dioxide: 3.0 MPa, 6.0 MPa, 7.5 MPa, 8.5 MPa, 9.6 MPa, 12.0 MPa and 14.0 MPa. It should be noted that these denominated CO₂ pressures are obtained by subtraction of the initial pressure of hydrogen from the total final pressure in the cell. They cannot indeed be taken as partial pressures, as the mixtures behave in a highly non-ideal way, even when they are supercritical gases. Notwithstanding, the phase behaviour of the α -pinene + carbon dioxide + hydrogen mixtures is very similar, at least in terms of phase boundaries and critical pressures, to the behaviour described by Pavlíček and Richter,¹⁴ and by Akgün *et al.*¹⁵ for α -pinene + CO₂ mixtures, if the carbon dioxide pressure is taken as defined above for the ternary mixture. In fact, visual observation through the sapphire window of the mixture inside the cell has shown that, for p_{CO_2} from 3.0 to 8.5 MPa, the reaction mixture presents two-phase (liquid–vapour) equilibrium, while at 12.0 and 14.0 MPa, it is in a single, supercritical phase. These conditions were maintained during the reaction time.

For the intermediate case of 9.6 MPa, the reaction starts in single phase conditions and continues in two phases. In fact, the formation of a liquid phase in the cell, after about 15 min of reaction, could be observed through the sapphire window. That pressure of carbon dioxide is very close to the critical pressures at the temperature of 323 K of α -pinene + CO₂ given by those authors. As explained by Chouchi *et al.*,⁸ at 9.6 MPa the reaction mixture starts in one phase, but the system enters into the two-phase region when enough pinene is produced by

Table 2 Product yields—mass percentage of pinane in relation to the total pinene + pinane—at the given reaction times (t), at a fixed hydrogen pressure of 4 MPa, and different carbon dioxide pressures (p_{CO_2})

t/min	$p_{\text{CO}_2}/\text{MPa}$						
	14	12	9.6	8.5	7.5	6	3
5	24	30	22	17	18	13	6
10	34	40	40	35	31	29	15
15	43	49	46	46	45	42	21
30	57	63	70	71	70	62	35
60	74	78	95	95	92	84	65
120	88	92	100	99	99	95	79

the reaction process, as pinane is less soluble in carbon dioxide than pinene.

The results are given in Table 2 as product yields—mass percentage of pinane, the reaction product, in relation to the total pinene + pinane—in each sample, taken at the given reaction times. These yields are graphically represented in Fig. 3.

The first samples, taken at five minutes, seem to indicate a direct dependence of initial rates on CO₂ pressure, but they probably only translate effects of pressure dependence of mixing reactants in the cell. Indeed, the subsequent samples, taken at 10 min and 15 min, show that the initial rates are remarkably independent of carbon dioxide pressure and of the phase behaviour of the system, except for the lower CO₂ pressure (3 MPa). As the reaction proceeds, and when about 50% conversion is attained, the reaction rates start diverging noticeably. The rates of mixtures at supercritical conditions (filled symbols in Fig. 3, corresponding to pressures of 12 MPa and 14 MPa) become lower than those of the biphasic mixtures at the highest pressures (7.5 MPa, 8.5 MPa and 9.6 MPa), when the conversions reach a level about 50%. The biphasic mixture at 3 MPa carbon dioxide pressure exhibits the lower conversions at all times, while the mixture at 6 MPa shows an intermediate behaviour.

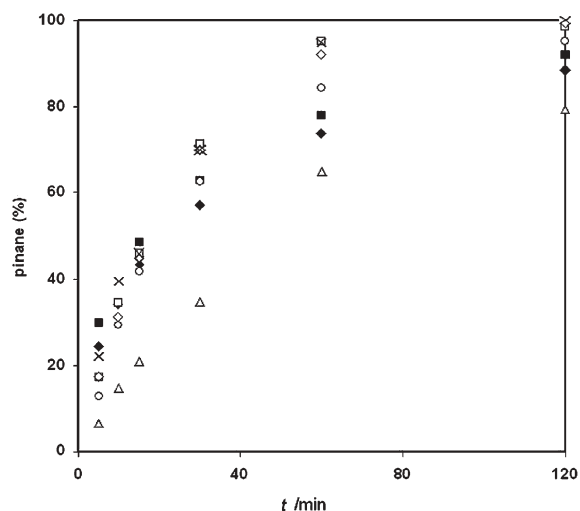


Fig. 3 Mass percentages of pinane, the reaction product, in relation to pinene + pinane, in samples taken at time t , using 4.0 MPa of H₂ and seven different pressures of carbon dioxide: (Δ) $p_{\text{CO}_2} = 3.0$ MPa; (\circ) $p_{\text{CO}_2} = 6.0$ MPa; (\diamond) $p_{\text{CO}_2} = 7.5$ MPa; (\square) $p_{\text{CO}_2} = 8.5$ MPa; (\times) $p_{\text{CO}_2} = 9.6$ MPa; (\blacksquare) $p_{\text{CO}_2} = 12.0$ MPa; (\blacktriangle) $p_{\text{CO}_2} = 14.0$ MPa.

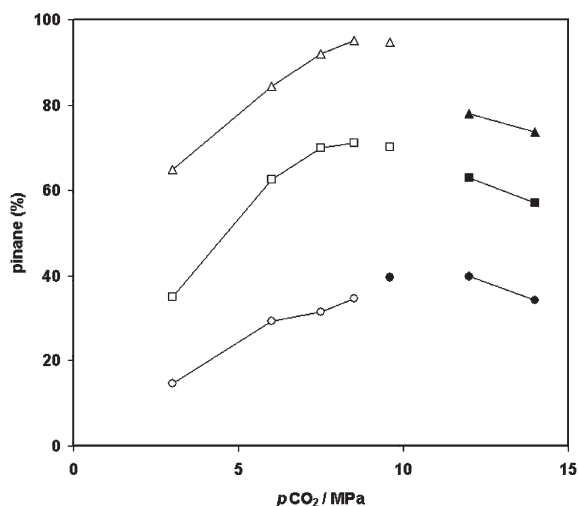


Fig. 4 Mass percentages of pinane, the reaction product, in relation to pinene + pinane, in samples taken at time: (●,○) 10 min; (■,□) 30 min; (▲,△) 60 min. Filled symbols correspond to single phase, supercritical mixtures, open symbols correspond to biphasic mixtures.

These trends are better perceived in Fig. 4, where the conversions at 10, 30 and 60 min are plotted as a function of the CO₂ pressure. In this figure, the open symbols denote biphasic mixtures and the filled ones, supercritical (single phase) mixtures.

An explanation for this behaviour might be that, except at a CO₂ pressure of 3 MPa, the access of hydrogen to the catalyst is sufficiently good to ensure enough material adsorbed at the surface of the catalyst for the reaction to proceed. Even in biphasic conditions, carbon dioxide dissolves in large amounts in the liquid terpene. Using the results for carbon dioxide + α -pinene^{14,15} as guide, the mass percentage of carbon dioxide in the liquid varies from 35% to more than 90%, at CO₂ pressures from 7.5 MPa to 9.6 MPa. This high content of carbon dioxide should significantly increase the solubility of hydrogen in the liquid, and its accessibility to the catalyst.

Although no measurements of the hydrogen solubility in α -pinene + CO₂ liquid mixtures have so far been performed, calculations can be performed. Pereda *et al.*¹⁶ have recently used group contribution equation of state models described by Pereda *et al.*¹⁷ to calculate the phase boundaries of the ternary α -pinene + CO₂ + H₂. Moreover, in their work on the hydrogenation of imides in ionic liquid + high pressure carbon dioxide, Leitner *et al.*¹⁸ have used a NMR technique to measure the hydrogen solubility in the liquid as a function of carbon dioxide pressure. Although their ionic liquid + CO₂ mixture is fundamentally different from α -pinene + CO₂, because the two-phase separation remains at least up to very high pressures, hydrogen shows a remarkable increase in solubility in the ionic liquid when CO₂ pressure increases above about 6 MPa.

3.3. The influence of carbon dioxide pressure on *cis/trans* pinane ratios

In order to further explore this hypothesis, the *cis/trans* pinane ratio was measured for each sample. Mechanisms have been

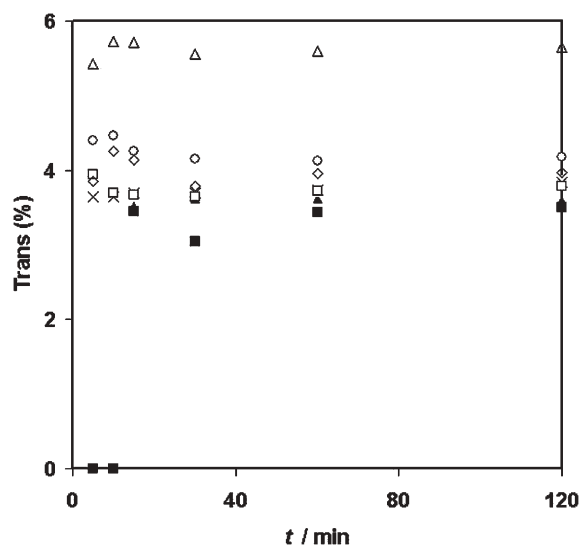


Fig. 5 Percentage of *trans*-pinane in the reaction product vs. time. Reaction conditions and symbols as in Fig. 3.

proposed by Ilyna and Semikolenov¹⁹ that explain the increase of selectivity of the reaction towards the *cis* isomer when hydrogen pressure increases, in a reaction carried out in biphasic conditions α -pinene (liquid) + hydrogen (high pressure gas). The *cis/trans* ratio might therefore be a sensitive indicator of the accessibility of hydrogen to the catalyst.

In Fig. 5, the *trans*/(*trans* + *cis*) percentage is plotted. The selectivity towards the *cis* isomer is clearly lower for the 3 MPa CO₂ pressure system, with an average *trans* percentage yield of 5.6%. This behaviour is consistent with the hypothesis that the lower conversion rates are due to reduced hydrogen accessibility to the catalyst.

At all higher pressures, the *trans* yield is around 4%, with the exception of the two higher pressures at 5 min and 10 min, where the *trans* isomer was not quantifiable. These results might however be due to the small concentration in pinane of these samples, which could have brought the small *trans* peak in the chromatograph below the detection limit of the apparatus. The mixtures at 9.6 MPa (either single phase, below 15 min, or biphasic) and at 8.5 MPa (always biphasic) yield very similar results. A slight trend towards higher *cis* selectivity (lower *trans*%) with higher carbon dioxide pressure is barely discernible.

The amount of hydrogen surrounding the catalyst is therefore sufficient to ensure high selectivity towards *cis*-pinane at all carbon dioxide pressures, except 3 MPa, whether the reacting system is biphasic or a single phase.

3.4. The influence of hydrogen pressure on reaction rates

In order to further study the accessibility of hydrogen to the catalyst in biphasic conditions, different initial pressures of hydrogen: 0.1 MPa, 2 MPa, 4 MPa, 6 MPa, and 8 MPa were used, at a fixed pressure of carbon dioxide of 8.5 MPa. In these experiments (with the obvious exception of atmospheric pressure), as in the experiments described above, hydrogen is always the reactant in excess, allowing, in principle, complete conversion of the α -pinene. The experiments at atmospheric pressure were performed after venting completely the

Table 3 Product yields—mass percentage of pinane in relation to the total pinene + pinane—at the given reaction times (t), at a fixed carbon dioxide pressure of 8.5 MPa, and different hydrogen pressures (p_{H_2})

t/min	$p_{\text{H}_2}/\text{MPa}$					
	8	6	4	4 ^a	2	0.1
5	21	34	21	17	39	8
10	39	54	37	35	50	9
15	53	68	48	46	70	11
30	80	89	71	71	90	15
60	98	98	90	95	97	21
120	99	99	97	99	98	24

^a Corresponds to the experiment in Table 2.

hydrogen used for reactivation of the catalyst. They aimed at sorting out the effect of the hydrogen stored inside the catalyst during the activation process, always performed before the start of each new experiment.

The values of the conversion yields obtained are given in Table 3. They are plotted in Fig. 6, as a function of time. In this figure, the results given in Table 2 for $p_{\text{CO}_2} = 8.5$ MPa and $p_{\text{H}_2} = 4$ MPa are also included. They agree well with the data obtained in the new experiment given in Table 3.

It may be concluded that there is no discernible influence of hydrogen pressure, down to 2 MPa, on the reaction rate. Another interesting observation is that even when no additional hydrogen is added, the reaction can proceed to some extent with the hydrogen stored in the catalyst material during the activation process.

The *trans*-pinane percentage yield, as defined above, is plotted in Fig. 7. Several conclusions may be drawn from the graphic:

(1) At atmospheric pressure of hydrogen, the yield of *trans* isomer is much higher than for any other condition. It increases with time, as the amount of hydrogen stored in the catalyst reacts without being replaced by fresh hydrogen brought from the bulk of the reaction mixture. This result is consistent with the hypothesis that the *trans*-pinane yield is a

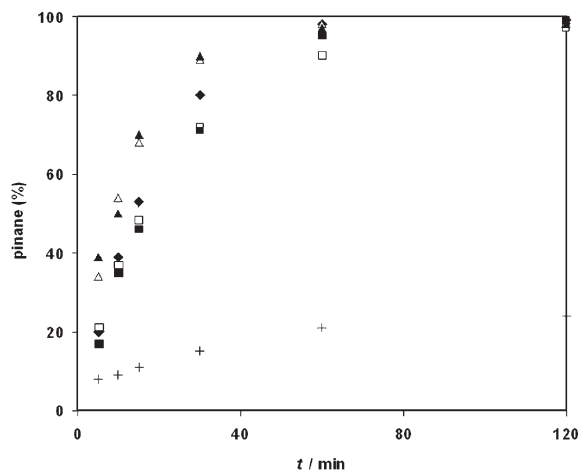


Fig. 6 Mass percentages of pinane, the reaction product, in relation to pinene + pinane, in samples taken at time t , using 8.5 MPa of CO_2 and five different pressures of H_2 : (+) $p_{\text{H}_2} = 0.1$ MPa; (▲) $p_{\text{H}_2} = 2.0$ MPa; (□) $p_{\text{CO}_2} = 4.0$ MPa; (■) $p_{\text{CO}_2} = 4.0$ MPa, Table 1; (△) $p_{\text{H}_2} = 6.0$ MPa; (◇) $p_{\text{H}_2} = 8.0$ MPa.

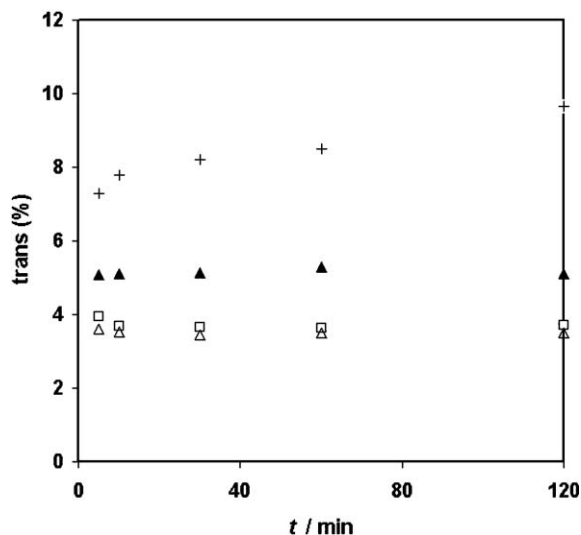


Fig. 7 Percentage of *trans*-pinane in the reaction product vs. time. Reaction conditions and symbols as in Fig. 6 ($p_{\text{H}_2} = 4.0$, Table 2, and $p_{\text{H}_2} = 8.0$ not shown).

sensitive indicator of the availability of hydrogen in the catalyst surroundings.

(2) At 4 MPa and 6 MPa, the *trans* isomer yields are virtually indistinguishable, and they average 3.6%, of the same order as shown in Fig. 5 for all CO_2 pressures above 7.5 MPa. At 2 MPa the selectivity towards the *cis* isomer is lower (the *trans*-pinane yield averages 5.1%), although the reaction rates are still high, as shown in Fig. 6.

Comparison with the results obtained at 3 MPa of CO_2 pressure and 4 MPa of hydrogen pressure, where the average *trans* yield is 5.6% and the reaction rates are clearly smaller, indicate that the *cis/trans* isomer ratio is affected by the reduction in hydrogen availability to the catalyst before any effect is felt on the reaction rate.

All these conclusions point to the concentration of α -pinene around the catalyst as the main factor that determines the reaction rates.

3.5. The influence of α -pinene concentration on the reaction rates

The concentration of α -pinene in the fluid crossing the catalyst bed can be calculated with reasonable precision, as 2 ml of this substance are used for each experiment, and the overall available volume in the cell is approx. 50 cm^3 . When the system is monophasic, at high pressures of carbon dioxide, the pinene concentration is uniform throughout the whole volume. At the start of each experiment, a simple calculation yields a concentration around 0.03 g cm^{-3} . When the system is biphasic, the liquid phase is the one in contact with the catalyst, because the circulation starts from the bottom of the cell. Most of the pinene will remain in the liquid phase, as its solubility in the gas phase is very small up to close to the critical pressure. Its concentration in the liquid depends essentially on the volume expansion of this phase as CO_2 is added. Rough estimates of this expansion by visual observation are from 1.5 to 3 times, as CO_2 pressure increases from 7.5 MPa to 9 MPa. Therefore, at around 8.5 MPa, the concentration of α -pinene close to the

catalyst is of the order of 0.3 g cm^{-3} , that is, one order of magnitude higher than in single-phase reaction mixtures.

Confirmation of these calculations was sought, by measuring the increase in the mass of solvent in the trap situated after the sample loop and due to the sample bubbling through it. These data are however subject to large experimental errors, due to the small mass of sample compared to the mass of solvent (hexane). Evaporation of hexane will occur, which will be highly dependent on the volume of gas being bubbled for each sample, and also on kinetic effects, which will determine how close to phase equilibrium the solvent and the gas will be. As both the quantities of gas and the kinetic effects were different when the loop contained either a liquid or a supercritical phase, the reliability of the observed results is poor. It should however be noted that large differences were observed between two-phase and supercritical conditions, and that the amounts of pinene in the sample loop measured at the start of the reaction were indeed one order of magnitude higher for the two-phase systems.

These results do not offer a straightforward explanation for the difference in rates between supercritical and two-phase conditions after about 50% conversion (given in Table 2 and Fig. 3 and 4). One possibility is that the initial concentration of α -pinene in the supercritical phase is sufficient to ensure good access to the catalyst either in liquid–vapour conditions or in supercritical ones. However, in these last cases, as the reaction proceeds, the adsorption equilibrium at the catalyst surface might be sufficiently displaced against this reactant, in favour of hydrogen, to slow down the reaction. In fact the balance between α -pinene and hydrogen in the mixture around the catalyst is certainly much lower in supercritical conditions than in the liquid phase in two-phase systems.

The other possibility is that the catalyst is poisoned faster by hydrogen + carbon dioxide (to produce carbon monoxide) when the mixture is in the single-phase state, slowing down the reaction in these conditions. In fact, mixtures are supercritical at high carbon dioxide pressures. Moreover, it is in these conditions that hydrogen has better access to the catalyst. Carrying out the reaction with biphasic mixtures, at relatively low carbon dioxide pressures, might therefore be a good way to protect platinum catalysts in hydrogenations in high pressure CO_2 media.

These results are consistent with the thermodynamic modelling of Pereda *et al.*,¹⁶ which showed that some of the hydrogenations described by Bhanage *et al.*¹⁰ were carried out in two-phase systems. As pointed out in the Introduction, their work on Pt-catalysed hydrogenations in CO_2 seems not to have been affected by problems of catalyst poisoning.

Chouchi *et al.*⁸ have also obtained fast hydrogenations of α -pinene at low pressures of carbon dioxide, where the three phases vapour, liquid and solid catalyst are present. They used a palladium catalyst and the difference in reaction rates between biphasic and supercritical they obtained was much larger than with the platinum catalysts used in this work.

4. Conclusions

These results show that the hydrogenation of α -pinene in high pressure carbon dioxide can proceed in good yields for very

distinct relative concentrations of the reactants, either in biphasic or supercritical conditions.

The access of α -pinene to the metal (Pt) in the catalyst is the most important factor determining the reaction rates, while mass transfer of hydrogen towards the catalyst is sufficiently fast in a wide range of conditions, including in biphasic mixtures.

The results indicate that biphasic conditions may protect the Pt catalyst from poisoning by carbon monoxide formed by reaction of hydrogen with carbon dioxide.

Acknowledgements

A. M. Banet Osuna thanks Fundação para a Ciência e a Tecnologia (FC&T, Lisbon, Portugal) for a postdoctoral fellowship SFRH/BPD/9138/2002. This work was financially supported by FC&T through project POCTI/QUI/38269/2001, and by the Marie Curie Research Training Network SuperGreenChem MCRTN-2004-504005. We thank Prof. Francisco Rodríguez-Reinoso and Dr Cristina Almansa, of the Inorganic Chemistry Department of the University of Alicante, for the TEM micrographs, and Marcio Temtem and Dr Teresa Casimiro for the production of the graphical contents entry.

References

- 1 E. J. Beckman, *J. Supercrit. Fluids*, 2004, **28**, 121.
- 2 R. Noyori, Ed., *Supercritical Fluids*, *Chem. Rev.*, 1999, **99**, 353.
- 3 *Chemical Synthesis in Supercritical Fluids*, ed. P. G. Jessop and W. Leitner, Wiley-VCH, Weinheim, 1999.
- 4 M. Härröd, S. van den Hark, M.-B. Macher and P. Møller, in *High Pressure Process Technology: Fundamentals and Applications*, ed. A. Bertucco and G. Vetter, Elsevier, Amsterdam, 2001, p. 496.
- 5 M. G. Hitzler, F. R. Smail, S. K. Ross and M. Poliakoff, *Org. Proc. Res. Dev.*, 1998, **2**, 137.
- 6 M. Wei, G. T. Musie, D. H. Busch and B. Subramanian, *J. Am. Chem. Soc.*, 2002, **124**, 2513.
- 7 J. A. Darr and M. Poliakoff, *Chem. Rev.*, 1999, **99**, 495.
- 8 D. Chouchi, D. Gourguillon, M. Courel, J. Vital and M. Nunes da Ponte, *Ind. Eng. Chem. Res.*, 2001, **40**, 2551.
- 9 B. Minder, T. Mallat, K. H. Pickel, K. Steiner and A. Baiker, *Catal. Lett.*, 1995, **34**, 1.
- 10 B. M. Bhanage, Y. Ikushima, M. Shirai and M. Arai, *Catal. Lett.*, 1999, **62**, 175.
- 11 L. Devetta, A. Giovanzana, P. Canu, A. Bertucco and B. J. Minder, *Catal. Today*, 1999, **48**, 337.
- 12 C. Prado Burguete, A. Linares-Solano, F. Rodriguez-Reinoso and C. Salinas-Martinez de Lecea, *J. Catal.*, 1989, **115**, 98.
- 13 G. del Angel, R. Melendrez, V. Bertin, J. M. Dominguez, P. Marecot and J. Barbier, in *Heterogeneous Catalysis and Fine Chemicals III*, ed. M. Guisnet *et al.*, Elsevier, Amsterdam, 1990, p. 171.
- 14 J. Pavlíček and M. Richter, *Fluid Phase Equilib.*, 1993, **90**, 125.
- 15 M. Akgün, N. A. Akgün and S. Dinçer, *J. Supercrit. Fluids*, 1999, **15**, 117.
- 16 S. Pereda, S. B. Bottini and E. A. Brignole, *Appl. Catal. A: General*, 2005, **281**, 129.
- 17 S. Pereda, S. B. Bottini and E. A. Brignole, *Fluid Phase Equilib.*, 2002, **194–197**, 493.
- 18 M. Solinas, A. Pfaltz, P. G. Cozzi and W. Leitner, *J. Am. Chem. Soc.*, 2004, **126**, 16142.
- 19 I. Ilyna and V. Semikolenov, *Proceedings of the 5th International Symposium on Heterogeneous Catalysis and Fine Chemicals*, Lyon, France, 1999.

Formation of carbon micro-sphere chains by defluorination of PTFE in a magnesium and supercritical carbon dioxide system

Qiang Wang, Fangyu Cao and Qianwang Chen*

Received 16th May 2005, Accepted 11th August 2005

First published as an Advance Article on the web 24th August 2005

DOI: 10.1039/b506890h

Well-crystallized carbon micro-spheres at the sub-micrometer scale were prepared by defluorination of polytetrafluoroethylene (PTFE) with metallic magnesium in supercritical carbon dioxide at 650 °C for 6 h. The products were characterized by X-ray diffraction, transmission electron microscopy, field-emission scanning electron microscopy and micro-Raman spectroscopy. FT-IR spectroscopy was used to monitor the extent of defluorination of PTFE. The produced carbon spheres tend to agglomerate to form chains and the possible mechanism of forming these carbon sphere chains in this system is tentatively discussed.

Introduction

As one of the most important fluorinated polymers, polytetrafluoroethylene (PTFE) is widely used because of its excellent properties, such as physical and chemical resistance, thermal stability, low coefficient of friction, low dielectric constant and high resistivity, hydrophobicity, *etc.*¹ However, because of the year-over-year increase in consumption, waste PTFE materials could become persistent solid pollutants which are difficult to degrade in the environment.² Due to the strong C–F bond (481 J mol⁻¹) in PTFE, conventional defluorination methods concentrate on hydrolysis at high temperatures and electrochemical reduction.³ Recently, many new methods of defluorination have been exploited. For example, some papers have reported that PTFE could react with alkali metals or their amalgams, forming active polyynes or porous carbon and metal fluorides.^{4–6} Huczko and his co-workers have developed a self-sustaining reaction using different metals and alloys for the defluorination of PTFE and generated novel nanostructures.⁷ Hlavaty reported that PTFE could be defluorinated and derivatized in a one step process by alkyl- and aryl-lithium in the presence of tetramethylethylenediamine (TMEDA) as catalyst.⁸ In 2004, Yang *et al.* treated PTFE in a hot solution of calcium hydroxide and obtained amorphous carbon and calcium fluorite.⁹

Different forms of carbon materials have been synthesized in our group by reduction of supercritical carbon dioxide with alkali metals in the past few years.^{10–12} Above the critical temperature and pressure ($T_c = 31.8$ °C, $P_c = 7.4$ MPa), CO₂ has a gas-like viscosity and a liquid-like density. These moderate critical conditions combined with the intrinsic characteristics of inexpensive, nonflammable, environmentally benign and easily separated products allow supercritical carbon dioxide to act as an ideal alternative solvent in synthetic chemistry.¹³ It is also known that supercritical carbon dioxide could be used as an alternative solvent in

fluorocarbon polymer synthesis and processing.¹⁴ Therefore, it is significant to examine the effect of defluorination of PTFE and investigate the structures of the carbon produced in the metal and supercritical carbon dioxide system. Although theoretical calculation shows that the thermolysis temperature of Mg/PTFE composition may exceed 3000 K,¹⁵ we report herein, for the first time, that PTFE can be defluorinated by metallic magnesium completely under the condition of supercritical carbon dioxide at 650 °C and most of the carbon products are chains consisting of carbon spheres at the sub-micrometer scale.

Experimental

In a typical run, 1.0–1.2 g of metallic magnesium (>99% purity 100–200 mesh, Shanghai Chem. Reagent. Corp.), 1.4–1.5 g of PTFE foils (FR101, Shanghai 3F New Materials Co., Ltd), and 10.0 g of freshly made dry ice (>99.9% purity) were sealed in a stainless steel autoclave with 15 mL capacity. The autoclave was put in an oven and heated at the rate of 10 °C min⁻¹, then kept at 650 °C for 6 h. After being cooled down to room temperature, the products were collected and washed with diluted hydrochloric acid to remove the residual magnesium and then alcohol and distilled water several times. The primary phase analysis suggested the sample was made up of carbon, magnesium fluoride and ferrite. In order to observe the morphology of the produced carbon, the sample was treated with a hot and concentrated solution of sodium carbonate and hydrochloric acid, respectively. The final sample was rinsed with pure alcohol, distilled water and dried under vacuum for 2 h.

Powder X-ray diffraction (XRD) analysis was performed on a Rigaku (Japan) D/max-rA X-ray diffractionmeter equipped with graphite monochromatized Cu K α radiation ($\lambda = 1.54178$ Å). The field emission scanning electron microscope (FESEM) and transmission electron microscope (TEM) observations were performed on a JSM-6700F (JEOL) and Hitachi H800. The FT-IR spectrum was carried out on a Bruker-Vector 22 FTIR spectrometer with KBr pellets. A LABRAM-HR confocal laser micro-Raman spectrometer was

Hefei National Laboratory for Physical Sciences at Microscale and Department of Materials Science & Engineering, University of Science & Technology of China, Hefei, 230026, China. E-mail: cqw@ustc.edu.cn; Fax: +86-0551-3607292; Tel: +86-0551-3607292

employed to characterize the product, operated at ambient temperature using the 514.5 nm line of an Ar-ion laser as the excitation source.

Results and discussion

Fig. 1(a) shows the XRD pattern of the powder sample prepared at 650 °C for 6 h after treatment with diluted HCl. The reflection peaks can be assigned to a mixture of graphite (JCPDS 75-1621), MgF₂ (labeled as “★” JCPDS 72-2231) and spinel-structured ferrite (labeled as “■” JCPDS 85-1436). No reflection of PTFE (JCPDS 47-2217) can be identified in this figure, indicating that the foils of PTFE have been completely transformed to carbon and magnesium fluoride under our experimental conditions. The ferrite phase might come from the components of the stainless steel cell. The XRD pattern of the sample after treatment with NaCO₃ and concentrated HCl solution is displayed in Fig. 1(b). In this figure, only the weak reflection peaks of ferrite can be seen along with the strong (002) peak of graphite, which suggests that most of the magnesium fluoride and ferrite are removed after treatment. Furthermore, at the 2θ range of 20–30°, there exists a broad and weak peak in contrast to the sharp (002) peak of graphite in Fig. 1(a) and (b), suggesting that the carbon produced exists in the forms of graphite and amorphous carbon.

The typical FESEM image (Fig. 2) reveals that a large number of chains connected by carbon micro-spheres with a diameter of less than 1 μm formed in the 650 °C sample. TEM observation further revealed spherical particles with diameters ranging from several hundreds of nanometers to 1 μm aligned in the form of chains as shown in Fig. 3(a). Also, a few amounts of amorphous carbon can be found in this figure, which is consistent with the XRD results. Fig. 3(b) shows that the carbon spheres in different dimensions are closely connected and the surface of these carbon spheres are not smooth, which has also been observed by Yamada *et al.*¹⁶ The selected area electron diffraction of the small sphere exhibits a

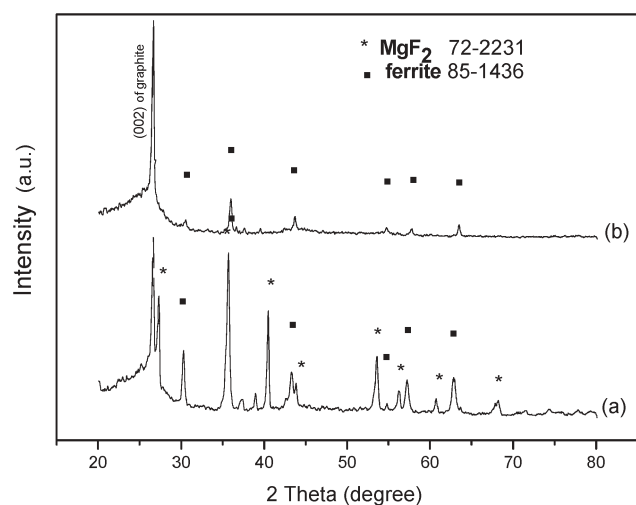


Fig. 1 (a) XRD pattern of the sample after the diluted HCl treatment. (b) XRD pattern of the same sample after the Na₂CO₃ and HCl treatment.

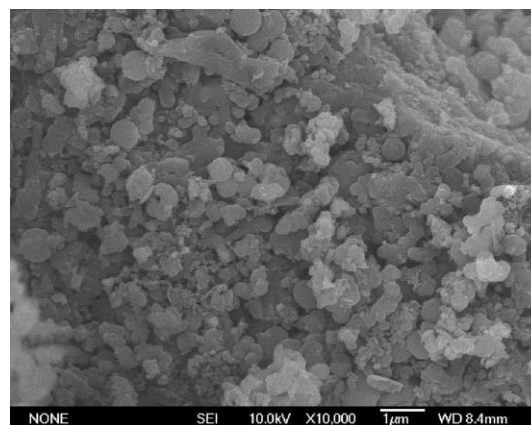


Fig. 2 FESEM image of the sample prepared at 650 °C for 6 h.

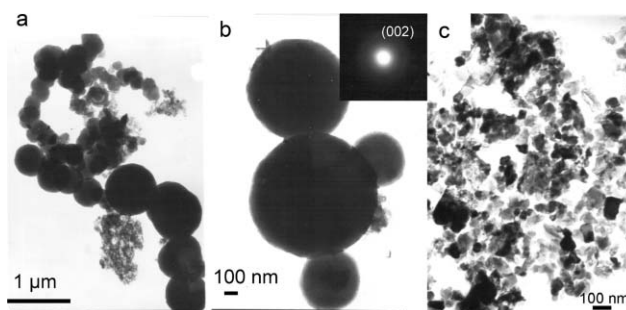


Fig. 3 (a) A typical TEM image of the carbon sphere chains. (b) A high magnification TEM image of a segment of the carbon sphere's chain and selected area electron diffraction (SAED) (inset). (c) TEM image of the sample prepared at 550 °C for 6 h.

clear (002) diffraction ring of graphite (inset of Fig. 3(b)), confirming that these spherical grains are well-crystallized carbon. Fig. 3(c) shows a typical TEM image of the sample prepared at 550 °C for 6 h; it can be seen that there are plenty of irregular grains and flakes (light gray) which might be residual PTFE or the defluorination intermediates of PTFE. From this result, it is shown that defluorination cannot be completed at temperatures lower than 650 °C, which is also verified by the FTIR analysis.

The Raman spectrum of the sample prepared at 650 °C is shown in Fig. 4. As the ordinary graphite-like carbon, the curve consists of two regions, usually denoted as G band and D band: the G band peaked at ~1590 cm⁻¹ associated with the E_{2g} in-plane graphite Raman active mode and the D band at ~1350 cm⁻¹ is a breathing mode of A_{1g} symmetry. In comparison with hexagonal graphite single crystal (single peak at 1580 cm⁻¹), the intensity of the D-band is known to be caused by the small grain size of the produced carbon spheres or the existence of amorphous carbon, while the position of the G band shifts up to the high frequency direction, which can be interpreted in terms of the conversion between amorphous carbon and graphite, proposed by Davydov *et al.*¹⁷ and Ferrari and Robertson.¹⁸ The spectrum shows no characteristic line at about 1900–2000 cm⁻¹ which is assigned to a stretching vibration of the sp carbon chain of polyynes, indicating no carbyne-like specimens exist in the final produced carbon.¹⁹

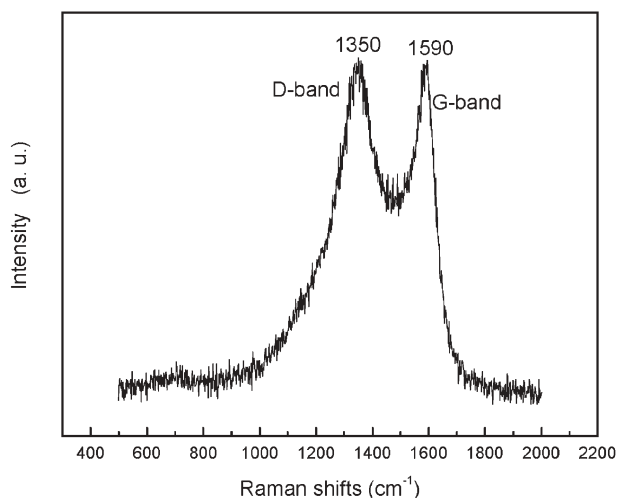


Fig. 4 Raman shifts of the carbon spheres prepared at 650 °C for 6 h.

Meanwhile, the ratio of I_G/I_D correlates with the in-plane graphite crystallite size L_a , according to the relationship: $L_a = 4.4I_G/I_D$ (in nm). The calculated value of L_a is 4.4 nm, implying the microcrystalline graphite planar crystal size is about 4.4 nm in the formed carbon micro-spheres.¹⁷

Being highly sensitive to the vibration mode of a specific bond or functional group, the IR spectrum is an ideal tool to monitor the extent of defluorination of PTFE at different experimental temperatures. The spectra of samples produced at 400 °C, 550 °C and 650 °C are shown in Fig. 5. The spectrum of the sample at 400 °C exhibits four characteristic strong absorption peaks at 1212 cm^{-1} , 1152 cm^{-1} , 639 cm^{-1} , 554 cm^{-1} and 503 cm^{-1} , which are assigned to the vibration of carbon-fluorine bonds ($-\text{CF}_2-$) in PTFE.²⁰ Therefore, it is reasonable to say that most of the PTFE are not decomposed at 400 °C in our experimental conditions. The corresponding absorption peaks of the sample at 550 °C are relatively weak, indicating some of the $-\text{CF}_2-$ bonds in PTFE have been diminished and that PTFE was partly but not completely

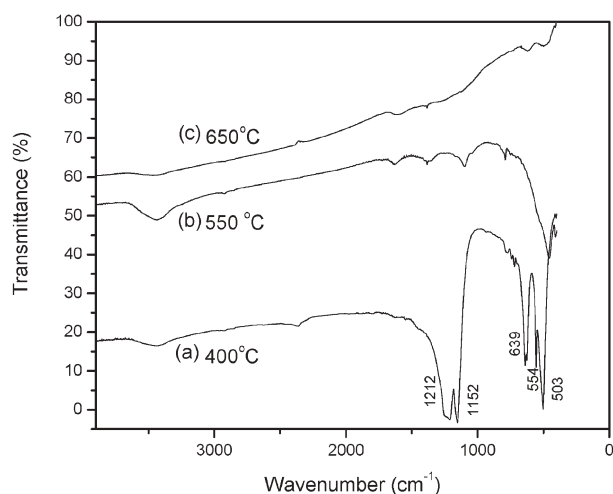


Fig. 5 FTIR spectra of the sample prepared at (a) 400 °C (b) 550 °C and (c) 650 °C.

defluorinated and carbonized at 550 °C. It is also confirmed by TEM observations. The IR spectrum of the sample prepared at 650 °C shows no absorption of the $-\text{CF}_2-$ bond or fragments of C_2F_4 , C_4F_8 or other organic functional groups, suggesting the defluorination of PTFE is completed at this temperature.²¹ Furthermore, the broad absorption peak at 3400 cm^{-1} and the weak absorption peaks at $\sim 1630 \text{ cm}^{-1}$ in the spectra shown in Fig. 5b and Fig. 5c could be assigned to the $-\text{OH}$ vibration mode of the absorbed water molecule of the sample.

CO_2 is a non-polar molecule, which exhibits great solubility of organic fluorocarbons. Despite this, very high temperatures are needed to dissolve PTFE, even in perfluorocarbon solvents, mainly to overcome the non-polar attractive forces between polymer segments that become magnified in the stereo-regular structure of the polymer's crystalline phase. Tuminello and co-workers studied the phase behavior of the dissolving of perfluorocarbon polymers in supercritical CO_2 by experiment and theoretical calculation and then predicted that PTFE should be dissolved in supercritical CO_2 at a temperature higher than 300 °C and a pressure higher than 100 MPa.²² In our sealed experimental system, CO_2 reaches the supercritical state easily at the beginning of the heating process and the pressure of supercritical CO_2 would be increasing with the experimental temperature. Therefore, it is reasonable to speculate that PTFE dissolved completely in supercritical CO_2 and formed a single phase mixture at a certain temperature. In addition, the phenomena of PTFE foils being swollen and powdered are also observed at 300 °C and 450 °C, respectively. For the reason that alkali metals would react with supercritical carbon dioxide at a relatively low temperature (200–300 °C) and produce amorphous carbon and flake graphite, metallic magnesium was chosen as the defluorination agent in the atmosphere of carbon dioxide because it is stable in carbon dioxide up to 700 °C.²³ Motiei reported that supercritical carbon dioxide can be reduced to carbon nanotubes and fullerene by metallic magnesium, however, the reaction occurs at a temperature as high as 1000 °C.²⁴ To further examine that these carbon spheres are the defluorinated products of PTFE, a similar procedure of heating magnesium and dry ice without adding PTFE at 650 °C for 6 h was conducted and no spherical carbon products were observed.

To investigate the effect of reaction condition on the formation of carbon sphere chains, a series of experiments were carried out by altering experimental parameters of the process. It is found that the reaction temperature played a critical role in the formation of these carbon spheres. At the reaction temperature of 550 °C and 600 °C, most of carbon products are irregular carbon grains and amorphous carbon revealed by TEM observations. A large amount of carbon spheres formed as the temperature was increased to 650 °C. The concept of "liquid metal nano-droplets" has been proposed to explain the formation mechanism of carbon spheres in the metallic lithium and supercritical CO_2 system in our previous research.²⁵ Magnesium melts at 650 °C, and its normal boiling temperature is 1090 °C. The vapor pressure of magnesium at 1000 °C is 350 mmHg. At a temperature of 650 °C, the magnesium powder melted and the liquid magnesium turns into nano-droplets, which might be dispersed in the mixture of supercritical of CO_2 and PTFE. Then, these Mg nano-droplets take

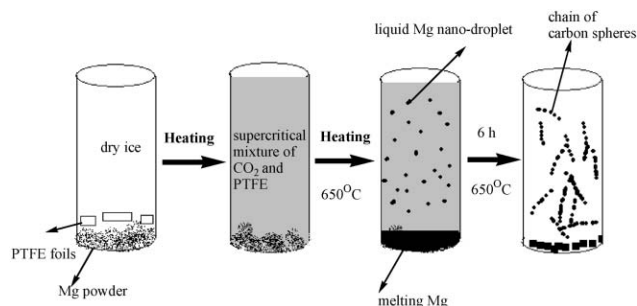


Fig. 6 Graphical description of the possible formation process of the carbon sphere chains.

the role of defluorination agents *via* the chemical reaction equation:



They also act as templates for carbon spheres to grow. The high pressures induced by CO₂ are favorable for the absorption of PTFE or its decomposed intermediates on the surfaces of Mg nano-droplets and may accelerate the electron transfer from Mg to PTFE or intermediates.²⁶ The produced carbon spheres are arranged in the shape of chains, which might be attributed to the linear structure of the PTFE molecule. The similar chain-like structure constructed by porous carbon has been observed in γ -irradiated PTFE reacting with potassium vapor at 1000 °C.⁶

A graphical description of this formation process is shown in Fig. 6. The PTFE foils firstly dissolved in the supercritical CO₂, forming a homogeneous mixture at a temperature of 400–500 °C in our reaction system. As the temperature increased to 650 °C, the magnesium powder melted and turned into nano-droplets in the mixture of CO₂–PTFE. For the rapid heating rate, most of the molecules of PTFE could not be decomposed in the heating procedure. When the linear molecular chains of PTFE react with magnesium nano-droplets, carbon spheres formed accompanied by the completion of defluorination. However, more detailed work is required to understand the exact formation mechanism of these carbon sphere chains. We also performed a similar experiment without adding dry ice; no carbon spheres were obtained and most of the carbon products were irregular carbon particles. When metallic magnesium is substituted by magnesia as defluorination agent, no spherical carbon products can be produced under the same experimental condition.

Conclusions

In summary, a simple chemical route degrading PTFE to carbon spheres has been illustrated in a magnesium and supercritical CO₂ system at 650 °C for 6 h. The produced

carbon micro-spheres have potential applications as reinforcement materials, supports for catalysts, hydrogen storage materials and anodes in lithium batteries. Magnesium fluoride is, as a by-product, widely used in the optical industry. In addition, this method could be applied to deal with other stable halogenous polymers.

Acknowledgements

This work was supported by the National Natural Science Foundation of China (20321101, 20125103 and 90206034).

References

- 1 J. H. Holloway, *J. Fluorine Chem.*, 2000, **104**, 3.
- 2 D. A. Ellis, S. A. Mabury, J. W. Martin and D. C. G. Muir, *Nature*, 2001, **412**, 321.
- 3 L. Kavan, *Chem. Rev.*, 1997, **97**, 3061.
- 4 S. Tasker, R. D. Chambers and J. P. S. Badyal, *J. Phys. Chem.*, 1994, **98**, 12442.
- 5 L. Kavan, F. P. Dousek, P. Janda and J. Weber, *Chem. Mater.*, 1999, **11**, 329.
- 6 T. Tzu Liang, Y. Yamada, N. Yoshizawa, S. Shiraishi and A. Oya, *Chem. Mater.*, 2001, **13**, 2933.
- 7 A. Huczko, H. Lange, G. Chojecki, S. Cudzilo, Y. Q. Zhu, H. W. Kroto and D. R. M. Walton, *J. Phys. Chem. B*, 2003, **107**, 2519.
- 8 J. Hlavaty, L. Kavan and Z. Bastl, *Angew. Makromol. Chem.*, 1996, **238**, 165.
- 9 X. G. Yang, C. Li, W. Wang, B. J. Yang, S. Y. Zhang and Y. T. Qian, *Chem. Commun.*, 2004, 342.
- 10 Z. S. Lou, Q. W. Chen, Y. F. Zhang, W. Wang and Y. T. Qian, *J. Am. Chem. Soc.*, 2003, **125**, 9302.
- 11 Z. S. Lou, Q. W. Chen, Y. T. Qian, W. Wang and Y. F. Zhang, *Angew. Chem. Int. Ed.*, 2003, **42**, 4501.
- 12 Z. S. Lou, C. L. Chen, Q. W. Chen and J. Gao, *Carbon*, 2005, **43**, 1084.
- 13 A. I. Cooper, *Adv. Mater.*, 2001, **13**, 1111.
- 14 L. Lei, H. Yokoyama, T. Nemoto and K. Sugiyama, *Adv. Mater.*, 2004, **16**, 1226.
- 15 S. Cudzilo and A. W. Trzcilski, *Pol. J. Appl. Chem.*, 2001, **26**, 25.
- 16 O. Tanaike, N. Yoshizawa, H. Hatori, Y. Yamada, S. Shiraishi and A. Oya, *Carbon*, 2002, **40**, 445.
- 17 V. A. Davydov, A. V. Rakhmanina, V. Agafonov, B. Narymbetov, J. P. Boudou and H. Szwarc, *Carbon*, 2004, **42**, 261.
- 18 A. C. Ferrari and J. Robertson, *Phys. Rev. B*, 2000, **61**, 14095.
- 19 L. Kavan, J. Hlavaty, J. Kastern and H. Kusmany, *Carbon*, 1995, **33**, 1321.
- 20 S. T. Li, E. Arenholz, J. Heitz and D. Bauerle, *Appl. Surf. Sci.*, 1998, **125**, 17.
- 21 G. B. Blanchet and S. I. Shah, *Appl. Phys. Lett.*, 1993, **62**, 1026.
- 22 W. H. Tuminello, G. T. Dee and M. A. McHugh, *Macromolecules*, 1995, **28**, 1506.
- 23 A. Abbud-Madrid, P. Omaly, M. C. Branch and J. W. Daily, 1996, Twenty-Sixth Symposium (International) on Combustion, The Combustion Institute, 1929–1936, Pittsburgh.
- 24 M. Motiei, Y. R. Hacohen, J. Calderon-Moreno and A. Gedanken, *J. Am. Chem. Soc.*, 2001, **123**, 8624.
- 25 Z. S. Lou, Q. W. Chen, J. Gao and Y. F. Zhang, *Carbon*, 2004, **42**, 229.
- 26 Q. W. Chen and D. W. Bahnemann, *J. Am. Chem. Soc.*, 2000, **122**, 970.

An efficient microwave-assisted green transformation of fused succinic anhydrides into *N*-aminosuccinimide derivatives of bicyclo[2.2.2]octene in water

Mitja Martelanc, Krištof Kranjc, Slovenko Polanc and Marijan Kočevar*

Received 14th June 2005, Accepted 10th August 2005

First published as an Advance Article on the web 24th August 2005

DOI: 10.1039/b508446f

A very efficient and clean green synthesis of highly substituted prochiral bicyclo[2.2.2]oct-7-enes, starting from bicyclo[2.2.2]oct-7-ene-2*exo*,3*exo*,5*exo*,6*exo*-tetracarboxylic acid 2,3:5,6-dianhydrides and a variety of hydrazines, is described.

Introduction

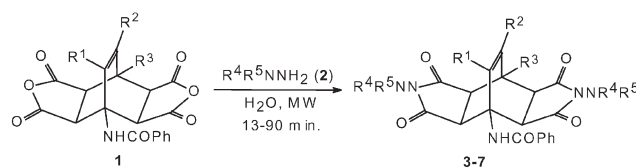
During recent years great efforts have been made in the field of green chemistry to adopt methods and processes that use less toxic chemicals, produce smaller amounts of by-products and use less energy.¹ As part of this “green” concept, toxic and/or flammable organic solvents are replaced by alternative non-toxic and non-flammable media or the reactions are carried out without the use of any solvent, and the classical sources of heating are often replaced by microwave (MW) heating.² Microwave-accelerated reactions have attracted considerable attention in the past decade due to their efficiency and eco-friendliness, yielding a variety of organic products.³ Similarly, among alternative green solvents, water was the solvent of choice for a variety of transformations.⁴ It is known to be one of the best green solvents and is also a medium microwave-absorbing solvent (with a very high dielectric constant and intermediate values for tangent delta and the dielectric loss).^{3b} Because of the above properties it is frequently utilized in combination with microwave irradiation.⁵

Our recent research interest in the transformations of cyclic α,β -didehydroamino acid derivatives⁶ containing the 2*H*-pyran-2-one unit in their structure resulted in the formation of bicyclo[2.2.2]oct-7-ene-2*exo*,3*exo*,5*exo*,6*exo*-tetracarboxylic acid 2,3:5,6-dianhydrides **1**^{7a} as well as in related fused succinimide derivatives.^{7b} Although bicyclo[2.2.2]oct-7-enes (bicyclo[2.2.2]oct-2-enes when unsubstituted) exhibiting a free or protected amino group at the bridgehead carbon atom are very rare,^{8a} they can be found in the skeleton of naturally occurring *Kopsia* alkaloids.^{8b} Derivatives **1** possess in their structure various functionalities (double-bond C=C, substituted amino group, two fused succinic anhydride units and a heterocyclic moiety) and, therefore, might serve as multifunctional building blocks in the synthesis. Our idea was to check the potential of their anhydride moieties for the double acylation of different nitrogen-containing nucleophiles. The anhydrides are known to react with amines and hydrazines producing the corresponding amides and imides.⁹ To our knowledge there is only one previous report of the

utilization of the fused bicyclo[2.2.2]octene system (but not containing an amino group at the bridgehead) in such a reaction with hydrazine hydrate and phenylhydrazine in an ethanolic solution.¹⁰ Two products were prepared in this investigation, but no details about the reaction times were given.

Results and discussion

Our idea was to explore the transformations of the prochiral derivatives of bicyclo[2.2.2]oct-7-enes **1** with different hydrazines **2** (hydrazine hydrate, alkyl hydrazines, aryl- and heteroarylhydrazines) toward the corresponding fused succinimides **3–7** (Scheme 1). Preliminary experiments with our compounds under conventional heating have shown that they require conditions more severe than just heating both reagents in ethanol. For example, heating for 1 h of the furyl derivative **1c** with 10 equivalents of methylhydrazine in ethanol (12 mL of EtOH/1 mmol of **1c**) followed by evaporation of the solvent resulted in the formation of the product **4c**, but it was accompanied with (most probably) at least an intermediary-formed product that did not completely disappear, even after 3 h of heating. Similarly, a reflux of **1c** with methylhydrazine (2.4 mmol/1 mmol of **1c**) for 3 h in DMF (12 mL of DMF/1 mmol of **1c**) resulted in **4c**, but accompanied by significant amount(s) of a side product(s). Analogous results were obtained in water: when refluxing **1c** with methylhydrazine (2.4 mmol/1 mmol of **1c**) for 1 h (12 mL H₂O/1 mmol of **1c**) the corresponding product **4c** was formed (in an about 80–85% conversion), though again accompanied by detectable amount(s) of a side product(s) and/or an intermediate(s); even after 4 h of heating the intermediate and/or side products can be detected by the ¹H NMR spectroscopy. Being encouraged by our previous preparation of various hydrazones from carbonyls and hydrazines using microwave irradiation of the



Scheme 1

Faculty of Chemistry and Chemical Technology, University of Ljubljana, Aškerčeva 5, SI-1000 Ljubljana, Slovenia.
E-mail: marijan.kocevar@fkkt.uni-lj.si; Fax: +386 1 2419220

starting compounds in solvent-free conditions,¹¹ we decided to perform this reaction in green conditions. So we have carried out the transformation of bicyclo[2.2.2]oct-7-enes **1** with different hydrazines **2** in an aqueous mixture at 100–160 °C in a pressurized tube (pressure up to 7 bar) under microwave irradiation in a focused monomode microwave device (CEM Discover). The transformation is complete within 90 min and the products **3a–c**, **4a–h**, **5–7** were isolated in high yields (80–95%) (Table 1). The reaction mixtures were heated in a sealed tube (10 mL) from room temperature to the final temperature (Table 1), and later held at this temperature for the total reaction time; the temperature was measured by using an external IR temperature sensor. It is worth mentioning that the starting compounds **1** are almost completely insoluble in water at room temperature, the same being true for the products **3–7**. We have no evidence, of course, about the solubility of all the components in water at the final temperature, but during a reflux in water at normal pressure there was a significant amount of non-soluble material. The reaction under such conditions leading to **4c** did take place to a significant extent in 1 h and nearly the same happened under MW conditions at 100 °C, though the reaction took place to a slightly greater extent; but at 150 °C the reaction was completed within 20 min of heating and no other product or impurity could be detected in the reaction mixture after the evaporation of water. The reaction is completely selective, *i.e.*, furyl or thienyl rings as well as the benzoylamino group were not disturbed during this reaction. Having in hand the above results, we decided to perform the above reaction by exploring the technique of simultaneous cooling in conjunction with microwave heating. This technique introduces a higher level of MW energy to the system, and cooling by passing a stream of compressed air over the reaction vessel makes it possible to maintain the mixture at the selected temperature. Such a technique is especially suitable for the reactions of thermally unstable substances.^{3b,5c,12} By applying this technique we have significantly shortened the reaction times (by up to 30%), but the yields remained the same (within the experimental accuracy). It was already shown in several experiments that the application of an external IR temperature measurement

during the “cooling-while-heating” method does not give an accurate bulk temperature of the reaction mixture; it gives lower values because of the air passing over the reaction vessel and the cooling of the outer surface of the vessel, where the measurement is conducted.¹² As a consequence, the faster reaction progress is not necessarily the result of just higher MW irradiation, but of the higher bulk temperature of the reaction mixture than that recorded by the IR sensor. To avoid this inconvenience, we performed the syntheses of products **4c** and **4g** in an 80 mL vessel equipped with a fiber-optic temperature measurement set-up. The analyses of the obtained results have shown that there was no significant enhancement (if any at all) of the reaction progress by the application of the “cooling-while-heating” technique.

Though the substrates **1** are practically insoluble in water the transformations comprising elimination of a molecule of water were completed within 90 min of irradiation with microwaves under the given conditions. It is important to mention that the same transformation requires higher temperatures, longer heating periods and/or greater excesses of hydrazines when carried out under conventional reflux conditions. Moreover, the work-up after the completion of the reaction in water under microwave irradiation is very simple — simply cooling down the mixture, filtering off the precipitated product and washing it with a small amount of water; without any need for an additional purification. Such an isolation procedure seems to be even simpler than that described for solvent-free synthesis.^{2a,11}

Conclusions

We have presented a highly efficient, environmentally benign, microwave-accelerated synthesis of fused *N*-aminosuccinimide derivatives of bicyclo[2.2.2]oct-7-enes starting from fused anhydrides and different hydrazines in an aqueous mixture in pressurized tubes. The reaction takes place in neutral conditions, without any need for catalysts (acid or base), and as a consequence it is highly selective. Further investigations of the scope and limitations of this efficient method and transformation are in progress.

Table 1 Reaction times and yield of products **3–7** under microwave conditions

Run	Starting 1 ^{7a,13}			2			Products 3–7	<i>t</i> /min ^a	Yield (%) ^b
	R ¹	R ²	R ³	R ⁴	R ⁵				
1	H	H	Me	1a	H	H	3a	50 ^c	94
2	H	4-(MeO)-C ₆ H ₄	Me	1b	H	H	3b	60 ^d	94
3	Me	H	2-furyl	1c	H	H	3c	50 ^c	92
4	H	H	Me	1a	H	Me	4a	13 ^c	94
5	H	4-(MeO)-C ₆ H ₄	Me	1b	H	Me	4b	90 ^d	95
6	Me	H	2-furyl	1c	H	Me	4c	20 ^d	92
7	H	H	Ph	1d	H	Me	4d	30 ^d	94
8	H	H	2-furyl	1e	H	Me	4e	20 ^d	93
9	Me	H	2-thienyl	1f	H	Me	4f	30 ^d	92
10	H			1g	H	Me	4g	40 ^c	80
11	H			1h	H	Me	4h	30 ^d	84
12	Me	H	2-furyl	1c	H	Py	5	80 ^d	83
13	Me	H	2-furyl	1c	H	Ph	6	75 ^d	92
14	Me	H	2-furyl	1c	Me	Me	7	70 ^{d,e}	80

^a Microwave irradiation in aqueous suspension at 100 °C (for **3**), at 150 °C (for **4,7**) and at 160 °C (for **5,6**) in a pressurized tube. ^b Yield of isolated compounds. ^c With 10% excess of hydrazines **2**. ^d With 20% excess of hydrazines **2**. ^e With 1.5 mL of solvent. Py: 2-Pyridyl.

Experimental

Melting points were determined on a Kofler micro hot stage, and are uncorrected. ^1H NMR spectra were recorded with a Bruker Avance DPX 300 spectrometer at 29 °C (unless otherwise stated) and 300 MHz using TMS as an internal standard. ^{13}C NMR spectra were recorded on the same instrument at 75 MHz and are referenced against the central line of the solvent signal (DMSO- d_6 septet at $\delta = 39.5$ ppm). The coupling constants (J) are given in Hz. IR spectra were obtained with a Bio-Rad FTS 3000MX (KBr pellets for all products). MS spectra were recorded with a VG-Analytical AutoSpec Q instrument. Elemental analyses (C, H, N) were performed with a Perkin Elmer 2400 Series II CHNS/O Analyzer. TLC was carried out on Fluka silica gel TLC-cards. The starting compounds **1** were prepared according to the published procedures;^{7a,13} all other reagents and solvents were used as received from commercial suppliers. Microwave reactions were conducted in air using a focused microwave unit (Discover by CEM Corporation, Matthews NC). The machine consists of a continuous, focused microwave power delivery system with an operator-selectable power output from 0 to 300 W. Reactions were performed in glass vessels (capacity 10 mL) sealed with a septum. The pressure was controlled by a load cell connected to the vessel *via* the septum. The temperature of the contents of the vessel was monitored using a calibrated infrared temperature control mounted under the reaction vessel. The mixtures were stirred with a Teflon-coated magnetic stir bar in the vessel. Temperature, pressure and power profiles were recorded using commercially available software provided by the manufacturer of the microwave unit.

General procedure

A mixture of the starting fused succinic anhydride derivative **1** (1 mmol) and hydrazine **2** (2.2–2.4 mmol) in 3 mL of distilled water (1.5 mL for the synthesis of **7**) was irradiated in the focused microwave equipment for the time specified (Table 1). The final temperature was set to 100 °C for **3a–c**, 150 °C for **4a–h** and **7**, or 160 °C for **5** and **6**; the power to 90 W, and the ramp time to 3 min. For typical temperature, pressure and

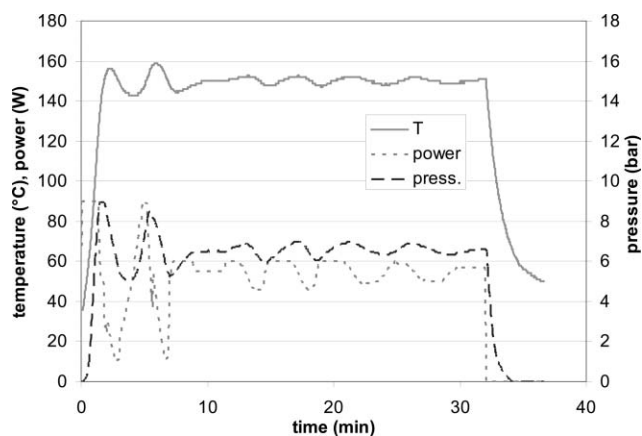


Fig. 1 Typical temperature (—), power (---) and pressure (- - -) profiles for the microwave irradiated synthesis of **4d**.

power profiles see Fig. 1. Thereafter, the reaction mixture was cooled, the precipitated solid was filtered off and washed with distilled water (0.5–1 mL).

Analytical and spectroscopic data of products 3–7

N-(2,6-Diamino-2,3,3a,4a,5,6,7,7a,8,8a-decahydro-8-methyl-1,3,5,7-tetraoxo-4,8-ethenobenzo[1,2-*c*:4,5-*c'*]dipyrrol-4(1*H*)-yl)benzamide (3a). Mp 305–308 °C (from EtOH). Found: C, 58.68; H, 5.01; N, 17.25. $\text{C}_{20}\text{H}_{19}\text{N}_5\text{O}_5$ requires C, 58.68; H, 4.68; N, 17.11%; $\nu_{\text{max}}(\text{KBr})/\text{cm}^{-1}$ 1773, 1717, 1693, 1639 and 1562; $\delta_{\text{H}}(300 \text{ MHz}; \text{DMSO-}d_6; \text{Me}_4\text{Si})$ 1.75 (3H, s, Me), 3.02 (2H, d, J 8.0, 7a-H, 8a-H), 4.23 (2H, d, J 8.0, 3a-H, 4a-H), 4.89 (4H, deg s, $2 \times \text{NNH}_2$), 5.83 (1H, d, J 8.6), 6.35 (1H, d, J 8.6) (9-H, 10-H), 7.53 (3H, m, Ph), 7.89 (2H, m, Ph) and 8.70 (1H, s, NH); $\delta_{\text{C}}(75.5 \text{ MHz}; \text{DMSO-}d_6)$ 19.1, 39.1, 41.8, 46.4, 57.6, 127.6, 128.0, 130.9, 131.1, 133.9, 135.7, 167.9, 172.0 and 173.2; m/z 409 (M^+ , 8%) and 105 (100).

N-(2,6-Diamino-2,3,3a,4a,5,6,7,7a,8,8a-decahydro-9-(4-methoxyphenyl)-8-methyl-1,3,5,7-tetraoxo-4,8-ethenobenzo[1,2-*c*:4,5-*c'*]dipyrrol-4(1*H*)-yl)benzamide (3b). Mp 262–264 °C (from EtOH). Found: C, 62.66; H, 4.91; N, 13.69. $\text{C}_{27}\text{H}_{25}\text{N}_5\text{O}_6$ requires C, 62.91; H, 4.89; N, 13.58%; $\nu_{\text{max}}(\text{KBr})/\text{cm}^{-1}$ 1773, 1712, 1644, 1605 and 1536; $\delta_{\text{H}}(300 \text{ MHz}; \text{DMSO-}d_6; \text{Me}_4\text{Si})$ 1.67 (3H, s, Me), 3.14 (2H, d, J 8.0, 7a-H, 8a-H), 3.74 (3H, s, OMe), 4.27 (2H, d, J 8.0, 3a-H, 4a-H), 5.02 (4H, s, $2 \times \text{NNH}_2$), 6.16 (1H, s, 10-H), 6.81 (4H, AA'BB', 4-MeO-C $_6$ H $_4$), 7.51 (3H, m, Ph), 7.90 (2H, m, Ph) and 8.68 (1H, s, NH); $\delta_{\text{C}}(75.5 \text{ MHz}; \text{DMSO-}d_6)$ 18.7, 41.9, 42.2, 47.2, 55.0, 58.1, 113.4, 127.0, 127.7, 128.0, 129.3, 129.7, 131.0, 135.7, 145.1, 158.7, 167.9, 172.0 and 173.4; m/z 515 (M^+ , 3%) and 69 (100).

N-[2,6-Diamino-8-(2-furyl)-2,3,3a,4a,5,6,7,7a,8,8a-decahydro-10-methyl-1,3,5,7-tetraoxo-4,8-ethenobenzo[1,2-*c*:4,5-*c'*]dipyrrol-4(1*H*)-yl]benzamide (3c). Mp 348 °C decomp. (from EtOAc). Found: C, 59.42; H, 4.67; N, 14.63. $\text{C}_{24}\text{H}_{21}\text{N}_5\text{O}_6 \cdot \frac{1}{2}\text{H}_2\text{O}$ requires C, 59.50; H, 4.58; N, 14.46%; $\nu_{\text{max}}(\text{KBr})/\text{cm}^{-1}$ 1774, 1712br, 1645 and 1524; $\delta_{\text{H}}(300 \text{ MHz}; \text{DMSO-}d_6; \text{Me}_4\text{Si})$ 1.89 (3H, d, J 1.3, Me), 3.56 (2H, d, J 8.1, 7a-H, 8a-H), 4.46 (2H, d, J 8.1, 3a-H, 4a-H), 4.85 (4H, s, $2 \times \text{NH}_2$), 6.16 (1H, deg q, 9-H), 6.39 (2H, m), 7.47 (1H, s), 7.57 (3H, m), 7.68 (1H, m) and 7.88 (2H, m) (Ph, furyl, NH); $\delta_{\text{C}}(75.5 \text{ MHz}; \text{DMSO-}d_6)$ 17.9, 41.5, 42.7, 46.2, 59.6, 107.6, 110.3, 122.6, 127.7, 128.3, 131.4, 135.5, 138.7, 142.0, 151.8, 168.0, 171.5 and 172.0; m/z 475 (M^+ , 0.5%) and 69 (100).

N-[2,3,3a,4a,5,6,7,7a,8,8a-Decahydro-8-methyl-2,6-bis(methylamino)-1,3,5,7-tetraoxo-4,8-ethenobenzo[1,2-*c*:4,5-*c'*]dipyrrol-4(1*H*)-yl]benzamide (4a). Mp 287–289 °C (from pyridine). Found: C, 60.47; H, 5.42; N, 16.27. $\text{C}_{22}\text{H}_{23}\text{N}_5\text{O}_5$ requires C, 60.40; H, 5.30; N, 16.01%; $\nu_{\text{max}}(\text{KBr})/\text{cm}^{-1}$ 3362, 3306, 3260, 1771, 1704br and 1652; $\delta_{\text{H}}(300 \text{ MHz}; \text{DMSO-}d_6; \text{Me}_4\text{Si})$ 1.75 (3H, s, Me), 2.37 (6H, d, J 5.4, $2 \times \text{NHCH}_3$), 3.01 (2H, d, J 8.1, 7a-H, 8a-H), 4.23 (2H, d, J 8.1, 3a-H, 4a-H), 5.48 (2H, q, J 5.4, $2 \times \text{NHMe}$), 5.89 (1H, d, J 8.7), 6.37 (1H, d, J 8.7) (9-H, 10-H), 7.52 (3H, m, Ph), 7.89 (2H, m, Ph) and 8.72 (1H, s, NHCOPh); $\delta_{\text{C}}(75.5 \text{ MHz}; \text{DMSO-}d_6)$ 19.0, 36.6, 39.2, 41.7,

46.3, 57.6, 127.7, 128.0, 130.9, 131.0, 133.8, 135.8, 168.0, 172.2 and 173.4; m/z 437 (M^+ , 8%) and 105 (100).

***N*-[2,3,3a,4a,5,6,7,7a,8,8a-Decahydro-9-(4-methoxyphenyl)-8-methyl-2,6-bis(methylamino)-1,3,5,7-tetraoxo-4,8-ethenobenzo[1,2-*c*:4,5-*c'*]dipyrrol-4(1*H*)-yl]benzamide (4b).** Mp 319–323 °C (from EtOAc). Found: C, 64.16; H, 5.61; N, 12.95. $C_{29}H_{29}N_5O_6$ requires C, 64.08; H, 5.38; N, 12.88%; $\nu_{\max}(\text{KBr})/\text{cm}^{-1}$ 1769, 1707br, 1607, 1536 and 1510; $\delta_{\text{H}}(300 \text{ MHz}; \text{DMSO-}d_6; \text{Me}_4\text{Si})$ 1.72 (3H, s, Me), 2.39 (6H, d, J 5.7, 2 \times NHCH_3), 3.15 (2H, d, J 8.2, 7a-H, 8a-H), 3.74 (3H, s, OMe), 4.27 (2H, d, J 8.2, 3a-H, 4a-H), 5.58 (2H, q, J 5.7, 2 \times NHMe), 6.23 (1H, s, 10-H), 6.85 (4H, m, 4-MeO-C₆H₄), 7.55 (3H, m, Ph), 7.91 (2H, m, Ph) and 8.70 (1H, s, NHCOPh); $\delta_{\text{C}}(75.5 \text{ MHz}; \text{DMSO-}d_6)$ 18.7, 36.7, 41.9, 42.3, 47.2, 55.1, 58.1, 113.6, 126.9, 127.7, 128.0, 128.9, 129.6, 131.0, 135.8, 144.9, 158.8, 168.1, 172.3 and 173.9; m/z 543 (M^+ , 12%) and 105 (100).

***N*-[8-(2-Furyl)-2,3,3a,4a,5,6,7,7a,8,8a-decahydro-10-methyl-2,6-bis(methylamino)-1,3,5,7-tetraoxo-4,8-ethenobenzo[1,2-*c*:4,5-*c'*]dipyrrol-4(1*H*)-yl]benzamide (4c).** Mp 292–295 °C (from EtOAc). Found: C, 61.99; H, 5.19; N, 13.94. $C_{26}H_{25}N_5O_6$ requires C, 62.02; H, 5.00; N, 13.91%; $\nu_{\max}(\text{KBr})/\text{cm}^{-1}$ 1775, 1713, 1639 and 1531; $\delta_{\text{H}}(300 \text{ MHz}; \text{DMSO-}d_6; \text{Me}_4\text{Si})$ 1.92 (3H, s, Me), 2.31 (6H, d, J 5.8, 2 \times NHCH_3), 3.54 (2H, d, J 8.1, 7a-H, 8a-H), 4.45 (2H, d, J 8.1, 3a-H, 4a-H), 5.43 (2H, q, J 5.8, 2 \times NHMe), 6.23 (1H, deg q, 9-H), 6.41 (2H, deg m), 7.60 (5H, m) and 7.87 (2H, m) (Ph, furyl, NHCOPh); $\delta_{\text{C}}(75.5 \text{ MHz}; \text{DMSO-}d_6)$ 17.8, 36.5, 41.3, 42.6, 46.0, 59.7, 107.7, 110.3, 122.7, 127.7, 128.2, 131.4, 135.5, 138.6, 142.0, 151.7, 168.1, 171.6 and 172.2; m/z 503 (M^+ , 5%) and 105 (100).

***N*-[2,3,3a,4a,5,6,7,7a,8,8a-Decahydro-2,6-bis(methylamino)-1,3,5,7-tetraoxo-8-phenyl-4,8-ethenobenzo[1,2-*c*:4,5-*c'*]dipyrrol-4(1*H*)-yl]benzamide (4d).** Mp 280–288 °C (from EtOAc). Found: C, 62.87; H, 5.32; N, 13.82. $C_{27}H_{25}N_5O_5 \cdot \text{H}_2\text{O}$ requires C, 62.66; H, 5.26; N, 13.53%; $\nu_{\max}(\text{KBr})/\text{cm}^{-1}$ 1773, 1711br, 1653 and 1541; $\delta_{\text{H}}(300 \text{ MHz}; \text{DMSO-}d_6; \text{Me}_4\text{Si})$ 2.31 (6H, d, J 5.7, 2 \times Me), 3.75 (2H, d, J 8.2, 7a-H, 8a-H), 4.37 (2H, d, J 8.2, 3a-H, 4a-H), 5.38 (2H, q, J 5.7, 2 \times NHMe), 6.58 (1H, d, J 9.0), 6.86 (1H, d, J 9.0) (9-H, 10-H), 7.29 (2H, m), 7.41 (2H, m), 7.54 (3H, m), 7.80 (1H, m), 7.92 (2H, m) (2 \times Ph) and 8.81 (1H, s, NHCOPh); $\delta_{\text{C}}(75.5 \text{ MHz}; \text{DMSO-}d_6)$ 36.5, 41.9, 45.7, 47.1, 58.2, 126.4, 127.3, 127.4, 127.7, 128.1, 129.4, 131.0, 131.5, 135.8, 138.6, 168.1, 171.9 and 172.2; m/z 499 (M^+ , 1%) and 105 (100). HRMS found 499.1868. $C_{27}H_{25}N_5O_5$ requires 499.1855.

***N*-[8-(2-Furyl)-2,3,3a,4a,5,6,7,7a,8,8a-decahydro-2,6-bis(methylamino)-1,3,5,7-tetraoxo-4,8-ethenobenzo[1,2-*c*:4,5-*c'*]dipyrrol-4(1*H*)-yl]benzamide (4e).** Mp 300–303 °C (from EtOH). Found: C, 61.17; H, 4.94; N, 14.09. $C_{25}H_{23}N_5O_6$ requires C, 61.34; H, 4.74; N, 14.31%; $\nu_{\max}(\text{KBr})/\text{cm}^{-1}$ 1771, 1704br, 1640, 1542 and 1506; $\delta_{\text{H}}(300 \text{ MHz}; \text{DMSO-}d_6; \text{Me}_4\text{Si})$ 2.32 (6H, d, J 5.7, 2 \times Me), 3.57 (2H, d, J 8.3, 7a-H, 8a-H), 4.37 (2H, d, J 8.3, 3a-H, 4a-H), 5.44 (2H, q, J 5.7, 2 \times NHMe), 6.44 (2H, m, 2H of furyl), 6.53 (2H, AB, J 8.9, 9-H, 10-H), 7.55 (3H, m, Ph), 7.68 (1H, m, 1H of furyl), 7.91 (2H, m, Ph) and 8.80 (1H, s,

NHCOPh); $\delta_{\text{C}}(75.5 \text{ MHz}; \text{DMSO-}d_6)$ 36.5, 41.5, 42.5, 45.9, 58.0, 107.8, 110.3, 127.7, 128.0, 129.0, 131.0, 131.9, 135.7, 142.1, 151.6, 168.0, 171.6 and 171.9; m/z 489 (M^+ , 2%) and 105 (100).

***N*-[2,3,3a,4a,5,6,7,7a,8,8a-Decahydro-10-methyl-2,6-bis(methylamino)-1,3,5,7-tetraoxo-8-(2-thienyl)-4,8-ethenobenzo[1,2-*c*:4,5-*c'*]dipyrrol-4(1*H*)-yl]benzamide (4f).** Mp 304–308 °C (from EtOAc). Found: C, 60.20; H, 4.94; N, 13.61. $C_{26}H_{25}N_5O_5\text{S}$ requires C, 60.10; H, 4.85; N, 13.48%; $\nu_{\max}(\text{KBr})/\text{cm}^{-1}$ 1774, 1711br, 1645 and 1525; $\delta_{\text{H}}(300 \text{ MHz}; \text{DMSO-}d_6; \text{Me}_4\text{Si}; 69 \text{ }^\circ\text{C})$ 1.92 (3H, s, Me), 2.35 (6H, d, J 5.6, 2 \times NHCH_3), 3.56 (2H, d, J 8.0, 7a-H, 8a-H), 4.47 (2H, d, J 8.0, 3a-H, 4a-H), 5.25 (2H, q, J 5.6, 2 \times NHMe), 6.30 (1H, deg q, 9-H), 7.01 (1H, m), 7.16 (1H, deg m), 7.32 (1H, s), 7.44 (1H, m), 7.55 (3H, m) and 7.88 (2H, m) (Ph, thienyl, NHCOPh); $\delta_{\text{C}}(75.5 \text{ MHz}; \text{DMSO-}d_6, 69 \text{ }^\circ\text{C})$ 17.3, 36.2, 41.6, 44.2, 48.8, 59.4, 124.2, 124.9, 126.2, 127.2, 128.0, 131.0, 135.4, 138.2, 143.4, 167.6, 171.0 and 171.5 (1 signal hidden); m/z 519 (M^+ , 3%) and 105 (100).

***N*-[1,3,3a,6,7,8,9,9b,10,11,13,14-Dodecahydro-2,12-bis(methylamino)-1,3,11,13-tetraoxo-4*H*-4,9a[3',4']-pyrrolonaphtho[1,2-*c*]furan-4-yl]benzamide (4g).** Mp 295–297 °C (from EtOAc). Found: C, 62.59; H, 5.84; N, 14.40. $C_{25}H_{27}N_5O_5$ requires C, 62.88; H, 5.70; N, 14.67%; $\nu_{\max}(\text{KBr})/\text{cm}^{-1}$ 1772, 1703br, 1649 and 1531; $\delta_{\text{H}}(300 \text{ MHz}; \text{DMSO-}d_6; \text{Me}_4\text{Si})$ 1.33 (2H, m, CH₂), 1.60 (2H, m, CH₂), 2.09 (2H, m, CH₂), 2.36 (6H, d, J 5.7, 2 \times Me), 2.63 (2H, m, CH₂), 3.03 (2H, d, J 8.0, 9b-H, 10-H), 4.14 (2H, d, J 8.0, 3a-H, 14-H), 5.50 (2H, q, J 5.7, 2 \times NHMe), 6.04 (1H, s, 5-H), 7.53 (3H, m, Ph), 7.88 (2H, m, Ph) and 8.60 (1H, s, NHCOPh); $\delta_{\text{C}}(75.5 \text{ MHz}; \text{DMSO-}d_6)$ 20.9, 22.8, 26.4, 29.1, 36.7, 40.5, 42.0, 47.2, 57.4, 123.4, 127.7, 128.0, 130.9, 135.8, 140.5, 167.9, 172.2 and 174.2; m/z 477 (M^+ , 6%) and 105 (100).

***N*-[2,3,3a,7,8,9,10,10b,12,13,14,15-Dodecahydro-2,13-bis(methylamino)-1,3,12,14-tetraoxo-1*H*,11*H*-4,10a[3',4']-endo-pyrrolocyclohept[*l*]isoindol-4(6*H*)-yl]benzamide (4h).** Mp 294–296 °C (from EtOAc). Found: C, 63.30; H, 6.03; N, 14.17. $C_{26}H_{29}N_5O_5$ requires C, 63.53; H, 5.95; N, 14.25%; $\nu_{\max}(\text{KBr})/\text{cm}^{-1}$ 1771, 1703br, 1665 and 1537; $\delta_{\text{H}}(300 \text{ MHz}; \text{DMSO-}d_6; \text{Me}_4\text{Si})$ 1.37 (2H, m, CH₂), 1.47 (2H, m, CH₂), 1.88 (2H, m, CH₂), 2.13 (2H, m, CH₂), 2.38 (6H, d, J 5.7, 2 \times Me), 2.63 (2H, m, CH₂), 2.99 (2H, d, J 8.0, 10b-H, 11-H), 4.17 (2H, d, J 8.0, 3a-H, 15-H), 5.52 (2H, q, J 5.7, 2 \times NHMe), 6.11 (1H, s, 5-H), 7.52 (3H, m, Ph), 7.89 (2H, m, Ph) and 8.62 (1H, s, NHCOPh); $\delta_{\text{C}}(75.5 \text{ MHz}; \text{DMSO-}d_6)$ 24.0, 26.7, 30.5, 32.6, 35.5, 36.7, 42.3, 46.9, 48.5, 57.0, 124.9, 127.7, 128.0, 130.9, 135.8, 145.2, 167.8, 172.0 and 174.1; m/z 491 (M^+ , 2%) and 105 (100).

***N*-[8-(2-Furyl)-2,3,3a,4a,5,6,7,7a,8,8a-decahydro-10-methyl-1,3,5,7-tetraoxo-2,6-bis(2-pyridylamino)-4,8-ethenobenzo[1,2-*c*:4,5-*c'*]dipyrrol-4(1*H*)-yl]benzamide (5).** Mp 249–252 °C (from EtOH). Found: C, 64.09; H, 4.50; N, 15.28. $C_{34}H_{27}N_7O_6 \cdot \frac{1}{2}\text{H}_2\text{O}$ requires C, 63.94; H, 4.42; N, 15.35%; $\nu_{\max}(\text{KBr})/\text{cm}^{-1}$ 1783, 1724br, 1679 and 1603; $\delta_{\text{H}}(300 \text{ MHz}; \text{DMSO-}d_6; \text{Me}_4\text{Si})$ 2.05 (3H, s, Me), 3.84 (2H, d, J 8.4, 7a-H, 8a-H), 4.69 (2H, d, J 8.4, 3a-H, 4a-H), 6.40 (3H, m), 6.54 (2H, m), 6.77 (2H, m), 7.54 (6H, m), 7.66 (1H, br s), 7.81 (2H, m), 8.03 (2H, d) (Ph, 2 \times Py, furyl, 9-H, NHCOPh) and 8.97 (2H,

s, $2 \times \text{NNHPy}$); δ_{C} (75.5 MHz; DMSO- d_6) 18.6, 41.6, 42.6, 46.1, 59.6, 107.1, 107.9, 110.3, 115.7, 123.6, 127.7, 128.2, 131.4, 135.4, 137.6, 139.3, 142.1, 147.5, 151.6, 156.2, 168.2, 172.0 and 172.4; m/z 629 (M^+ , 5%), 105 (53) and 91 (100).

***N*-[8-(2-Furyl)-2,3,3a,4a,5,6,7,7a,8,8a-decahydro-10-methyl-1,3,5,7-tetraoxo-2,6-bis(phenylamino)-4,8-ethenobenzo[1,2-*c*:4,5-*c'*]dipyrrol-4(1*H*)-yl]benzamide (6).** Mp 295–297 °C (from EtOH). Found: C, 68.69; H, 4.80; N, 11.06. $\text{C}_{36}\text{H}_{29}\text{N}_5\text{O}_6$ requires C, 68.89; H, 4.66; N, 11.16%; ν_{max} (KBr)/ cm^{-1} 1787, 1727br, 1655 and 1603; δ_{H} (300 MHz; DMSO- d_6 ; Me_4Si) 2.06 (3H, s, Me), 3.81 (2H, d, *J* 8.4, 7a-H, 8a-H), 4.72 (2H, d, *J* 8.4, 3a-H, 4a-H), 6.40 (1H, m), 6.46 (1H, m), 6.58 (5H, m), 6.77 (2H, m), 7.16 (4H, m), 7.50 (3H, m), 7.67 (1H, br s), 7.72 (1H, br s), 7.80 (2H, m) ($3 \times \text{Ph}$, furyl, 9-H, *NHCOPh*) and 8.26 (2H, s, $2 \times \text{NNHPy}$); δ_{C} (75.5 MHz; DMSO- d_6) 18.6, 41.7, 42.7, 46.3, 59.7, 108.0, 110.3, 112.3, 119.7, 124.1, 127.8, 128.1, 128.8, 131.3, 135.4, 140.1, 142.2, 146.0, 151.4, 168.4, 172.1 and 172.7; m/z 627 (M^+ , 8%), 105 (38) and 69 (100).

***N*-[8-(2-Furyl)-2,3,3a,4a,5,6,7,7a,8,8a-decahydro-10-methyl-2,6-bis(dimethylamino)-1,3,5,7-tetraoxo-4,8-ethenobenzo[1,2-*c*:4,5-*c'*]dipyrrol-4(1*H*)-yl]benzamide (7).** Mp 290–294 (from EtOH). Found: C, 62.99; H, 5.71; N, 12.88. $\text{C}_{28}\text{H}_{29}\text{N}_5\text{O}_6$ requires C, 63.27; H, 5.50; N, 13.17%; ν_{max} (KBr)/ cm^{-1} 1786, 1726br, 1660 and 1603; δ_{H} (300 MHz; DMSO- d_6 ; Me_4Si) 1.95 (3H, d, *J* 1.2, Me), 2.59 (12H, s, $2 \times \text{NMe}_2$), 3.46 (2H, d, *J* 8.4, 7a-H, 8a-H), 4.37 (2H, d, *J* 8.4, 3a-H, 4a-H), 6.28 (1H, br s), 6.41 (2H, m), 7.59 (5H, m) and 7.86 (2H, m) (Ph, furyl, 9-H, NH); δ_{C} (75.5 MHz; DMSO- d_6) 17.7, 41.0, 42.7, 43.0, 45.9, 59.6, 107.7, 110.3, 122.8, 127.7, 128.2, 131.3, 135.5, 138.8, 141.9, 151.7, 168.0, 172.0 and 173.0; m/z 531 (M^+ , 10%) and 105 (100).

Acknowledgements

We thank the Ministry of Higher Education, Science and Technology of the Republic of Slovenia for financial support (P1-0230-0103 and J1-6693-0103). Dr B. Kralj and Dr D. Žigon (Center for Mass Spectroscopy, “Jožef Stefan” Institute, Ljubljana, Slovenia) are gratefully acknowledged for mass measurements.

Notes and references

- 1 A. Matlack, *Green Chem.*, 2003, **5**, G7–G12.
- 2 (a) K. Tanaka, *Solvent-free Organic Synthesis*, Wiley-VCH, Weinheim, 2003; (b) *Ionic Liquids in Synthesis*, ed. P. Wasserscheid and T. Welton, Wiley-VCH, Weinheim, 2003; (c) *Chemical Synthesis Using Supercritical Fluids*, ed. P. G. Jessop and W. Leitner, Wiley-VCH, Weinheim, 1999.
- 3 (a) *Microwaves in Organic Synthesis*, ed. A. Loupy, Wiley-VCH, Weinheim, 2002; (b) B. L. Hayes, *Microwave Synthesis: Chemistry at the Speed of Light*, CEM Publishing, Matthews NC, 2002; (c) R. S. Varma, *Green Chem.*, 1999, **1**, 43–55; (d) P. Lidström, J. Tierney, B. Wathey and J. Westman, *Tetrahedron*, 2001, **57**, 9225–9283; (e) M. Nüchter, B. Ondruschka, W. Bonrath and A. Gum, *Green Chem.*, 2004, **6**, 128–141; (f) C. O. Kappe, *Angew. Chem., Int. Ed.*, 2004, **43**, 6250–6284; (g) A. de la Hoz, A. Díaz-Ortiz and A. Moreno, *Chem. Soc. Rev.*, 2005, **34**, 164–178.
- 4 (a) C.-J. Li and T.-H. Chan, *Organic Reactions in Aqueous Media*, Wiley, New York, 1997; (b) *Organic Synthesis in Water*, ed. P. A. Grieco, Blackie Academic and Professional, London, 1998; (c) D. J. Adams, P. J. Dyson and S. J. Tavener, *Chemistry in Alternative Reaction Media*, Wiley, New York, 2004; (d) U. M. Lindström, *Chem. Rev.*, 2002, **102**, 2751–2772.
- 5 (a) J. An, L. Bagnell, T. Cablewski, C. R. Strauss and R. W. Trainor, *J. Org. Chem.*, 1997, **62**, 2505–2511; (b) N. E. Leadbeater and M. Marco, *Angew. Chem. Int. Ed.*, 2003, **42**, 1407–1409; (c) R. K. Arvella and N. E. Leadbeater, *Org. Lett.*, 2005, **7**, 2101–2104; (d) Y. Ju and R. S. Varma, *Org. Lett.*, 2005, **7**, 2409–2411; (e) A. Miyazawa, K. Tanaka, T. Sakakura, M. Tashiro, H. Tashiro, G. K. S. Prakash and G. A. Olah, *Chem. Commun.*, 2005, 2104–2106.
- 6 (a) U. Schmidt, A. Lieberknecht and J. Wild, *Synthesis*, 1988, 159–172; (b) R. O. Duthaler, *Tetrahedron*, 1994, **50**, 1539–1650.
- 7 (a) K. Kranjc, I. Leban, S. Polanc and M. Kočevar, *Heterocycles*, 2002, **58**, 183–190; (b) K. Kranjc, S. Polanc and M. Kočevar, *Org. Lett.*, 2003, **5**, 2833–2836.
- 8 (a) A. S. Kende, J. Lan and D. Arad, *Tetrahedron Lett.*, 2002, **43**, 5237–5239; (b) P. Magnus, L. Gazzard, L. Hobson, A. H. Payne, T. J. Rainey, N. Westlund and V. Lynch, *Tetrahedron*, 2002, **58**, 3423–3443.
- 9 (a) M. A. Ogliaruso and J. F. Wolfe, *Synthesis of Carboxylic Acids, Esters and Their Derivatives*, Wiley, New York, 1991, pp. 198–217; (b) *The chemistry of amides*, ed. J. Zabicky, Interscience Publ., London, 1970.
- 10 S. M. Verma and H. Maurya, *Indian J. Chem.*, 1985, **24B**, 447–449.
- 11 (a) M. Ješelnik, R. S. Varma, S. Polanc and M. Kočevar, *Chem. Commun.*, 2001, 1716–1717; (b) M. Ješelnik, R. S. Varma, S. Polanc and M. Kočevar, *Green Chem.*, 2002, **4**, 35–38.
- 12 N. E. Leadbeater, S. J. Pillsbury, E. Shanahan and V. A. Williams, *Tetrahedron*, 2005, **61**, 3565–3585.
- 13 The starting compound **1c** was prepared from 3-benzoylamino-6-(2-furyl)-4-methyl-2*H*-pyran-2-one and maleic anhydride by the same method as described for **1e** in ref. 7a.

Green process for hydrogen production from cellulose derivative using visible light-harvesting function of Mg chlorophyll-*a*

Noriko Himeshima and Yutaka Amai*

Received 29th March 2005, Accepted 26th August 2005

First published as an Advance Article on the web 9th September 2005

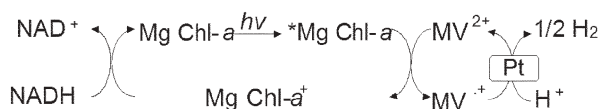
DOI: 10.1039/b504377h

A green process for hydrogen production, coupling hydrolysis of cellulose derivative, methylcellulose (MC_n) with different average molecular weights of 15 000, 21 000, 26 000, 41 000, 63 000 and 86 000, by cellulase and glucose dehydrogenase (GDH) and hydrogen production with platinum colloid as a catalyst using the visible light-harvesting function of Mg chlorophyll-*a* (Mg Chl-*a*) from *Spilurina*, has been developed. When the sample solution containing MC_n , cellulase, nicotinamide adenine dinucleotide (NAD^+), GDH, Mg Chl-*a*, methylviologen (MV^{2+} , an electron carrier reagent) and platinum colloid is irradiated, continuous hydrogen production is observed with irradiation time. For all systems using MC_n , the amount of hydrogen production is more than 10 μmol after 4 h irradiation. Hydrogen production is not affected by the polymerization degree of MC_n .

Introduction

In the research fields of environmental science and the development of energy sources, hydrogen gas production from renewable resources of timber waste, including cellulose, lignin, *etc.* is important.^{1–5} Cellulose and other polysaccharides can be hydrolyzed to monosaccharides, such as glucose, with hydrolysis enzymes. Biohydrogen production systems from glucose using a combination of glucose dehydrogenase (GDH) and hydrogenase have been reported.^{6–8} Moreover, enzymatic photoinduced hydrogen production from polysaccharides, such as cellulose, has been desired.

Studies on visible-light induced hydrogen production systems consisting of an electron donor, photosensitizer, electron carrier and a catalyst have been reported.^{9–10} In this system, the photosensitizer molecule is an important component. To develop an effective hydrogen production system, a photosensitizer molecule with an absorption band in the visible-light region is desired. Mg chlorophyll-*a* (Mg Chl-*a*), which acts as a light-harvesting molecule in photosynthesis in green plants,¹¹ is a suitable photosensitizer. On the other hand, methylviologen (MV^{2+}) and platinum colloid are useful as an electron carrier and catalyst for hydrogen production, respectively.^{9,12–15} We previously reported photoinduced hydrogen production with a system consisting of NADH, Mg Chl-*a*, MV^{2+} and platinum colloid as shown in Scheme 1.^{12,13} In this system NADH is a sacrificial reagent



Scheme 1 Visible light-induced hydrogen production system with platinum colloid *via* MV^{2+} photoreduction using the light-harvesting function of Mg Chl-*a* in the presence of NADH.

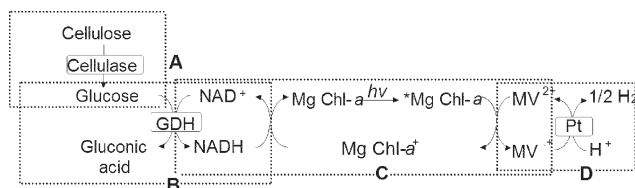
and the oxidized electron donor, NAD^+ is consumed in the reaction system. However, if NADH could be regenerated, photoinduced hydrogen production would be accomplished without NAD^+ consumption. Since GDH uses NAD^+ as a cofactor, photoinduced hydrogen production can be developed using the combination of two reactions. One is the NADH regeneration with GDH and the other one is a hydrogen production system with photosensitizer, electron relay reagent, and catalyst. We have previously reported enzymatic photoinduced hydrogen production from sucrose or maltose as renewable bio-resources using the light-harvesting function of Mg Chl-*a*,^{16–19} photoinduced hydrogen production from methylcellulose using the light-harvesting function of Mg Chl-*a*, has also been accomplished.^{18,19} However, the degree of polymerization and the molecular weight of the cellulose used in the photoinduced hydrogen production system are important factors. Thus, the relation between the degree of polymerization, molecular weight of cellulose and the amount of hydrogen production will be examined by using solubilized cellulose, methylcellulose as a cellulose derivative, in the photoinduced hydrogen production system. We have reported the preliminary result about the relation between the degree of polymerization, molecular weight of cellulose and the amount of hydrogen production as a research note.²⁰ However, the detailed conclusion of the relation between the degree of polymerization, molecular weight of cellulose and the amount of hydrogen production is not obtained.

In this paper we describe a green process for hydrogen production by coupling methylcellulose with different molecular weight, hydrolysis with cellulase and GDH, and hydrogen production with platinum colloid *via* the photo-reduction of MV^{2+} using the visible light-harvesting function of Mg Chl-*a* as shown in Scheme 2.

Experimental

Mg Chl-*a* from *Spilurina*, GDH from *Bacillus* sp., and methylcellulose (MC_n) were purchased from Wako Pure Chemical

Department of Applied Chemistry, Oita University, Dannoharu 700, Oita, Japan. E-mail: amai@cc.oita-u.ac.jp; Fax: +81 97 554 7972; Tel: +81 97 554 7972



Scheme 2 Green process for visible light-induced hydrogen production system coupling cellulose hydrolysis with cellulase and GDH and hydrogen production with platinum colloid *via* MV^{2+} photoreduction using the light-harvesting function of Mg Chl-*a*.

Industry Co. Ltd. Methylcellulose (MC_n) with average molecular weights of 15 000, 21 000, 26 000, 41 000, 63 000 and 86 000, are defined as the MC_1 , MC_2 , MC_3 , MC_4 , MC_5 and MC_6 . Methylviologen dichloride (MV^{2+}), and cetyltrimethylammonium bromide (CTAB) were obtained from Tokyo Kasei Co. Ltd. NAD^+ and NADH were purchased from Oriental Yeast Co. Ltd. Cellulase from *Aspergillus niger* was obtained from Sigma. Hydrogen hexachloroplatinate hexahydrate and sodium citrate dihydrate were obtained from Kanto Chemical Co. Ltd. D_2O was purchased from Sigma Co. Ltd. The other chemicals were analytical grade or the highest grade available. Mg Chl-*a* was solubilized with 10 mM of CTAB, since Mg Chl-*a* is insoluble in aqueous solution.

Enzyme activity

One unit of GDH activity is defined as the amount of enzyme required to reduce 1.0 μmol NAD^+ to NADH per min in the presence of glucose. One unit of cellulase activity is defined as the amount of enzyme required to reduce 1.0 μmol methylcellulose to 6-methylglucose per min.

Preparation of platinum colloid

A suspension of platinum colloid is prepared by refluxing hydrogen hexachloroplatinate(IV) hexahydrate and sodium citrate.¹⁴ A solution of 400 ml of water containing 30 mg of hydrogen hexachloroplatinate hexahydrate is heated to boiling using a heater mantle and a magnetic stirrer for 1.5 h and then a solution of 30 ml of water containing 600 mg of sodium citrate dihydrate is added and refluxed at 100 °C for 4 h. The particle size is estimated to be 1.5 nm. The prepared platinum colloid has the ability to release 0.7 μmol hydrogen in the reaction system of 10 μl platinum colloid, 1.2×10^{-5} mmol MV^{2+} and 7.7×10^{-5} mmol sodium dithionite in 4 ml of 0.15 mmol Tris-HCl buffer (pH 7.4) at 30 °C for 10 min. One unit of platinum colloid activity is defined as release of 1.0 μmol of hydrogen per min.

Glucose formation with MC_n and cellulase

The reaction is started by adding cellulase (4.0 units) to a solution containing MC_n (1.2 μmol , cellobiose unit) in potassium phosphate buffer (pH 7.0) (process A in Scheme 2). Formation of the products in the reaction mixture is analyzed using HPLC with an electrical conductivity detector (Shimadzu CDD-10A_{VP}) (column temperature: 40 °C, column: polystyrene sulfonate column Shimadzu SCR-H, elutant: *p*-toluene sulfonic acid and flow rate: 0.8 ml min⁻¹).

NADH formation with MC_n cellulase and GDH

The reaction is started by adding NAD^+ (0.6 μmol) to a solution containing MC_n (1.2 μmol , cellobiose unit), cellulase (4 units) and GDH (5 units) in phosphate buffer (pH 7.0) (process A and B in Scheme 2). The reduction of NAD^+ to NADH by GDH is determined by following the specific absorption at 340 nm assuming a molar extinction coefficient of $6.3 \times 10^3 \text{ M}^{-1} \text{ cm}^{-1}$.

Photoreduction of MV^{2+}

Photoreduction of MV^{2+} is tested in a reaction mixture containing NAD^+ (15 μmol), MC_n (60 μmol , cellobiose unit), cellulase (4 units), NAD^+ (7.5 μmol), GDH (5 units), Mg Chl-*a* (27 nmol), and MV^{2+} (1.2 μmol) in 3.0 ml of 30 μmol potassium phosphate buffer (pH 7.0) (process A, B and C in Scheme 2). The solution is deaerated by repeated freeze-pump-thaw cycles and irradiated with a 200 W tungsten lamp at a distance of 3.0 cm. Wavelengths less than 390 nm are removed with a Toshiba L-39 cut-off filter. Reduction of MV^{2+} is monitored using an UV-vis spectrophotometer set at 605 nm assuming a molar extinction coefficient of $1.3 \times 10^4 \text{ M}^{-1} \text{ cm}^{-1}$.²¹

Photoinduced hydrogen production

Photoinduced hydrogen production is tested in a reaction mixture containing MC_n (60 μmol , cellobiose unit), cellulase (4 units), GDH (5 units), NAD^+ (7.5 μmol), Mg Chl-*a* (27 nmol), MV^{2+} (1.2 μmol) and platinum colloid (0.5 unit) in 3.0 ml of 30 μmol potassium phosphate buffer (pH 7.0). The solution is deaerated by 6 freeze-pump-thaw cycles, and flushed with argon gas. The amount of hydrogen produced and the other produced gases are measured with a Shimadzu GC-14B gas chromatograph (detector: TCD, column temperature: 40 °C, column: active charcoal with particle size 60–80 mesh, carrier gas: nitrogen gas, carrier gas flow rate: 24 ml min⁻¹).

Results and discussion

Glucose formation with MC_n and cellulase

When the sample solution containing MC_n and cellulase is incubated for 10 min, methylglucose (2-, 3- or 6-methylglucose) is formed. For all systems, total methylglucose (2.4 μmol) is produced after 10 min incubation. This result shows that the methylcellulose hydrolysis to methylglucose with cellulase proceeds rapidly and the yield is *ca.* 100% after 10 min incubation.

NADH formation with MC_n , cellulase and GDH

When a sample solution containing MC_n , cellulase, NAD^+ and GDH is incubated, the time dependence of NADH production is shown in Fig. 1. For all systems, 0.6 μmol NADH is formed and the yield of NAD^+ to NADH is *ca.* 100% after 40 min incubation. Little change in NADH formation rate is observed for any MC_n . Thus, MC_n hydrolysis rate with cellulase (step A in Scheme 2) is independent of the molecular weight of MC_n . In contrast, no formation of NADH is

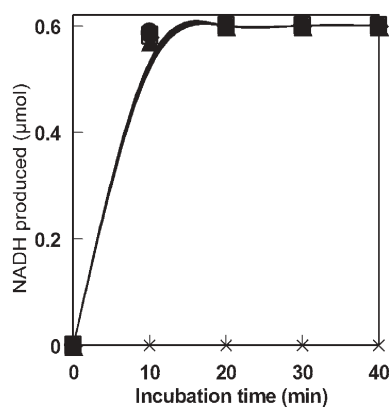


Fig. 1 Time dependence of NADH production with MC_n (1.2 μmol cellobiose unit), cellulase (4.0 units), NAD^+ (0.6 μmol) and GDH (5.0 units) in 3 ml of 30 μmol potassium phosphate buffer (pH 7.0). Closed square: MC_1 , closed circle: MC_2 , closed triangle: MC_3 , closed diamond: MC_4 , open square: MC_5 and open circle: MC_6 . X: without cellulase.

observed in a solution containing methylcellulose, GDH and NAD^+ without cellulase.

Photoreduction of MV^{2+}

Time dependence of the MV^+ concentration in a system containing MC_n , cellulase, GDH, NAD^+ , Mg Chl-*a*, and MV^{2+} with visible light irradiation is shown in Fig. 2. The absorption band at 605 nm attributed to MV^+ increases with irradiation time. For all NAD^+ concentrations, ca. 0.24 μmol reduced MV^{2+} is produced and the yield of MV^{2+} to MV^+ is estimated to be ca. 20% after 40 min irradiation. The photoreduction is

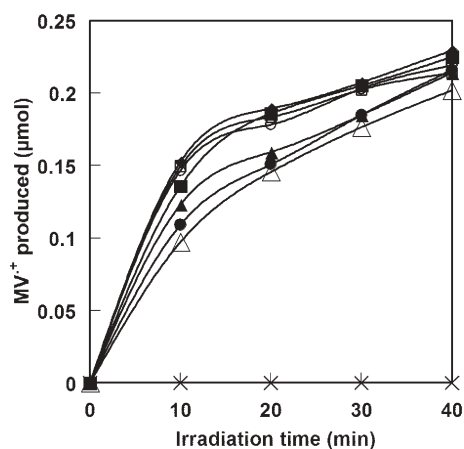


Fig. 2 The time dependence of the reduced MV^{2+} concentration under steady state irradiation with visible light using 200 W tungsten lamp at a distance of 3.0 cm. The sample solution consisting of MC_n (60 μmol cellobiose unit), cellulase (4.0 units), NAD^+ (7.5 μmol), GDH (5.0 units), Mg Chl-*a* (27 nmol) and MV^{2+} (1.2 μmol) in 3 ml of 30 μmol phosphate buffer (pH 7.0). Closed square: MC_1 , closed circle: MC_2 , closed triangle: MC_3 , closed diamond: MC_4 , open square: MC_5 and open circle: MC_6 . X: without NAD^+ . Open triangle: 30 μmol potassium phosphate buffer prepared using D_2O is used as the reaction media (pH 7.0).

independent of the concentrations of NAD^+ , methylcellulose, cellulase and GDH. In contrast, the reduction depends on the concentrations of Mg Chl-*a* and MV^{2+} . Thus, the rate-limiting step in the MV^{2+} reduction (processes A, B and C in Scheme 2) is the electron transfer process from the photoexcited Mg Chl-*a* ($^*\text{Mg Chl-}a$) to MV^{2+} (process C in Scheme 2). MV^{2+} is not reduced without NAD^+ (Fig. 2, X symbol) or without irradiation. These results show that the MV^{2+} photoreduction proceeds by coupling the methylcellulose hydrolysis with cellulase and GDH (processes A and B in Scheme 2) and MV^{2+} reduction using the light-harvesting function of Mg Chl-*a* (process C in Scheme 2).

Photoinduced hydrogen production

Fig. 3 shows the time dependence of hydrogen production by the visible light in the system containing MC_n , cellulase, GDH, NAD^+ , Mg Chl-*a*, MV^{2+} , and platinum colloid. When the sample solution is irradiated, hydrogen production is observed as shown in Fig. 3. For all systems, hydrogen is produced continuously and the amount of hydrogen production is more than 10 μmol after 4 h irradiation. From the results of gas analysis using gas chromatography, hydrogen and argon gases are detected and other gases such as carbon dioxide are not detected.

For the systems using MC_1 and MC_4 , the amount of hydrogen production is 12 μmol . In contrast, the amount of hydrogen production is 10 μmol in the system using MC_2 . However, there is little difference in the amount of hydrogen production. These results show that the hydrogen production rate is also independent of the polymerization degree of MC_n . For all cases, the amount of hydrogen produced is larger than that of the initial NAD^+ (7.5 μmol). This result indicates that NADH formed by cellulase and GDH is oxidized to NAD^+ in the photoinduced hydrogen production and the formed NAD^+ is reduced to NADH by the MC_n hydrolysis with cellulase and

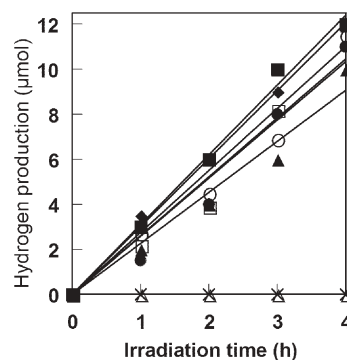


Fig. 3 Time dependence of hydrogen production under steady state irradiation with visible light using 200 W tungsten lamp at a distance of 3.0 cm. The sample solution consisted of MC_n (60 μmol cellobiose unit), cellulase (4.0 units), NAD^+ (7.5 μmol), GDH (5.0 units), Mg Chl-*a* (27 nmol), MV^{2+} (1.2 μmol) and platinum colloid (0.5 units) in 3 ml of 30 μmol phosphate buffer (pH 7.0). Closed square: MC_1 , closed circle: MC_2 , closed triangle: MC_3 , closed diamond: MC_4 , open square: MC_5 and open circle: MC_6 . X: without NAD^+ . Open triangle: 30 μmol potassium phosphate buffer prepared using D_2O as the reaction media (pH 7.0).

GDH, and then the formed NADH is used as an electron donor in the photoinduced hydrogen production.

In contrast, no hydrogen production is observed without irradiation as shown in Fig. 3 (data not shown). Moreover, hydrogen is also not evolved in the absence of NAD⁺ (X symbol).

The by-product formation in the reaction mixture was analyzed using HPLC. Methylgluconic acid is produced as by-product. Methylgluconic acid is formed by oxidation of methylglucose (formed by methylcellulose hydrolysis with cellulase) with GDH as shown in steps A and B of Scheme 2. These results strongly suggest that the visible light-induced hydrogen production proceeded by coupling the methylcellulose hydrolysis with cellulase and GDH and the hydrogen production with platinum colloid using the light-harvesting function of Mg Chl-*a* as shown in Scheme 2.

Next, to investigate the proton source of the hydrogen production in the system containing MC_{*n*}, cellulase, GDH, NAD⁺, Mg Chl-*a*, MV²⁺, and platinum colloid, the 30 μmol potassium phosphate buffer prepared using D₂O was used as the reaction media (pH 7.0). In this experiment, MC₂ was used. At first, the photoreduction of MV²⁺ was attempted in potassium phosphate buffer prepared using D₂O. The time dependence of the MV⁺ concentration in potassium phosphate buffer prepared using D₂O is shown in Fig. 2 (open triangles). The photoreduction of MV²⁺ proceeds in potassium phosphate buffer prepared using D₂O. However, no hydrogen production in potassium phosphate buffer prepared using D₂O was observed as shown in Fig. 3 (open triangles). This result shows that the platinum colloid cannot catalyze the reduction of D⁺ to D₂. Thus, the hydrogen produced originates from protons in the reaction media.

Next let us focus on the effect of reaction pH on the hydrogen production. Fig. 4 also shows the time dependence of the photoinduced hydrogen production in the system containing MC₂, cellulase, GDH, NAD⁺, Mg Chl-*a*, MV²⁺,

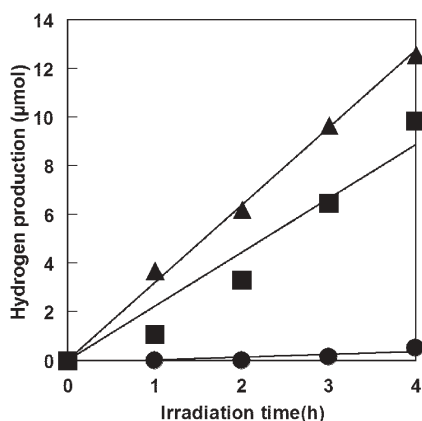


Fig. 4 Time dependence of hydrogen production with steady state visible light irradiation using 200 W tungsten lamp at a distance of 3.0 cm under various pH conditions. The sample solution consisting of MC₂ (60 μmol cellobiose unit), cellulase (4.0 units), NAD⁺ (7.5 μmol), GDH (5.0 units), Mg Chl-*a* (27 nmol), MV²⁺ (1.2 μmol) and platinum colloid (0.5 units) in 3 ml of 30 μmol phosphate buffer. The reaction pH: (closed circle): 5, (closed triangle): 7, (closed square): 8.

and platinum colloid irradiated with visible light under various pH conditions between 5 and 8. The hydrogen production rate is highest at pH 7. As the optimum pH for GDH activity is above 6.7, the hydrogen production rate decreases at pH 5 due to the deactivation of GDH. As the proton concentration decreases at pH 8, the hydrogen production rate also decreases.

The view to engineering application

Next let us focus on the engineering application of this photoinduced hydrogen production system. By using this process, the amount of hydrogen production is estimated to be 12 μmol after 4 h irradiation. As the quantum yield is 2.0% by potassium ferrioxalate actinometry method, the conversion ratio of MC_{*n*} (initial: 20 μmol) to hydrogen gas is up to 20%. The total volume of the reaction vessel used in this work is 15.0 ml. The *ca.* 4.0 μmol (8.0 μg) of hydrogen gas is obtained with 1 h irradiation. Thus 0.27 mol of hydrogen will be obtained using a 1.0 m³ reaction vessel. The 3.0 ml reaction mixture includes 64.7 μg of platinum in this system (the 0.5 units of platinum colloid is equal to 0.11 mM). To obtain 1.0 kg of hydrogen using this process with 1 h irradiation, 8.1 kg of platinum is needed. From these results, this process is suitable for producing hydrogen from cellulose derivatives rather than for producing usable energy.

Now we are attempting the scale-up of the reaction and hydrogen production using sunlight for the development of economic processing.

Conclusion

In conclusion, a green process for hydrogen production coupling hydrolysis of methylcellulose (MC_{*n*}) with different molecular weights with cellulase and GDH and hydrogen production with platinum colloid *via* MV²⁺ photoreduction using the light-harvesting function of Mg Chl-*a* is developed and continuous hydrogen gas production is achieved. Only gluconic acid from the cellulose derivative is produced as a by-product and no carbon dioxide gas is evolved in the present reaction system. Thus, renewable bio-resources have been effectively used to produce hydrogen gas through an environmentally clean process.

Acknowledgements

This work was partially supported by Special Fund from The Iwatani Naoji Foundation and a Grant-in-Aid for Scientific Research Areas (417) from the Ministry of Education, Culture, Sports, Science and Technology, Japan.

References

- 1 L. C. Helena and R. P. Overend, *Fuel Process Technol.*, 2001, **71**, 187.
- 2 M. J. Barbosa, J. M. Rocha, J. Tramper and R. H. Wijffels, *J. Biotechnol.*, 2001, **85**, 25.
- 3 L. Garcia, R. French, S. Czernik and E. Chornet, *Appl. Catal., A*, 2000, **201**, 225.
- 4 D. Wang, *Fuel Energy Abstr.*, 1998, **39**, 188.
- 5 T. Minowa and S. Inoue, *Renewable Energy*, 1999, **16**, 1114.

- 6 J. Woodward, M. Orr, K. Cordray and E. Greenbaum, *Nature*, 2000, **405**, 1014.
- 7 T. Inoue, S. N. Kumar, T. Kamachi and I. Okura, *Chem. Lett.*, 1999, 147.
- 8 J. Woodward, S. M. Mattingly, M. Danson, D. Hough, N. Ward and M. Adams, *Nature Biotechnol.*, 1996, **14**, 872.
- 9 J. R. Darwent, P. Douglas, A. Harriman, G. Porter and M. C. Richoux, *Coord. Chem. Rev.*, 1982, **44**, 93.
- 10 I. Okura, *Coord. Chem. Rev.*, 1985, **68**, 53.
- 11 H. Scheer, *Chlorophylls*, CRC Press, London, 1991.
- 12 Y. Tomonou and Y. Amai, *BioMetals*, 2002, **15**, 391.
- 13 Y. Tomonou and Y. Amai, *BioMetals*, 2003, **16**, 419.
- 14 P. A. Brugger, P. Cuendet and M. Grätzel, *J. Am. Chem. Soc.*, 1981, **103**, 2923.
- 15 J. Kiwi and M. Grätzel, *J. Am. Chem. Soc.*, 1979, **101**, 7214.
- 16 Y. Saiki and Y. Amai, *Bioconjugate Chem.*, 2002, **13**, 898.
- 17 N. Himeshima and Y. Amai, *Biotechnol. Lett.*, 2002, **24**, 1647.
- 18 N. Himeshima and Y. Amai, *Biotechnol. Lett.*, 2002, **24**, 1935.
- 19 N. Himeshima and Y. Amai, *Energy Fuels*, 2003, **17**, 1641.
- 20 N. Himeshima and Y. Amai, *Polymer J.*, 2004, **36**, 352.
- 21 T. Watanabe and K. Honda, *J. Phys. Chem.*, 1982, **86**, 2617.

A ternary mechanism for the facilitated transfer of metal ions into room-temperature ionic liquids (RTILs): implications for the “greenness” of RTILs as extraction solvents†

Mark L. Dietz* and Dominique C. Stepinski

Received 20th June 2005, Accepted 18th August 2005

First published as an Advance Article on the web 8th September 2005

DOI: 10.1039/b508604c

Partitioning of sodium ions between aqueous nitrate media and 1-alkyl-3-methylimidazolium bis[(trifluoromethyl)sulfonyl]imides ($C_n\text{mim}^+\text{Tf}_2\text{N}^-$) in the presence of dicyclohexano-18-crown-6 is shown to take place *via* as many as three pathways: conventional nitrate complex extraction and/or either or both of two ion-exchange processes, the relative importance of which is determined by aqueous acidity and the hydrophobicity of the ionic liquid cation. Contrary to expectations, increasing the alkyl chain length of the IL cation (from $C_5\text{mim}^+$ to $C_{10}\text{mim}^+$) is insufficient to eliminate the possibility of ion exchange as a mode of metal ion partitioning between the two phases, an observation with negative implications for the utility of ILs as environmentally benign extraction solvents.

Introduction

Growing recognition of the advantages afforded by ionic liquids (ILs) as replacements for conventional molecular solvents in numerous synthetic,^{1–4} catalytic,^{4–6} and electrochemical^{7,8} applications has led to increasing interest in their potential utility in various separation processes.^{9–19} Of particular interest in this laboratory have been the possibilities offered by these novel solvents as the basis for more environmentally benign systems for the liquid–liquid extraction of metal ions.²⁰ In an effort to devise guidelines for the rational design of IL-based extraction systems for metal ion separation, we have sought to develop an understanding of the fundamental aspects of the transfer of a metal ion from an aqueous phase into an ionic liquid in the presence of various types of ligands, among them crown ethers,^{21–23} neutral organophosphorus compounds,²⁴ and their mixtures.²⁵ In earlier reports,^{21,22} we presented evidence that the transfer of a strontium ion from aqueous nitrate media into certain 1-alkyl-3-methylimidazolium bis[(trifluoromethyl)sulfonyl]imides (abbreviated hereafter as $C_n\text{mim}^+\text{Tf}_2\text{N}^-$) in the presence of dicyclohexano-18-crown-6 (DCH18C6) involves exchange of the cationic 1 : 1 strontium : DCH18C6 complex for the cationic constituent of the ionic liquid, an observation with obvious negative implications for the “greenness” of ionic liquids as extraction solvents. Implicit in this observation is that as the hydrophobicity of the IL cation increases, the

ion-exchange process should become more difficult, and in fact, an increase in the length of the alkyl chain appended to the IL cation has been shown to lead to both decreased strontium extraction²¹ and a gradual change in the mode of its partitioning from ion exchange (for $n = 5$) to nitrate complex extraction (for $n = 10$).²³ In the course of studies to determine the generality of these observations, we have examined the partitioning of a representative alkali metal cation, Na^+ , between $C_n\text{mim}^+\text{Tf}_2\text{N}^-$ ($n = 5–10$) ILs and aqueous nitrate media in the presence of DCH18C6. Unexpectedly, the results obtained reveal the presence of another, previously unreported pathway for metal ion partitioning into ionic liquids, and demonstrate that merely increasing the IL cation hydrophobicity is not always sufficient to eliminate the possibility of ion exchange as a mode of metal ion transfer into an ionic liquid in the presence of a neutral extractant.

Experimental

Materials

The ionic liquids were prepared according to published methods.²⁶ The DCH18C6 used was a commercial mixture of the *cis-syn-cis* (A) and *cis-anti-cis* (B) isomers (Aldrich, Milwaukee, WI), consistent with prior studies.^{14,21,23} Aqueous acid solutions were prepared using Milli-Q2 water and Ultrex[®] nitric acid (J. T. Baker Chemical Co.).

Methods

All sodium distribution ratios were determined radiometrically using a commercial Na-22 tracer, assayed *via* gamma spectroscopy using standard procedures²⁷ modified only by use of a single acid contact as a preconditioning step. The extent of aqueous phase dissolution of the $C_n\text{mim}^+$ cation was determined by ¹H NMR. A temperature of *ca.* 23 °C was employed for all measurements.

Chemistry Division, Argonne National Laboratory, Argonne, IL 60439, USA. E-mail: mdietz@anl.gov.; Fax: +1 (630) 252-7501; Tel: +1 (630) 252-3647

† The submitted manuscript has been created by the University of Chicago as Operator of Argonne National Laboratory under contract number W-31-109-ENG-38 with the US Department of Energy. The US Government retains for itself, and others acting on its behalf, a paid-up, nonexclusive, irrevocable worldwide license in said article to reproduce, prepare derivative works, distribute copies to the public, and perform publicly, and display publicly, by or on behalf of the Government.

Results and discussion

As is well known, electroneutrality must be maintained in the transfer of a metal ion from an aqueous phase into an organic solvent.²⁸ In conventional (*i.e.*, molecular) solvents employing neutral extractants, such as in the extraction of a metal cation into an aliphatic alcohol by a crown ether, this is accomplished by the coextraction of aqueous phase anions.²⁹ In the extraction of Na^+ from acidic nitrate media into 1-octanol by DCH18C6, for example, the 1 : 1 sodium–crown ether complex³⁰ must be accompanied by a nitrate ion:



Not surprisingly, the nitric acid dependency of D_{Na} for DCH18C6 in such a system (Fig. 1) is characterized by an increase in sodium partitioning with increasing nitrate (*i.e.*, nitric acid) concentration (until high acidities are reached, at which point the effects of metal–nitrate complex formation and acid extraction by the crown ether result in a rollover of the dependency³¹). In contrast, the acid dependency of D_{Na} in both $\text{C}_5\text{mim}^+\text{Tf}_2\text{N}^-$ and $\text{C}_{10}\text{mim}^+\text{Tf}_2\text{N}^-$ (Fig. 1) exhibits a significant decline in sodium partitioning as the acidity is increased. Such a decline, as has been noted previously,²¹ is inconsistent with the extraction of a metal–nitrate complex.

That D_{Na} decreases with nitric acid concentration for both C_nmim^+ systems is unexpected, given earlier results for strontium ion extraction,²³ for which the increase in IL cation hydrophobicity that accompanies the change from C_5mim^+ to $\text{C}_{10}\text{mim}^+$ was found to be sufficient to induce a change in the mode of strontium transfer from ion exchange to nitrate complex partitioning and thus, to produce an acid dependency for $\text{C}_{10}\text{mim}^+\text{Tf}_2\text{N}^-$ exhibiting a positive slope. This result suggests that the transfer of Na^+ from acidic nitrate media into

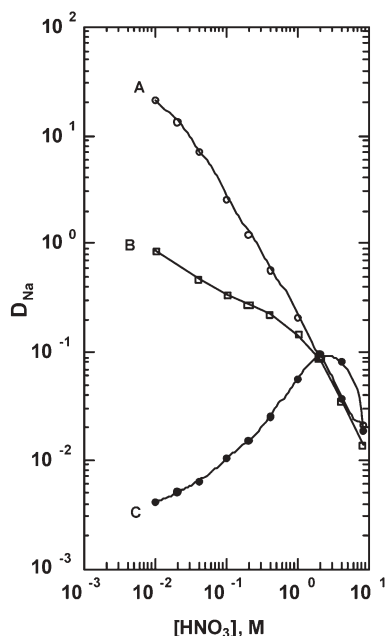
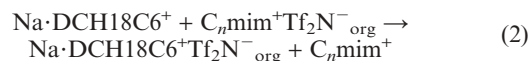


Fig. 1 Nitric acid dependency of D_{Na} for DCH18C6 (0.1 M) in (A) $\text{C}_5\text{mim}^+\text{Tf}_2\text{N}^-$, (B) $\text{C}_{10}\text{mim}^+\text{Tf}_2\text{N}^-$, and (C) 1-octanol.

the ionic liquids in the presence of a crown ether may involve a process other than the direct exchange of the 1 : 1 complex for the IL cation (eqn (2)), an interpretation supported by a close examination of the acid dependencies of D_{Na} at high (≥ 1 M) nitric acid concentrations.



In this region, a log–log plot of D_{Na} versus $[\text{HNO}_3]$ for $\text{C}_{10}\text{mim}^+\text{Tf}_2\text{N}^-$ yields a line ($R = 0.993$) of negative near-unit slope (-1.14). A similar linear decrease (slope = -1.10 ; $R = 0.994$) in $\log D_{\text{Na}}$ with $\log [\text{HNO}_3]$ is observed for $\text{C}_5\text{mim}^+\text{Tf}_2\text{N}^-$ over this same range of acidities, indicating that the transfer of a sodium ion is accompanied by release of a hydrogen ion from the IL phase. Given that the ionic liquids bear no ionizable hydrogens and that the extractant is neutral, this would not initially appear to be reasonable. Numerous prior studies, however, have established that DCH18C6 can extract significant quantities of various mineral acids, including nitric acid, from aqueous solution.^{31–37} Moreover, our measurements of metal ion partitioning involve a preliminary equilibration of the IL phase with aqueous nitric acid, thus providing an opportunity for conversion of the crown ether to a DCH18C6 : acid adduct prior to introduction of a sodium ion. Examination of the infrared spectrum of the IL phase before and after its equilibration with nitric acid (1 M), in fact, shows that, in contrast to conventional organic solvents (in which nitric acid adducts with DCH18C6 typically comprise *undissociated* HNO_3 molecules),³¹ acid extraction by the crown ether results in the formation of a DCH18C6 : hydronium ion adduct in the ionic liquid. (This is demonstrated both by the presence of absorbance bands characteristic of oxonium salts,³⁸ most notably a prominent band centered at *ca.* 2184 cm^{-1} , and the close correspondence of the spectrum to that of the ionic liquid following its equilibration with perchloric acid, with which DCH18C6 is known to form a hydronium ion complex.³⁹) Thus, at sufficiently high acidity, sodium partitioning apparently involves the following process:



That this process clearly cannot occur without conversion of the crown ether to the acid adduct, along with the fact that extraction of sodium occurs even in the absence of acid and that for $\text{C}_{10}\text{mim}^+\text{Tf}_2\text{N}^-$ (but not for $\text{C}_5\text{mim}^+\text{Tf}_2\text{N}^-$) this extraction is accompanied by some co-extraction of nitrate ion (*ca.* 60% of that required to maintain electrical neutrality), indicates that the *overall* extraction process must be described by a combination of three processes: sodium nitrate–crown ether complex partitioning (eqn (1)), exchange of the 1 : 1 sodium–crown ether complex for the IL cation (eqn (2)), and crown ether-mediated $\text{Na}^+/\text{H}_3\text{O}^+$ exchange (eqn (3)), their relative importance determined by the aqueous acidity and the hydrophobicity of the IL cation. To the best of our knowledge, such a “ternary (*i.e.*, three-path) partitioning mechanism” has no counterpart in extraction systems employing crown ethers in conventional molecular solvents.

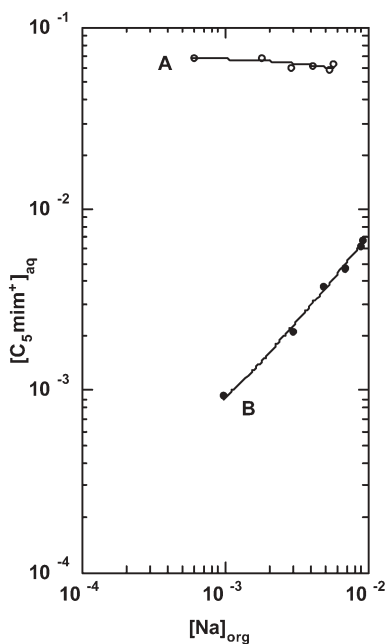
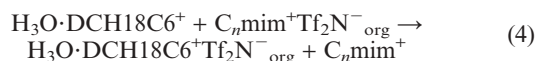


Fig. 2 Effect of sodium extraction ($[Na^+]_{aq, initial}$: 0.001–0.01 M) by DCH18C6 (0.1 M) in $C_5mim^+Tf_2N^-$ on the solubilization of the C_5mim^+ cation in (A) 0.20 M HNO_3 or (B) water. (Each value of $[C_5mim^+]$ represents the difference between that observed in the presence and absence of DCH18C6 at a given $[Na^+]_{aq, initial}$ concentration. Values of $[Na]_{org}$ were calculated from the % extraction values under the same conditions.)

Additional support for the presence of two distinct ion-exchange processes in the partitioning of sodium ions is found in the results of measurements of the aqueous concentration of the C_5mim^+ cation as a function of sodium ion loading of the IL phase using either water or 0.25 M nitric acid as the aqueous phase (Fig. 2). In the former system, a near first power dependence of $[IL^+]_{aq}$ upon the concentration of extracted sodium is observed (slope = 0.88; $R = 0.997$), as expected from eqn (2). In contrast, for the acidic aqueous phase, increased sodium loading yields no increase in the aqueous concentration of the IL cation, as expected from eqn (3). It is important to note, however, that although sodium ion extraction *via* its exchange for a hydronium ion in $H_3O \cdot DCH18C6^+$ (eqn (3)) results in no *direct* loss of IL^+ to the aqueous phase, the formation and partitioning of the DCH18C6 : hydronium ion adduct (during acid preconditioning of the organic phase) would itself be expected to lead to solubilization of the ionic liquid:



In fact, increasing the initial organic phase concentration of the crown ether in $C_5mim^+Tf_2N^-$ in the presence of excess aqueous acid (e.g., 1 M HNO_3) is accompanied by a corresponding increase (slope = +0.83; $R = 0.993$) in the concentration of the IL cation in the aqueous phase. Thus, either of the two ion-exchange processes by which a sodium ion reaches the IL phase ultimately requires transfer of C_nmim^+ to the aqueous phase.

Conclusions

These results, in addition to their obvious importance in elucidating the fundamental aspects of metal ion transfer into ILs, have significant practical (and unfortunately, negative) implications for their application as environmentally benign extraction solvents. First, among the various factors determining the suitability of ionic liquids as replacements for conventional molecular solvents in separations applications is that of the mutual solubility of ILs and water (and/or aqueous acid solutions). As shown in this study, the aqueous solubility of an ionic liquid can be increased merely by the presence of a neutral ligand (here, a crown ether) capable of extracting significant quantities of acid. Such effects, which are not normally a consideration in selecting a conventional extraction solvent, represent an important and heretofore unrecognized limitation of ionic liquids in this application. Next, as we have noted previously,²¹ an extraction system in which metal ion partitioning is accompanied by increased dissolution of the ionic liquid in the aqueous phase cannot be regarded as “green”. Although our earlier results²³ suggested that simply increasing the hydrophobicity of the IL cation (from C_5mim^+ to $C_{10}mim^+$) could eliminate the possibility of ion exchange as a mode of metal ion partitioning between acidic media and ILs containing neutral extractants and the accompanying solubilization of the ionic liquid, this is clearly not always the case. Finally, despite the ostensible chemical simplicity of an alkali or alkaline earth cation/neutral crown ether system, the process involved in the transfer of the cation into an ionic liquid in the presence of a crown ether is surprisingly complex. Although such complexity can, in principle, provide a wealth of opportunities for the design of IL-based extraction systems of improved efficiency and selectivity, the full potential of ionic liquids as environmentally benign extraction solvents will clearly not be realized until methods are devised to reduce or eliminate the aqueous dissolution of the IL that can accompany metal ion partitioning. Work addressing this issue is now underway in this laboratory.

Acknowledgements

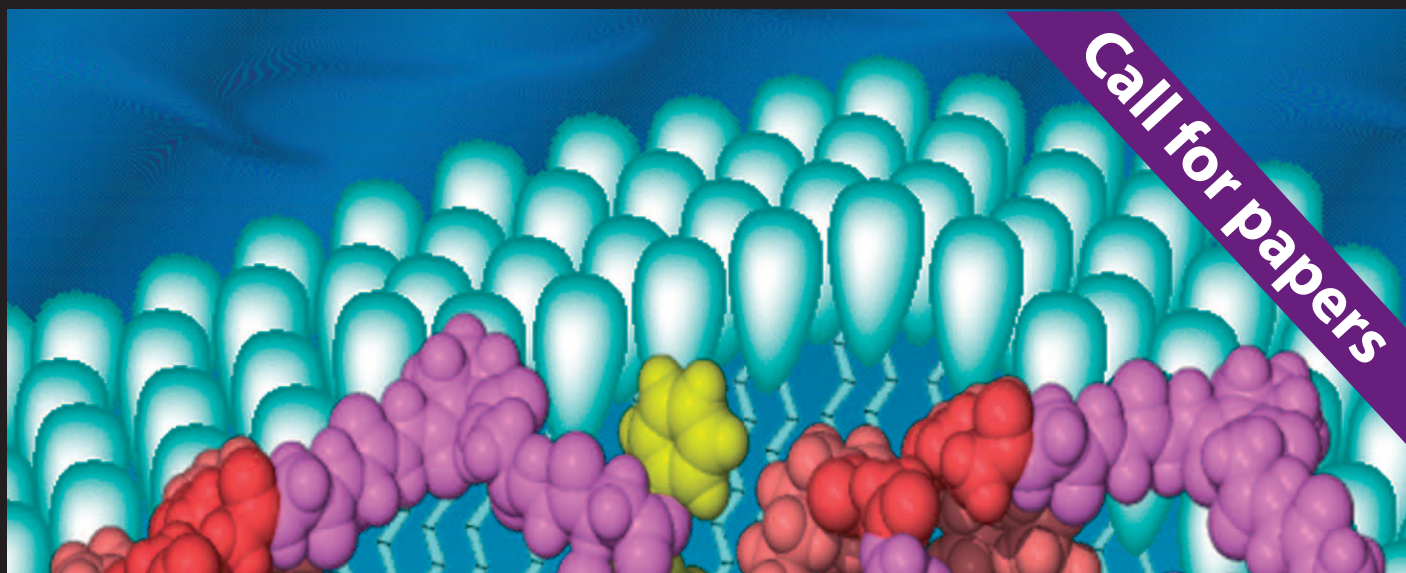
This work was performed under the auspices of the Office of Basic Energy Sciences, Division of Chemical Sciences, United States Department of Energy, under contract number W-31-109-ENG-38.

References

- 1 K. R. Seddon, *J. Chem. Technol. Biotechnol.*, 1997, **68**, 351.
- 2 J. D. Holbrey and K. R. Seddon, *Clean Prod. Processes*, 1999, **1**, 223.
- 3 M. J. Earle and K. R. Seddon, *Pure Appl. Chem.*, 2000, **72**, 1391.
- 4 H. Olivier-Bourbigou and L. Magna, *J. Mol. Catal. A: Chem.*, 2002, **182**, 419.
- 5 K. R. Seddon, *Kinet. Catal.*, 1996, **37**, 693.
- 6 D. Zhao, M. Wu, Y. Kou and E. Min, *Catal. Today*, 2002, **74**, 157.
- 7 J. Fuller, R. T. Carlin and R. A. Osteryoung, *J. Electrochem. Soc.*, 1997, **144**, 3881.
- 8 R. T. Carlin and J. Fuller, in *Proceedings of the 12th Annual Battery Conference on Applications and Advances-1997*, ed. H. A. Frank, E. T. Seo, Institute of Electrical and Electronics Engineers, New York, 1997, pp. 261–266.

- 9 J. L. Anthony, E. J. Maginn and J. F. Brennecke, in: *Ionic Liquids: Industrial Applications for Green Chemistry*, ed. R. D. Rogers, K. R. Seddon, ACS Symposium Series 818, American Chemical Society, Washington, DC, 2002, pp. 260–269.
- 10 L. A. Blanchard, Z. Gu and J. F. Brennecke, *J. Phys. Chem. B*, 2001, **105**, 2437.
- 11 A. G. Fadeev and M. M. Meagher, *Chem. Commun.*, 2001, 295.
- 12 L. C. Branco, J. G. Crespo and C. A. M. Afonso, *Angew. Chem., Int. Ed.*, 2002, **41**, 2771.
- 13 L. C. Branco, J. G. Crespo and C. A. M. Afonso, *Chem.—Eur. J.*, 2002, **8**, 3865.
- 14 S. Dai, Y. H. Ju and C. E. Barnes, *J. Chem. Soc., Dalton Trans.*, 1999, 1201.
- 15 A. E. Visser, R. P. Swatloski, W. M. Reichert, S. T. Griffin and R. D. Rogers, *Ind. Eng. Chem. Res.*, 2000, **39**, 3596.
- 16 A. E. Visser, R. P. Swatloski, D. H. Hartman, J. G. Huddleston and R. D. Rogers, in *Calixarenes for Separations*, ed. G. J. Lumetta, R. D. Rogers, A. S. Gopalan, ACS Symposium Series 757, American Chemical Society, Washington, DC, 2000, pp. 223–236.
- 17 A. E. Visser, R. P. Swatloski, S. T. Griffin, D. H. Hartman and R. D. Rogers, *Sep. Sci. Technol.*, 2001, **36**, 785.
- 18 S. Chun, S. V. Dzyuba and R. A. Bartsch, *Anal. Chem.*, 2001, **73**, 3737.
- 19 A. E. Visser, R. P. Swatloski, W. M. Reichert, R. Mayton, S. Sheff, A. Wierzbicki, J. H. Davis, Jr. and R. D. Rogers, *Chem. Commun.*, 2001, 135.
- 20 M. L. Dietz, J. A. Dzielawa, M. P. Jensen and M. A. Firestone, in *Ionic Liquids as Green Solvents. Progress and Prospects*, ed. R. D. Rogers, K. R. Seddon, ACS Symposium Series 856; American Chemical Society, Washington, DC, 2003, pp. 526–543.
- 21 M. L. Dietz and J. A. Dzielawa, *Chem. Commun.*, 2001, 2124.
- 22 M. P. Jensen, J. A. Dzielawa, P. Rickert and M. L. Dietz, *J. Am. Chem. Soc.*, 2002, **124**, 10664.
- 23 M. L. Dietz, J. A. Dzielawa, I. Laszak, B. A. Young and M. P. Jensen, *Green Chem.*, 2003, **5**, 682.
- 24 A. E. Visser, M. P. Jensen, I. Laszak, K. L. Nash, G. R. Choppin and R. D. Rogers, *Inorg. Chem.*, 2003, **42**, 2197.
- 25 D. C. Stepinski, M. P. Jensen, J. A. Dzielawa and M. L. Dietz, *Green Chem.*, 2005, **7**, 151.
- 26 P. Bonhôte, A.-P. Dias, N. Papageorgiou, K. Kalyanasundaram and M. Grätzel, *Inorg. Chem.*, 1996, **35**, 1168.
- 27 E. P. Horwitz, M. L. Dietz, D. M. Nelson, J. J. LaRosa and W. D. Fairman, *Anal. Chim. Acta*, 1990, **238**, 263.
- 28 M. L. Dietz, A. H. Bond, B. P. Hay, R. Chiarizia, V. J. Huber and A. W. Herlinger, *Chem. Commun.*, 1999, 1177.
- 29 E. P. Horwitz, M. L. Dietz and D. E. Fisher, *Solvent Extr. Ion Exch.*, 1990, **8**, 199.
- 30 G. W. Gokel, *Crown Ethers and Cryptands*, Royal Society of Chemistry, Cambridge, 1991.
- 31 M. L. Dietz, A. H. Bond, M. Clapper and J. W. Finch, *Radiochim. Acta*, 1999, **85**, 119.
- 32 V. V. Yakshin, V. M. Abashkin, N. G. Zhukova, N. A. Tsarenko and B. N. Laskorin, *Dokl. Akad. Nauk SSSR*, 1979, **247**, 1398 (CAN 91:199668).
- 33 A. M. Rozen, Z. I. Nikolotova, N. A. Kartasheva, N. G. Luk'yanenko and A. V. Bogatshii, *Dokl. Akad. Nauk SSSR*, 1982, **263**, 1165 (CAN 97:61870).
- 34 V. V. Yakshin, M. B. Korshunov, A. T. Fedorova and B. N. Laskorin, *Dokl. Akad. Nauk SSSR*, 1984, **279**, 407 (CAN 102:120874).
- 35 E. A. Filippov, V. V. Yakshin, V. M. Abashkin, V. G. Fomenkov and I. S. Serebryakov, *Radiokhimiya*, 1982, **24**, 214 (CAN 96:206290).
- 36 V. M. Abashkin, V. V. Yakshin and B. N. Laskorin, *Dokl. Akad. Nauk SSSR*, 1981, **257**, 1374 (CAN 95:50301).
- 37 V. M. Abashkin, V. V. Yakshin, I. A. Komolova, A. I. Zarubin and B. N. Laskorin, *Dokl. Akad. Nauk SSSR*, 1987, **296**, 622 (CAN 108:83016).
- 38 R. M. Izatt, B. L. Haymore and J. J. Christensen, *J. Chem. Soc., Chem. Comm.*, 1972, 1308.
- 39 R. M. Izatt, B. L. Haymore, J. S. Bradshaw and J. J. Christensen, *Inorg. Chem.*, 1975, **14**, 3132.

Call for papers



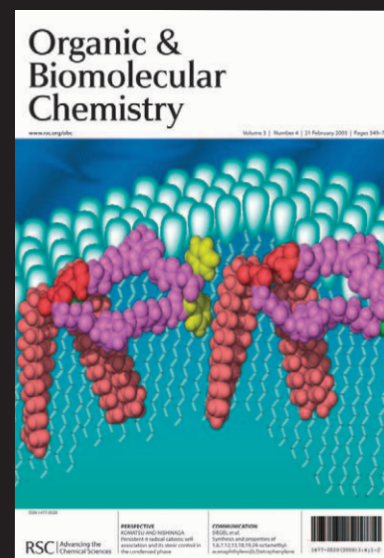
09030532

Organic & Biomolecular Chemistry

A major peer-reviewed international, high quality journal covering the full breadth of synthetic, physical and biomolecular organic chemistry.

Publish your review, article, or communication in OBC and benefit from:

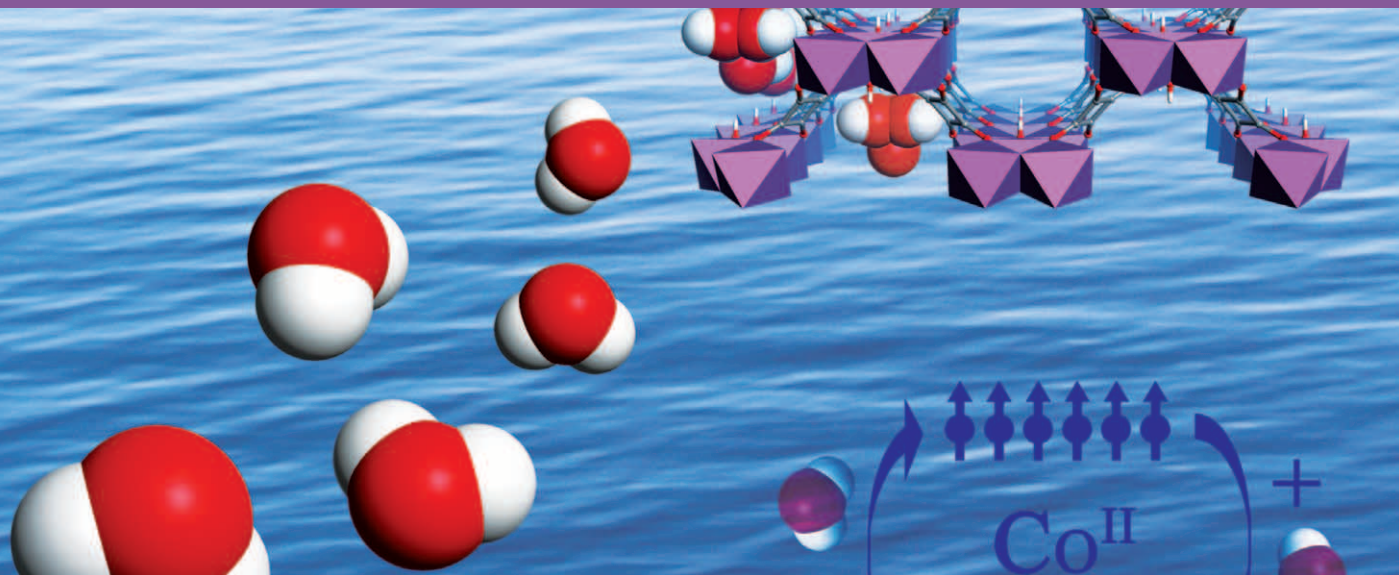
- The fastest times to publication (80 days for full papers, 40 days for communications)
- High visibility (OBC is indexed in MEDLINE)
- Free colour (where scientifically justified)
- Electronic submission and manuscript tracking via ReSource (www.rsc.org/ReSource)
- A first class professional service
- No page charges



Submit today!

RSC Publishing

www.rsc.org/obc



ChemComm

The leading international journal for the publication of communications on important new developments in the chemical sciences.

- Weekly publication
- Impact factor: 3.997
- Rapid publication – typically 60 days
- 3 page communications – providing authors with the flexibility to develop their results and discussion
- 40 years publishing excellent research
- High visibility – indexed in MEDLINE
- Host of the RSC's new journal, *Molecular BioSystems*

